A comparison of Eulerian-Lagrangian methods for the solution of the transport equation

Anabela Pacheco de Oliveira

B.Sc., Universidade Técnica de Lisboa, 1990

A thesis submitted to the faculty of the
Oregon Graduate Institute of Science & Technology
in partial fulfillment of the
requirements for the degree of
Master of Science
in
Environmental Science and Engineering

January 1994

The thesis "A comparison of Eulerian-Lagrangian methods for the solution of the transport equation" by Anabela Pacheco de Oliveira has been examined and approved by the following Examination Committee:

António M. Baptista, PhD., Thesis Advisor

William Fish, PhD., Associate Professor

Steve Otto, PhD., Assistant Professor

E. Eric Adams, PhD.,
Massachusetts Institute of Technology

To my mother, Sereia

À minha mãe, Sereia

ACKNOWLEDGEMENTS

I would like to express my appreciation and gratitude to Dr. António Baptista, whose experience, encouragement and numerous suggestions have been invaluable throughout this work. António and Izildinha's friendship was also a source of support, and facilitated my integration in a new society.

I would also like to express my gratitude to the other members of my thesis committee Dr. William Fish, Dr. Steve Otto and Dr. Eric Adams, for their review of this thesis and their valuable suggestions.

Special thanks to Paul Turner, for providing the wonderful software with which all figures were generated. His patience and competence in changing and adapting the original software for my work are deeply appreciated.

The life of graduate students couples is far from being easy: duplicated stress, duplicated deadlines and, in our case, the need to adapt to a new language and culture. André Fortunato has been both a loving and proud husband, and an excellent colleague. This work would not have been possible without his many suggestions, his insightful advice and many, many helpful discussions. He has offered love and comfort when I was feeling down and encouragement when I was willing to quit. I love you André.

I am especially thankful to my cats, Fox and Eddy. They were always ready to help me forget my work and to force me to have a good time (pet me, feed me, clean the litter box!).

The love and encouragement of my mother, to whom this thesis is dedicated, have always helped me throughout life. Her dedication to her children and all sacrifices she went through to provide me with the best education available are deeply appreciated.

A deep-hearted thanks to my brother, my sister-in-law and to my wonderful nephews, André and Miguel. They were a constant source of love and support. Thanks are also due to my mother- and father-in-law, for their friendship and encouragement throughout the last two years. The cheerful support of my friends in Portugal and of Miguel Remédio and José Menaia were much appreciated.

Finally, I would like to acknowledge the Junta Nacional de Investigação Científica e Tecnológica, Portugal, who provided me with the financial support through the grant BM/1354/91-RN (Programa Ciência). I also acknowledge the support of my former employer, Laboratório Nacional de Engenharia Civil.

TABLE OF CONTENTS

LIST OF TABLES

LIST OF FIGURES

ABSTRACT

A comparison of Eulerian-Lagrangian methods for the solution of the transport equation

Anabela Pacheco de Oliveira

Oregon Graduate Institute of Science & Technology, 1993

Supervising Professor: António M. Baptista

We present an extensive formal and experimental comparison of the accuracy and stability of selected finite-element Eulerian-Lagrangian methods (FE-ELMs) for the solution of the 1D transport equation.

The comparison shows that recent FE-ELMs that use the perspective of integration (rather than the more conventional perspective of interpolation) to treat initial conditions at the feet of the characteristic lines have excellent accuracy properties. Although some "integration" FE-ELMs are only conditionally stable, the associated constraints are expected to be minor for most applications of interest.

Motivation for the comparison was provided by the on-going development of a new generation of multi-dimensional Eulerian-Lagrangian water quality models, oriented towards surface water applications, and addressing tracers with increasingly complex chemical and biological pathways.

While this motivation may appear remote for a theoretical study of numerical methods, the need for the information now generated is strong, and the practical contributions are significant. Indeed, the need stems from the fear (partly rooted in accumulated experience) that complex water quality models may magnify remaining shortcomings in

fundamental aspects of the solution of the transport equation, such as stability, mass conservation, and ability to accurately transport sharp gradients of concentration.

Practical contributions include:

- the recommendation to initiate the systematic replacement of "interpolation" FE-ELMs by "integration" FE-ELMs, as the reference strategy to solve for hydraulic transport in the family of ELA water quality models (ELA, ELAcol, ELAsed, ELAmet, etc.);
- the development of basic data and understanding necessary for the informed use of "integration" FE-ELMs; an example is the development of basic data necessary to drive the semi-automatic generation of finite element grids tailor-made for the simulation of transport processes by "integration" FE-ELMs.

CHAPTER 1

Introduction

Context

Surface water bodies have always played an essential role in the development of human civilization. Under the pressure of multiple and conflicting demands, however, many such water bodies have shown stress signals for several decades. While awareness for the need of balanced management approaches has grown considerably, such approaches require an understanding of pathways of water, sediments and environmental tracers that only slowly is being acquired.

Numerical modeling has quickly overcome analytical and scale modeling as a tool of choice for the analysis of environmental processes and their relationship with the use of surface waters. In spite of very significant progress, however, the modeling community has yet to develop complex water quality models whose reliability is broadly accepted. The problem is at least three fold:

- some important environmental processes are not understood to the point where they can be correctly described by a set of mathematical equations;

- sources and empirical parameters are often difficult to quantify for specific sites/ situations;

- some fundamental questions related to the accuracy of numerical methods remain unresolved.

It is somewhat surprising that the third of these aspects remains unquestionably a limiting factor of our modeling ability. In this context, difficulties that are associated with

the solution of the transport equation are particularly surprising and frustrating. While we are moving towards a new generation of water quality models (where chemistry and biology are represented in ever increasing detail, and increasing spatial and temporal resolution), it is prudent and relevant to re-examine some of the basic issues surrounding the numerical solution of the transport equation. The present thesis is a contribution to such a re-examination.

Numerical methods for the solution of the transport equation

The fate of environmental tracers is described by the transport equation, eventually coupled with appropriate transformation equations. In this thesis, we will concentrate on the one-dimensional hydraulic transport of conservative and passive scalars, for which the transport equation reduces to:

$$\frac{\partial c}{\partial t} + u\frac{\partial c}{\partial x} = D\frac{\partial^2 c}{\partial x^2} \tag{1.1}$$

where c is the concentration of the tracer, u is the flow velocity and D is the diffusion coefficient. Since this equation will be approximated by a numerical method, it will be discretized in time with a time step Δt, and in space with a grid spacing Δx.

The physics of each of the two transport processes represented in Equation (1.1), advection and diffusion, are rather distinct:

- advection carries mass in the direction of the flow;
- diffusion carries mass in the direction of the lower concentrations.

Distinct physics maps into distinct mathematical properties: Equation (1.1) is predominantly hyperbolic if advection is dominant, and predominantly parabolic if diffusion is dominant. Also, distinct mathematics maps into distinct numerics, with advection-dominated transport often being more challenging to solve numerically than diffusion-dominated transport.

Early numerical methods did not explicitly recognize the contrasting physical, mathematical, and numerical nature of advection and diffusion. However, this recognition has triggered the development of a multitude of methods over the last couple of decades. Some of these methods deliberately targeted either advection-dominated or diffusion-dominated transport while others attempted to cover the full spectrum.

Because of the large number of numerical methods now available to solve the transport equation, it is useful to group these methods into broad classes. We will consider in this discussion three classes: Eulerian, Lagrangian and Eulerian-Lagrangian methods[1].

Eulerian methods solve the Eulerian form of the transport equation at the nodes of a fixed grid, thus handling the hyperbolic and parabolic operators simultaneously. Although this procedure has shown to be accurate for diffusion-dominated problems, it leads to spurious spatial oscillations for Peclet numbers ($Pe = u\Delta x/D$) larger than 2, when sharp gradients of concentration are present [*Roache,* 1982]. These oscillations may be eliminated by adding artificial diffusion, either by specifically imposing an excessive diffusion coefficient or by letting the numerical method introduce numerical diffusion (upwind methods). However, artificially damping oscillations changes the physics of the problem being solved, which may not be acceptable for specific applications.

Numerical oscillations can also be eliminated through the refinement of the computational grid, in order to reduce Pe. Doing so, however, increases the computational costs. In addition, the grid refinement limits the size of the time step, since Eulerian methods are often limited to Courant numbers ($\beta = u\Delta t/\Delta x$) smaller than one. For explicit methods, this restriction is due to stability constrains (Courant-Lewy stability criterion). For implicit methods, it is necessary to keep β small, since the accuracy of these methods decreases rapidly with increasing Courant numbers. Recent higher-order upwind schemes were able to considerably reduce the excessive numerical diffusion without unreasonable

1. A fourth relevant class not discussed here is constituted by particle methods.

grid refinements [*Westerink, et al*, 1989], but they still suffer from Courant number limitations.

Lagrangian methods solve the Lagrangian form of the transport equation in a grid that moves with the flow, thus avoiding the need to handle simultaneously the advective and diffusion operators. These methods are theoretically good approaches for advection-dominated problems, but they have seldom been implemented in application-oriented models due to practical difficulties such as the deformation of grids in the presence of complex flows.

Eulerian-Lagrangian methods (ELMs) combine the advantages of the Lagrangian treatment of advection with the convenience of a fixed computational grid [*Daubert*, 1974, *Holly and Preissmann*, 1977, *Glass and Rodi*, 1982, *Baptista, et al.*, 1984, *Baptista*, 1986 and 1987, *Celia, et al.*, 1990, *Cheng, et al.*, 1984, *Dimou*, 1992, *Hasbani, et al.*, 1983, *Hauguel*, 1985, *Leith*, 1965, *Russell*, 1985 and 1989, *Varoglu and Finn*, 1982, *Wang, et al.*, 1988, *Wood and Baptista*, 1993, *Yeh, et al.*, 1992, *Zisman*, 1990]. This is achieved through the effective decoupling of the advection and diffusion terms: advection is solved along trajectories that follow the flow (characteristic lines), while diffusion is solved in an Eulerian grid, either by finite differences or finite elements. Through this approach, ELMs are able to solve transport problems ranging from advection-dominated to diffusion-dominated. Since ELMs solve for advection in a Lagrangian form, they overcome the Courant number restriction, and large time steps can be used.

ELM solutions typically comprise three basic steps (Figure 1.1):

- definition of characteristic lines that follow the flow backwards from the present time step to the previous one;
- determination of concentrations at the feet of the characteristic lines; and,
- solution of the Lagrangian form of the diffusion equation, using concentrations at the feet of the characteristic lines as initial conditions.

The decoupling of advection and diffusion also gives ELMs the ability to handle effectively processes with very distinct time scales. While tracking in advection is usually solved with a very small time step, diffusion can be solved with a much larger time step. In addition, chemical transformations can be treated either in the advection [*Wood and Baptista,* 1993] or the diffusion steps.

When the ELMs are coupled with finite elements (FE-ELM), they become particularly well suited to the modeling of regions with very irregular domains, such as coasts and estuaries. The FE approach also provides the ability to refine the domain locally (for instance, near sources) in a simple and efficient way. FE-ELMs have been applied with success in the past, for the study of the transport of pollutants in estuarine and coastal systems [*Baptista, et al.,* 1984, *Cheng, et al.,* 1984, *Hauguel,* 1985, *Wang, et al.,* 1988, *Dimou,* 1992, *Wood and Baptista,* 1993].

Background and recent trends in Eulerian-Lagrangian methods

Although ELMs constitute a very attractive approach to solve advection-dominated problems, there is still room for improvement, in particular concerning mass conservation and the trade-off between accuracy and cost.

Mass conservation is one of the critical issues in ELMs [*Baptista,* 1987, *Dimou,* 1992]. Indeed, these methods are not inherently conservative, and mass loss or gain has been detected in many applications, being particularly significant when long term simulations are involved.

These mass imbalances are often traceable back to (a) the coupling of flow and transport models, (b) the tracking in the advective step, and (c) the treatment of boundary conditions. The coupling between flow and transport models can lead to mass imbalances when the flow field is not conservative. In order to have a Lagrangian treatment of advec-

tion, ELMs solve for the non-conservative form of the transport equation, assuming that the continuity equation is exactly satisfied:

$$\underbrace{\frac{\partial c}{\partial t} + u_i \frac{\partial c}{\partial x_i} = \frac{1}{H}\frac{\partial}{\partial x_i}\left(D_{ij}\frac{\partial c}{\partial x_j}\right)}_{\text{non-conservative form of the transport equation}} \underbrace{- \frac{1}{H}\left(\frac{\partial H}{\partial t} + \frac{\partial}{\partial x_i}(u_i H)\right) c}_{\text{dropped term in ELMs}} \qquad (1.2)$$

where H is the total water depth. Therefore, when flow is not conservative, the dropped term from the conservative transport equation will lead to mass errors in the transport simulation. The tracking performed with a non-conservative flow field generates deviations in the location of the feet of the characteristic lines that lead to mass errors.

In addition, the weak formulation of some flow models, can be another source of mass errors in the transport simulation, since the no-flow restriction at the land boundaries is imposed as a natural boundary condition. The velocity oscillations that results from the relaxing of the no-flow boundary condition, can lead to the leakage of the mass through closed boundaries.

Mass errors in the advective step are primarily controlled by the accuracy of the particle backtracking [*Baptista,* 1987, *Dimou,* 1992]. As with a non-conservative flow field, tracking errors lead to errors in the evaluation of the feet of the characteristic lines. Therefore, the mass errors in the transport simulation will be similar for both problems. Studies done in the past showed that very accurate tracking schemes are required, to keep the concentration field conservative [*Baptista et al,* 1984], especially in the presence of sharp velocity gradients. These studies have also presented tracking techniques that are accurate enough to preserve mass, although at significant computational costs.

The implementation of boundary conditions in ELMs can also compromise the conservation of mass if the concentrations are significant near the boundaries. For instance, the ambiguity in imposing the boundary conditions associated with the tradi-

tional ELM formulations can lead to mass errors if a considerable mass of the tracer is entering the domain. Recently proposed Eulerian Lagrangian Localized Adjoint Methods (ELLAMs) constitute a formally more satisfying way to treat boundary conditions [*Celia, et al,* 1990, *Zisman,* 1990].

The advective step has been identified as a major source of numerical errors in ELMs [*Baptista,* 1987, *Dimou,* 1992]. It can be responsible for the presence of both considerable numerical diffusion and numerical dispersion. Numerical dispersion affects the formulations with quadratic and higher order elements and it results mainly from phase errors that are associated with the different types of nodes in these elements [*Baptista,* 1986 and 1987]. In contrast, numerical diffusion plagues the results from all formulations, and it is strongly controlled both by the domain discretization and by the definition of the initial conditions for the diffusion equation.

In the past, the definition of the initial conditions for the diffusion equation was identified as an interpolation problem, and several interpolators were proposed and formally analyzed [*Leith,* 1965, *Holly and Preissmann,* 1977, *Baptista, et al.*, 1984, *Baptista,* 1986, *Baptista,* 1987]. They have been classified in two broad groups: compact methods, in which the concentration at the feet of the characteristic lines is interpolated from the concentrations at the nodes of the element that contains the foot of the relevant characteristic line (core element); and non-compact methods, where the interpolation functions include the contribution of nodes outside the core element [*Baptista,* 1987].

In a search for increasingly more accurate algorithms, both compact and non-compact high order interpolators were proposed and analyzed [*Baptista,* 1987]. Several non-compact interpolators presented very attractive properties in 1D, but their extension to multiple dimensions poses unattractive practical problems, ranging from ambiguity to high computational costs. The compact cubic or higher order interpolators were found to be unstable.

The quadratic compact interpolator was considered to be one of the best options and it has been implemented in several ELM transport models for surface waters [*Wood and Baptista,* 1993, *Baptista, et al,* 1984, *Dimou,* 1992]. However, in the presence of sharp gradients, the necessary grid refinement for acceptable accuracy can lead to very high computational costs.

In an attempt to develop a more efficient and accurate technique, several ELMs proposed over the last decade [*Yeh, et al.,* 1992, *Hasbani, et al.,* 1983, *Russell,* 1985] share a new approach: they deal with the definition of the initial conditions for the diffusion equation as an integration rather than an interpolation problem. By doing so, these methods take explicit advantage of FE concepts, and become fundamentally different from corresponding finite difference ELMs.

If the Courant number is not an integer, the concentration between the feet of consecutive characteristic lines is a piecewise function (Figure 1.2). *Interpolation* ELMs evaluate the concentrations at the feet of the characteristic lines, either by a compact or non-compact approach, and define the concentration between these points by polynomial shape functions. These polynomial functions provide the basis for the evaluation of the integrals in the diffusion step. The errors associated with this integration depend on the interpolation technique and on the order of the shape functions. *Integration* ELMs identify the integration as the key operation to be performed. In order to reduce the errors in the advective step, they propose more accurate approaches to the definition of initial conditions for the diffusion equation. One approach (piecewise ELMs) seeks an exact evaluation of the integrals, taking into account the piecewise shape of the concentration at the feet of the characteristic lines; another approach (quadrature ELMs) uses a numerical integration.

One possible implementation of the piecewise integration concept [*Yeh, et al.,* 1992] is to evaluate integrals at the feet of the characteristic lines exactly, either numerically or analytically, by sub-dividing the domain in regions where the integrands are C^{∞} functions (Figure 1.3). Sub-regions are defined both by the nodes and by other "notable"

points, leading to a final concentration defined by a piecewise function inside each element. The notable points, which generally correspond to discontinuities in the first derivative of concentration, are forward tracked at each time step along with the nodes found between two consecutive feet of characteristic lines (Figure 1.3). Numerical tests performed with this method showed excellent accuracy [*Yeh, et al,* 1992]. However, the associated costs may become unsustainable for practical applications since the number of notable points required to reproduce the concentration in each element increases rapidly with time.

Yeh's implementation of the piecewise integration concept is theoretically very attractive, but the increase of the number of notable points in time may compromise the feasibility of this method in multiple dimensions. In an attempt to overcome this problem, we propose a simpler implementation of the same concept, which eliminates the accumulation of notable points (Figure 1.4). In each time step, the concentration after the advective step is defined by the concentration at the feet of the characteristic lines and the concentration at the nodes found between two consecutive feet of characteristic lines. The piecewise shape is used for the evaluation of the integrals, but is eliminated during the diffusion step. The final concentration is thus defined by the shape functions only, leading to a controlled, time-step independent cost. The initial conditions for the diffusion equation will only be exact in a per-time-step basis, but the method will be shown to have quite good accuracy.

Quadrature ELMs handle the definition of the initial conditions for the diffusion equation from a numerical integration perspective: quadrature points, defined at the time level in which the equation is being solved, are backtracked instead of the nodes. The quadrature points are then used in the numerical integration at the feet of the characteristic lines, providing a straightforward evaluation of the integrals (Figure 1.5). Previous studies showed that quadrature ELMs can be very accurate [*Hasbani, et al.,* 1983], but are only conditionally stable [*Morton, et al,* 1988]. One of the most attractive features of these methods is their simple implementation in multiple dimensions.

Another class of ELMs, denoted Eulerian-Lagrangian Localized Adjoint Methods (ELLAMs), has been proposed in recent years [*Celia, et al.*, 1990, *Russell*, 1989, *Zisman*, 1990]. Borrowing some concepts from older methods [*Varoglu and Finn*, 1982, *Hauguel*, 1985], ELLAMs provide a systematic treatment of boundary conditions.

This flexible approach to the implementation of boundary conditions gives rise to a conservative numerical scheme, in a constant coefficients context [*Celia, et al.*, 1990, *Russell*, 1989]. For variable coefficients, both tracking errors and non-conservative flow fields lead to mass imbalances that are not addressed by ELLAMs [*Russell*, 1989]. ELLAMs also provide an useful framework to the ELM concept, in which context both interpolation and integration methods can be interpreted.

Integration (piecewise and quadrature) methods constitute a potentially attractive alternative to interpolation ELMs. However, as in many fast-evolving areas, little effort has been dedicated to the systematic analysis of the characteristics of these methods or to the comparison of their properties with well-established methods. This analysis becomes especially important nowadays, when the development of efficient and accurate 3D models is necessary in many areas.

Objectives, methodology and structure

We seek to consolidate selected aspects of the current knowledge of FE-ELMs for the transport equation. Primary objectives are:

- To understand the numerical properties of integration FE-ELMs

  • Rationale: Integration FE-ELMs provide a conceptually very attractive approach to the definition of the initial conditions for the diffusion equation. However, previous analysis of integration FE-ELMs were mostly based on isolated tests, which limits the current understanding of their properties. Our

goal is to analyze the formal properties of the methods (accuracy and stability) in a systematic way, explicitly analyzing dependencies on controlling dimensionless numbers.

- To compare integration and interpolation FE-ELMs

  • Rationale: Little effort has been devoted to compare integration ELMs with more conventional interpolation ELMs, except through episodic numerical experimentation. A systematic comparative analysis is important to help modelers select a technique for implementation in multiple-dimension models. Detailed studies done in the past for interpolation methods [*Baptista,* 1987] provide the theoretical support for the choice of currently used techniques. In this work, we seek to address part of the controlling parameters for the selection of new techniques, through a combination of formal analysis and numerical experimentation.

To achieve the stated goals, selected integration ELMs and two interpolation ELMs will be subject to systematic formal analysis of propagation and truncation errors, and to extensive numerical experimentation. The formal analysis provides insight on the accuracy and stability of each method, as a function of controlling dimensionless numbers (Courant number, Diffusion number and Dimensionless wavelength). The numerical experimentation tests the performance of the methods in well-established test cases, and examines the ability of each method to preserve mass in simple test cases.

For simplicity, this study is conducted in one dimension and for constant velocity and diffusion coefficient. Because of this simplicity, we are able to characterize the methods in a systematic and general way, which is essential for an unbiased comparison. However, we will be unable to address some relevant issues that are associated with a non-constant velocity field, such as the computational cost and the mass conservation.

This thesis is divided into three chapters, including this Introduction. Chapter 2 constitutes the core of the thesis. Written as a stand-alone contribution, intended for sub-

mission to *International Journal for Numerical Methods in Fluids*, it describes and systematically compares the methods selected for analysis. Chapter 3 places our findings in the context of the evolution of ELMs and explores directions for future research.

References

Baptista, A. M., E. E. Adams, and K. D. Stolzenbach, Eulerian- Lagrangian analysis of pollutant transport in shallow water, *Technical Report no. 296*, MIT R.M. Parsons Laboratory, Cambridge, Mass, 1984.

Baptista, A. M., Accurate Numerical Modeling of Advection-Dominated Transport of Passive Scalars: A contribution, Laboratório Nacional de Engenharia Civil, Lisbon, Portugal, 1986.

Baptista, A. M., Solution of Advection-Dominated Transport by Eulerian-Lagrangian Methods using the Backwards Method of Characteristics, Ph.D. Dissertation, Massachusetts Institute of Technology, Cambridge, Mass, 1987.

Celia, M. A., T. F. Russell, I. Herrera, R. E. Ewing, An Eulerian-Lagrangian Localized Adjoint Method for the Advection-Diffusion Equation, *Advances in Water Resources*, *13*(4), pp. 187-206, 1990.

Cheng, R. T., V. Casulli, and S. N. Milford, Eulerian-Lagrangian Solution of the Convection-Dispersion Equation in natural Coordinates, *Water Resources Research, 20*(7), pp. 944-952, 1984.

Daubert, O., *Programme HYP1 - Rapport C41/74/12*, Laboratoire National D'Hydraulique, Chatou, France, 1974.

Dimou, K., 3-D Hybrid Eulerian-Lagrangian / Particle Tracking Model for Simulating Mass Transport in Coastal Water Bodies, Ph.D. Dissertation, Massachusetts Institute of Technology, Cambridge, Mass, 1992.

Glass, J. and W. Rodi, A Higher Order Numerical Scheme for Scalar Transport, *Comp. Meth. in Appl. Mech. and Eng., 31*, pp. 337-358, 1982.

Hasbani, Y., E. Livne, and M. Bercovier, Finite Elements and Characteristics Applied to Advection-Diffusion Equations, *Computers and Fluids, 11*, pp. 71-83, 1983.

Hauguel, A., Numerical Modelling of Complex Industrian and Environmental Flows, *Proceedings of the International Symposium on Refined Flow Modelling and Turbulence Measurements, I*, Iowa, 1989

Holly, F. M. and A. Preissmann, Accurate Calculation of Transport in Two Dimensions, *Journal of the Hydraulics Division, ASCE, 103*, pp. 1259-1278, 1977.

Leith, C. E., Numerical Simulation of the Earth's Atmosphere, *Methods in Computational Physics, 4*, pp. 1-28, 1965.

Morton, K. W., A. Priestley, and E. Suli, Stability of the Lagrange-Galerkin Method with Non-exact Integration, *Mathematical Modelling and Numerical Analysis, 22*(4), pp. 625-653, 1988.

Roache, P., *Computational Fluid Dynamics*, Hermosa Publ., 1982

Russell, T. F., Time Stepping along characteristic with incomplete iteration for a Galerkin approximation of Miscible Displacement in Porous Media, *SIAM J. of Numerical Analysis, 22*(5), pp. 970-1013, 1985.

Russell, T. F., Eulerian-Lagrangian Localized Adjoint Methods for Advection-Dominated Problems, *Proceedings of the 13th Biennial Conference on Numerical Analysis*, Pitman, Dundee, Scotland, 1989.

Russell, T. F. and R.V. Trujillo, Eulerian-Lagrangian Localized Adjoint Methods with Variable Coefficients in Multiple Dimensions, *Proceedings of the Ninth International Conference on Computational Methods in Water Resources*, Denver, 1992.

Varoglu, E. and W. D. Liam Finn, Utilization of the Method of Characteristics to solve accurately Two-Dimensional Transport Problems by Finite Elements, *International Journal for Numerical Methods in Fluids, 2*, pp. 173-184, 1982.

Wang, J. D., S. V. Cofer-Shabica, and J. Chin Fatt, Finite Element Characteristic Advection Model, *Journal of Hydraulic Engineering, ASCE, 114*, pp. 1098-1114, 1988.

Westerink, J. J. and D. Shea, Consistent Higher Degree Petrov-Galerkin Methods for the Solution of the Transient Convection-Diffusion Equation, *International Journal for Numerical Methods in Engineering, 28*, pp. 1077-1101, 1989

Wood, T. M. and A. M. Baptista, A model for Diagnostic Analysis of Estuarine Geochemistry, *Water Resources Research, 29*(1), pp. 51-71, 1993.

Yeh, G. T., J. R. Chang, and T. E. Short, An Exact Peak Capturing and Oscillation-Free Scheme to Solve Advection-Dispersion Transport Equations, *Water Resources Research, 28*(11), pp. 2937-2951, 1992.

Zisman, S., Simulation of Contaminant Transport in Groundwater Systems using Eulerian-Lagrangian Localized Adjoint Methods, M.S. Thesis, Massachusetts Institute of Technology, Cambridge, Mass, 1990.

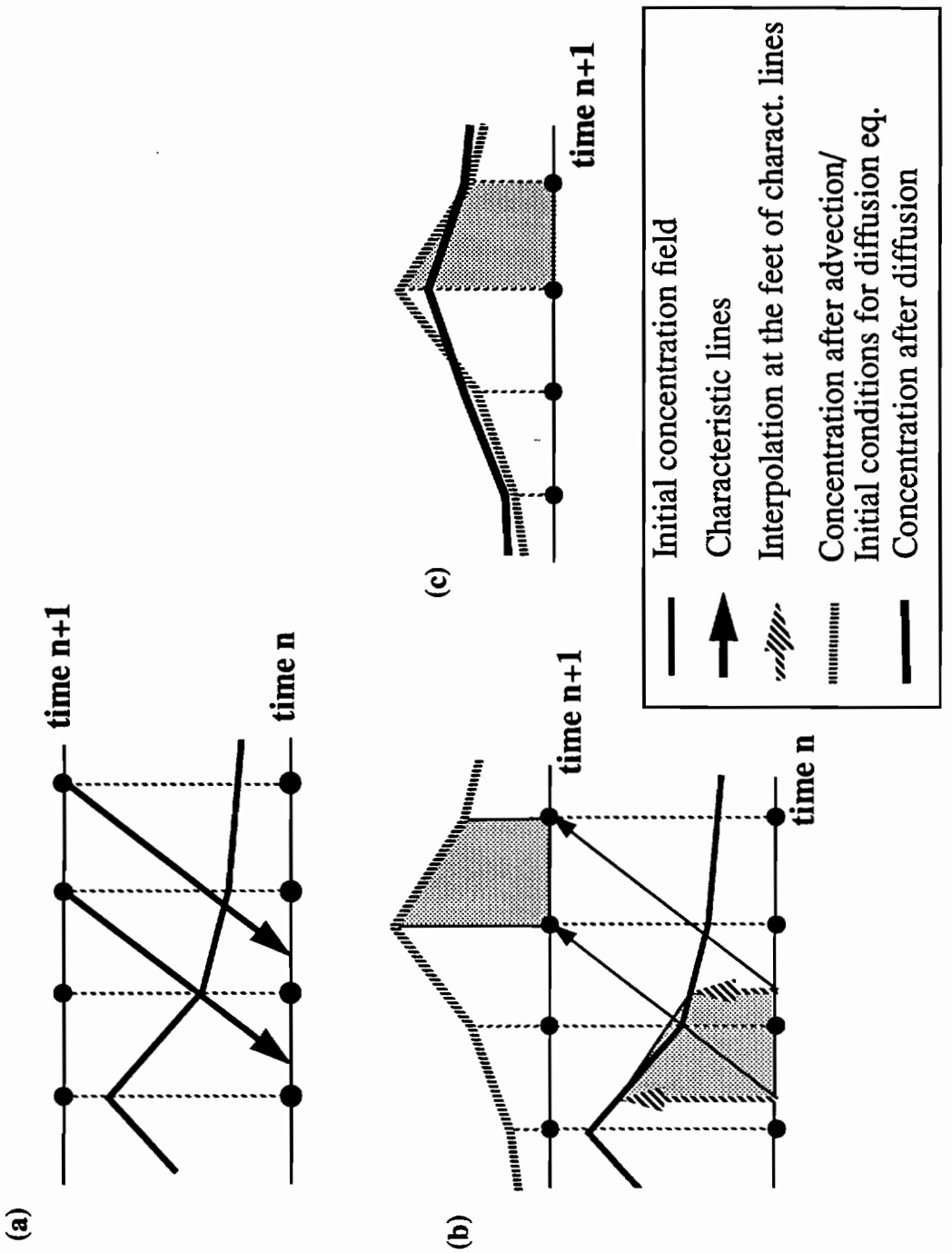

Figure 1.1 Basic steps of Eulerian Lagrangian methods: (a) definition of the characteristic lines; (b) interpolation of the concentration at the feet of the characteristic lines; (c) solution of the Lagrangian form of the diffusion equation.

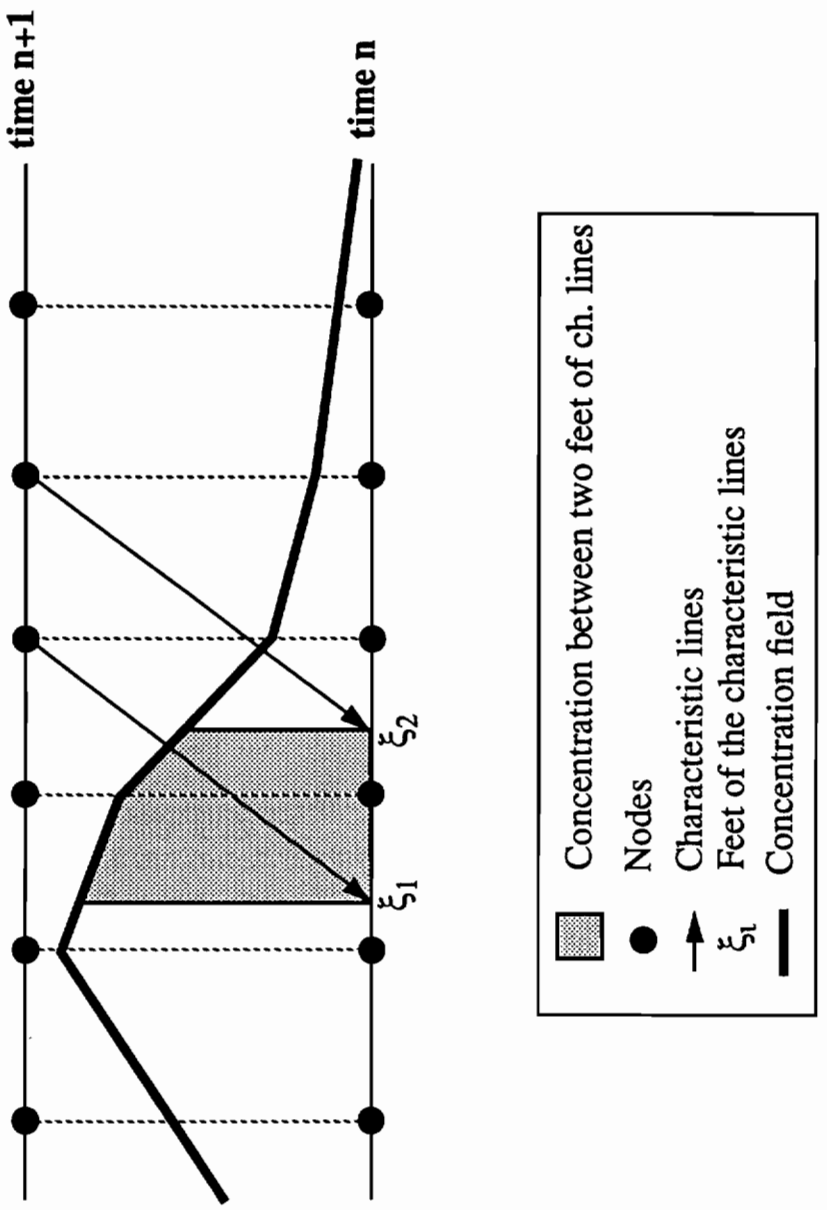

Figure 1.2 Concentration between two consecutive feet of the characteristic lines, for non-zero fractional part of the Courant number

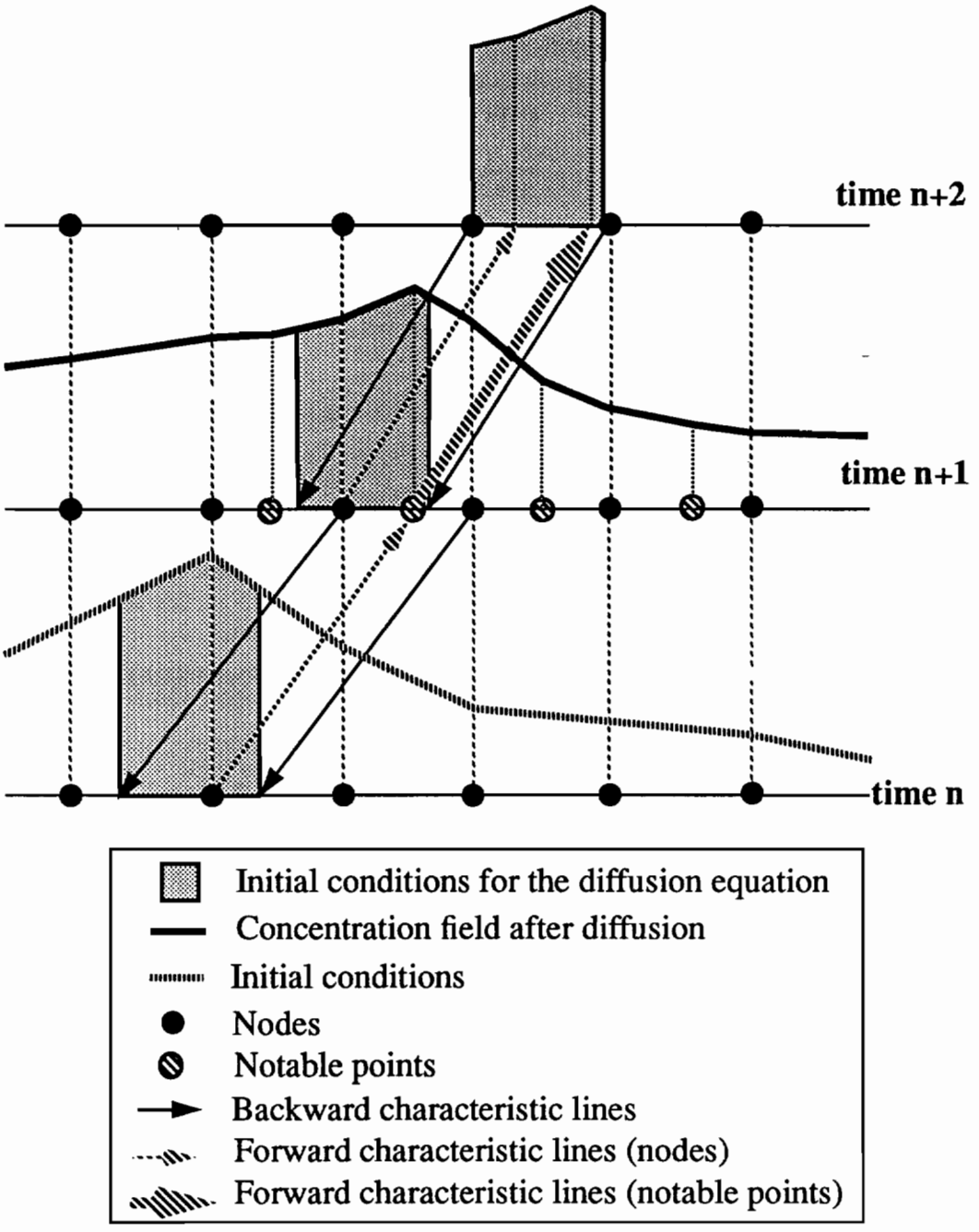

Figure 1.3 Original piecewise ELM procedure for two consecutive time steps: initial conditions for the diffusion equation supported by nodes and notable points.

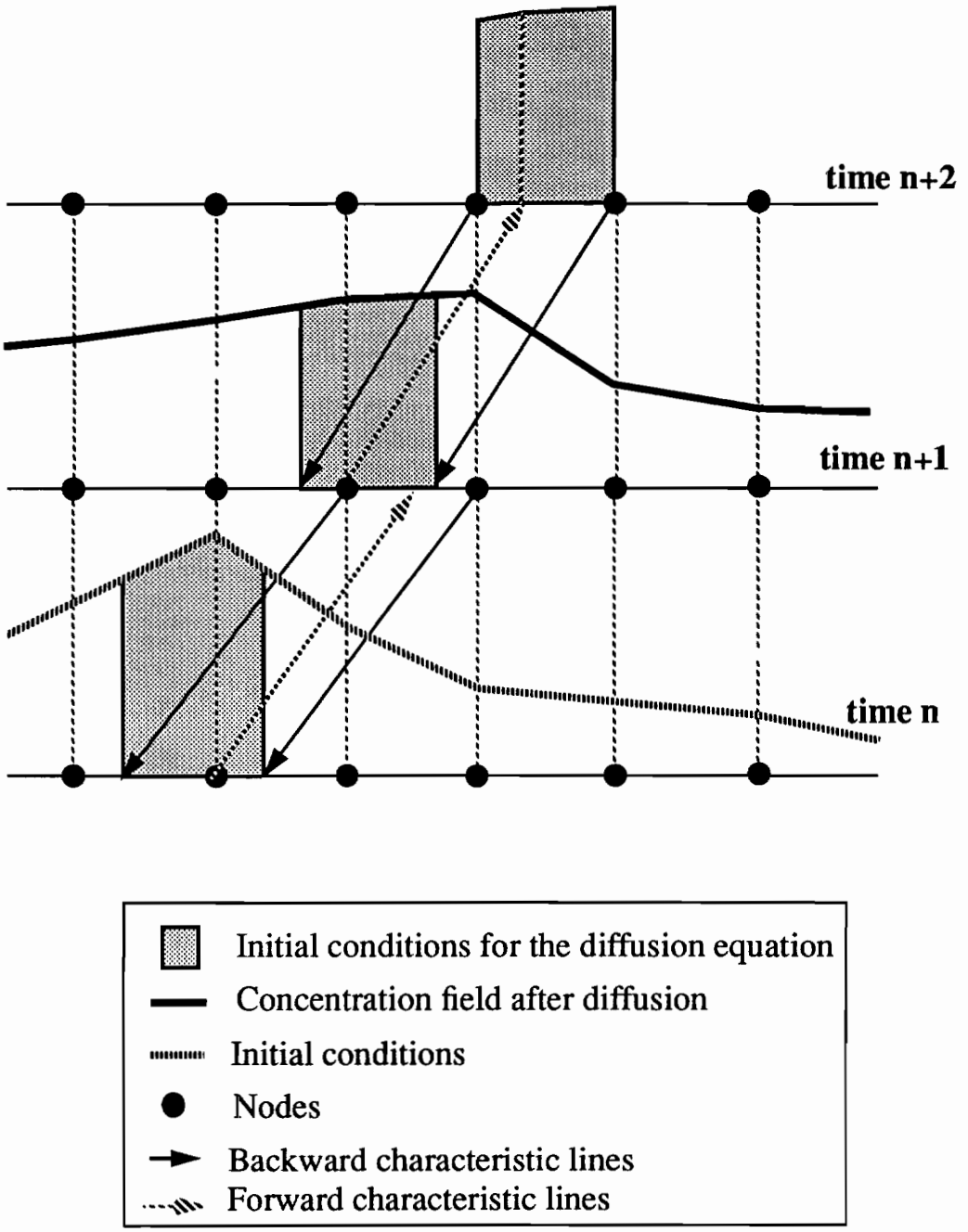

Figure 1.4 Proposed piecewise ELM: initial conditions for the diffusion equation defined only by the nodes.

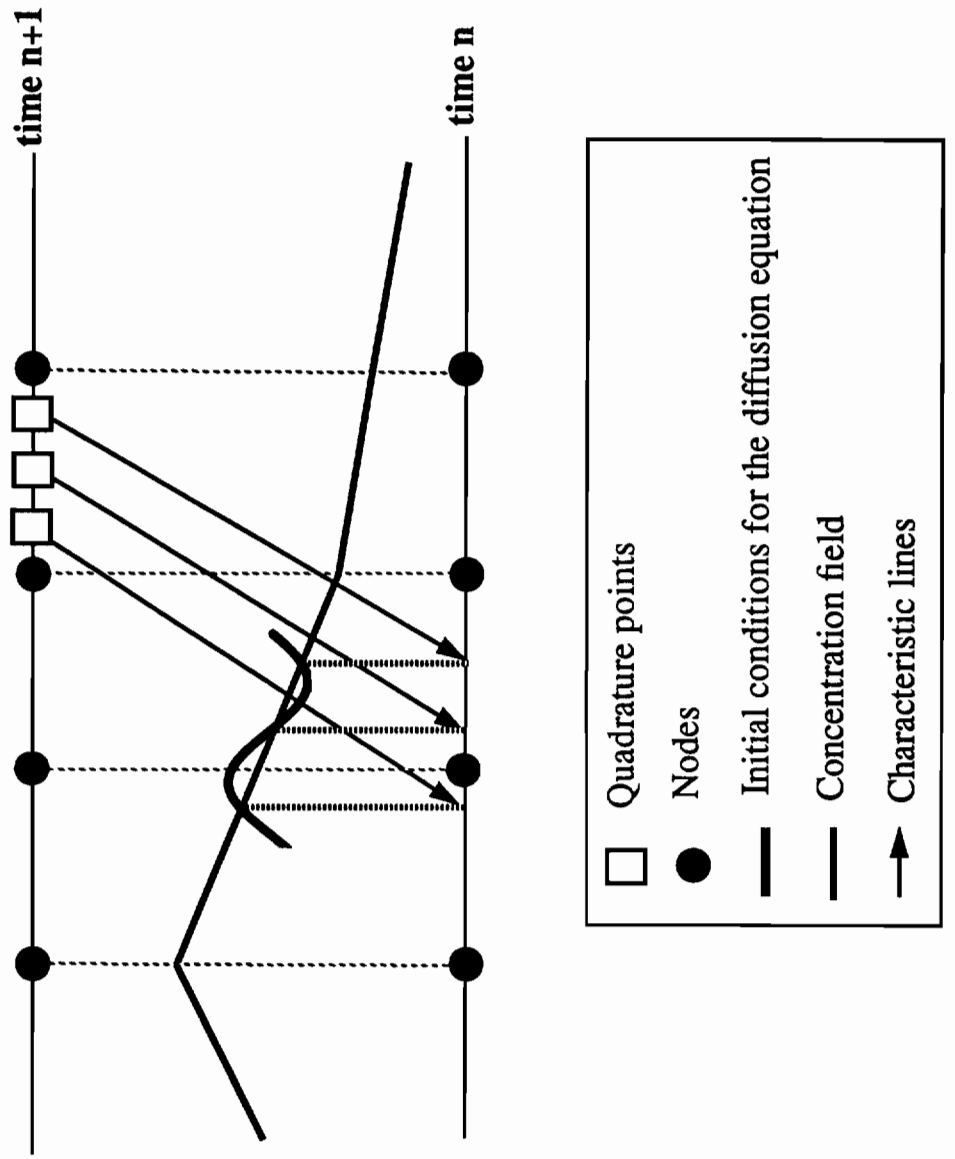

Figure 1.5 Quadrature ELMs: initial conditions for the diffusion equation defined by a polynomial function specified by the number and type of quadrature points (e.g. n Gauss quadrature points => polynomial of order $2n$-2).

CHAPTER 2

A comparison of Eulerian-Lagrangian methods for the solution of the transport equation

Abstract

Selected "interpolation" and "integration" finite element Eulerian-Lagrangian methods are systematically compared, through a combination of formal analysis (propagation and truncation errors) and numerical experimentation. While no method emerges as optimal, we show that methods that approach conditions at the feet of the characteristic lines with the perspective of "integration" rather than "interpolation" tend to have superior accuracy. Among integration methods, however, those based on the notion of tracking quadrature points, are mildly affected by conditional stability.

Introduction

Eulerian Lagrangian Methods (ELMs) have evolved much over the last three decades, to become one of the most attractive techniques for the solution of advection-dominated transport. The basic concept of ELMs is simple: the transport equation is solved in Lagrangian form "along" characteristic lines, effectively decoupling the advection and diffusion terms but retaining the convenience of fixed computational grids. There are many different ways to implement this concept, and several ELMs have been proposed over the years [*Daubert,* 1974, *Holly and Preissmann,* 1977, *Glass and Rodi,* 1982, *Baptista, et al.,* 1984, *Baptista,* 1986 and 1987, *Celia, et al.,* 1990, *Cheng, et al.,* 1984, *Dimou,* 1992, *Hasbani, et al.,* 1983, *Hauguel,* 1985, *Leith,* 1965, *Russell,* 1985 and 1989, *Varoglu*

and Finn, 1982, *Wang, et al.,* 1988, *Wood and Baptista,* 1993, *Yeh, et al.,* 1992, *Zisman,* 1990, *Neuman,* 1981 and 1984].

As frequently happens in fast-evolving areas, much more attention has been paid to the development of new ELMs than to the systematic comparison of existing ones. This paper updates, by including representative new methods, earlier research [*Baptista,* 1986 and 1987] on the comparison and understanding of ELMs. The comparison concentrates on finite-element based ELMs (FE-ELMs), and is restricted to the case of constant-coefficient, one-dimensional transport on uniform grids.

The paper is divided into five main sections, besides this ***Introduction. Background*** presents a brief history of the evolution of ELMs, and introduces the three classes of methods selected for analysis. Out of necessity, some new nomenclature is introduced. While this nomenclature may be transitory, it creates a guiding taxonomy that helps the reader throughout the paper, and addresses a growing need for systematics in numerical analysis.

Selected Methods provides the rationale for the choice of the specific methods adopted, and describes their formulation. All formulations are presented for the case of constant coefficients and one-dimensional uniform grids, but all methods can and several have been applied in much less restrictive settings. Additional nomenclature is introduced, completing the taxonomy adopted in the paper.

Formal Analysis examines the accuracy and stability of the selected methods, based on formal analysis of truncation and propagation errors. Error formulae are compiled in tables, and errors are mapped in ways that foster the analysis of the accuracy and stability of individual methods, and prompt comparisons among methods or classes of methods. An integrating discussion of truncation and propagation errors is presented, primarily aimed at anticipating and explaining trends of behavior.

Numerical Experimentation provides a complementary examination of the accuracy and stability of the selected methods. Tests and error measures are extracted from or influenced by the Convection-Diffusion forum [*Baptista, et al.*, 1986, *Adams, et al.*, 1993]. The analysis of the numerical results is guided by and compared against the results of the formal analysis in the previous section.

Final Considerations provides an overview of the results presented in the paper, and examines how these results may impact future research on ELMs and the development of a new generation of Eulerian-Lagrangian models for environmental application in surface waters.

Background[1]

The basic concept, if not the terminology and full usefulness, of Eulerian-Lagrangian methods was introduced in the mid-sixties [*Leith*, 1965]. In an attempt to avoid the wiggles that plague finite-difference (FD) centered solutions of the advection-dominated transport equation, Leith proposed to solve

$$\frac{Dc}{Dt} \equiv \frac{\partial c}{\partial t} + u\frac{\partial c}{\partial x} = D\frac{\partial^2 c}{\partial x^2} \tag{2.1}$$

using the discrete algorithm:

$$\frac{c_j^{n+1} - c_\xi}{\Delta t} = D\frac{c_{j+1}^n - 2c_j^n + c_{j-1}^n}{\Delta x^2} \tag{2.2}$$

where c is the concentration, u is the velocity, D is the diffusion coefficient and ξ denotes the feet of characteristic lines that follow the flow backwards (Figure 2.1(a)). The location of the foot of each characteristic line is obtained by integration (trivial, for uniform velocities):

1. Consistently with the scope of the paper, this section concentrates on the fundamentals of existing methods, as applied to 1D constant coefficient transport. We will also assume that u is positive.

$$x_\xi = x_j - \int_{t_{n+1}}^{t_n} u d\tau \equiv x_j - u\Delta t \tag{2.3}$$

and the associated concentrations are obtained by interpolation or extrapolation:

$$c_\xi = c_j^n + \frac{c_j^n - c_{j-1}^n}{\Delta x}(x_\xi - x_j) \tag{2.4}$$

Leith's method effectively decouples advection from diffusion. The decoupling process is physically-based, in the sense that it results naturally from the introduction of backward characteristic lines that follow the flow. Three distinct steps are involved in the overall solution:

- step 1: definition of the characteristic lines, and determination of the location of their "feet" (x^ξ);
- step 2: determination of the concentrations at the feet of the characteristic lines (c^ξ); and
- step 3: solution of the Lagrangian form of the diffusion equation, using the concentrations at the feet of the characteristic lines as initial conditions.

Both the decoupling strategy and the three generic solution steps identified above are identifying characteristics of Eulerian-Lagrangian methods. However, Leith's proposed method had a major limitation. Indeed, examination of Equation (2.4) shows that the concentration at the foot of the characteristic lines is determined from the concentrations at nodes j and j-1; hence, for Courant numbers larger than one, this determination involves an extrapolation and the algorithm becomes unstable. Furthermore, the replacement of Equation (2.4) into Equation (2.2) leads to:

$$\frac{c_j^{n+1} - c_j^n}{\Delta t} + u\frac{c_j^n - c_{j-1}^n}{\Delta x} = D\frac{c_{j+1}^n - 2c_j^n + c_{j-1}^n}{\Delta x^2} \tag{2.5}$$

which shows that the advection term is effectively approximated by a conventional upwind scheme: hence, Leith's method can be easily interpreted as essentially an Eulerian upwind method.

It took over a decade for Leith's pioneering concept to lead to the truly distinctive group of methods now known as ELMs. *Daubert* [1974] may have been the first to recognize that Courant number restrictions could be avoided by interpolating between the nodes bounding the foot of each characteristic line (Figure 2.1(b)), rather than by extrapolating from the vicinity of the head of the characteristic line (Figure 2.1(a)). In its conceptual simplicity, this recognition may qualify as the single most important development in ELM history.

Daubert also recognized that interpolating linearly to find concentrations at the feet of the characteristic lines is a major source of errors, and allowed for higher order (quadratic) interpolations. Following these early steps, the optimization of the strategy for interpolation at the foot of the characteristic lines became a focus for ELM research during the 80's. As a result, a large number of interpolators were developed, none of which can be recognized as "optimal" as shown by two systematic reviews [*Baptista*, 1986 and 1987].

Coincidentally with the search for optimal interpolators, the notion of using ELMs in a finite element (FE) context became progressively more popular. Early FE-ELMs [*Holly and Preissmann*, 1977, *Neuman*, 1981, *Baptista, et al.*, 1984, *Hauguel*, 1985] differed "mechanically" but not in any fundamental conceptual way from the corresponding FD-ELMs. In particular, only recently [*Russell*, 1985, *Yeh, et al.*, 1992] have ELMs started to take advantage of the fact that, in a finite element context, the problem of "interpolation" at the feet of the characteristic lines can effectively be expressed as an "integration" problem.

To illustrate this point, consider the evaluation of the contribution of element k to the weak weighted residual statement:

$$\int_{\Omega_k} \phi_m \frac{Dc}{Dt} dx = -D \int_{\Omega_k} \frac{\partial \phi_m}{\partial x} \frac{\partial c}{\partial x} dx + boundary\ \ terms \tag{2.6}$$

where ϕ_m are the weighting functions.

The evaluation of the integrals poses no problem at time $n+1$, where the derivatives of the elemental shape functions are continuous. However, integrals at time n (Figure 2.2) involve shape functions from more than one element; hence concentration derivatives are discontinuous over the region of integration. The form in which these discontinuities at time n are addressed provides an important distinguishing criterion among FE-ELMs.

"Interpolation FE-ELMs" [*Baptista, et al.*,1984, *Holly and Preissmann,* 1977, *Leith,* 1965, *Baptista,* 1987] simply "ignore" the discontinuity of ∇c. The concentrations and concentration derivatives are evaluated at the feet of the characteristic lines and assigned to a polynomial interpolation function. This interpolation function provides the basis for the integration (Figure 2.2(a)), which may be analytical or numerical. Systematic comparisons of alternative interpolation functions [*Baptista*, 1986 and 1987] show that unsatisfactory compromises between cost/feasibility and accuracy become necessary and limit the implementation of the most accurate interpolation ELMs in multi-dimensions. The implication is that while interpolation ELMs have proved satisfactory for many practical applications, there is significant room for improvement.

"Quadrature FE-ELMs" [*Hasbani, et al.*, 1983, *Russell*, 1985] explicitly recognize that the operation that one has ultimately to deal with is an integration, and take a conceptually very distinct approach: rather than tracking nodes backwards from $n+1$ to n, these methods track quadrature points (Figure 2.2(c)), which are then used as a basis of a necessarily numerical integration (typically Gauss or Lobatto quadrature). Quadrature ELMs are generally less damping than interpolation ELMs, but, as shown in latter sections, they often have only conditional stability. A very positive characteristic of quadrature ELMs is their straightforward implementation in multiple dimensions.

"Piecewise integration FE-ELMs" also recognize the key role of integration. These methods track nodes and/or other "notable points" both from $n+1$ to n and from n to $n+1$; hence, the domain of integration is effectively divided into sub-domains, in each of which integrals can be evaluated *exactly* or very accurately, either numerically or analyti-

cally. Notable points tracked from n to n+1 may (Figure 2.2(b)) or may not correspond to discontinuities in first derivatives of concentration. These methods were introduced by *Yeh, et al.* [1992], borrowing some concepts from *Neuman* [1984]; a simpler implementation is proposed and analyzed in this paper.

The three classes of methods identified above cover most FE-ELMs currently available. A fourth and important class, however, is constituted by the "Eulerian-Lagrangian Localized Adjoint methods" (ELLAMs). The term ELLAM has evolved from the research of Russel, Herrera, Celia, and co-workers [*Russell,* 1989, *Celia, et al.,* 1990, *Zisman,* 1990], although methods with similar characteristics were introduced earlier [*Varoglu and Finn, 1982, Hauguel,* 1985]. Loosely speaking, ELLAMs are FE-ELMs where the weighting functions are defined in the space-time domain, and are formally chosen to represent or approximate a solution of the homogeneous adjoint equation.

ELLAMs provide a nicely formal approach to the treatment of boundary conditions, and enforce global mass conservation for constant coefficients [*Celia, et al.*,1990, *Russell,* 1989]. Maybe more importantly, ELLAMs provide a general framework from which to interpret other classes of FE-ELMs. In particular, we will show later that, for constant coefficients, ELLAMs revert in the interior of the domain to specific forms of either quadrature ELMs or piecewise ELMs, depending upon whether numerical or exact integration is chosen.

Selected methods

In this section, we first present two alternative generic ELM formulations: Galerkin ELMs and ELLAMs. We then show how one or both generic formulations can be customized to obtain the five specific ELMs chosen for detailed comparison in this paper. These five ELMs cover the range of interpolation and (piecewise or quadrature) integration methods introduced in the previous section.

Generic formulations

Galerkin formulation

The Lagrangian form of the transport equation is discretized in time as (Figure 2.1(b)):

$$\frac{c^{n+1}-c^{\xi}}{\Delta t}-\alpha D\frac{\partial^2 c}{\partial x^2}\bigg|_{n+1}-(1-\alpha)D\frac{\partial^2 c}{\partial x^2}\bigg|_{\xi}=0 \tag{2.7}$$

where α is the time discretization weight.

Standard application of a weak Galerkin weighted residual finite element formulation leads to:

$$\sum_{k=1}^{N_{elems}}\{\frac{1}{\Delta t}(\Psi_{kj}^{n+1}-\Psi_{kj}^{\xi})+D[\alpha\Phi_{kj}^{n+1}+(1-\alpha)\Phi_{kj}^{\xi}]\}+BT=0 \tag{2.8}$$

with:

$$\Psi_{kj}^{m}=\int_{\Omega_k}c^{m}\phi_j dx \qquad \Phi_{kj}^{m}=\int_{\Omega_k}\frac{\partial c}{\partial x}\bigg|^{m}\frac{\partial\phi_j}{\partial x}dx \tag{2.9}$$

or, in local coordinates:

$$\Psi_{kj}^{m}=\frac{\Delta x}{2}\int_{-1}^{1}c^{m}\phi_j dr \qquad \Phi_{kj}^{m}=\frac{2}{\Delta x}\int_{-1}^{1}\frac{\partial c}{\partial r}\bigg|^{m}\frac{\partial\phi_j}{\partial r}dr \tag{2.10}$$

where ϕ_j are weighting functions that coincide, on an elemental basis, with the shape functions. The boundary terms (*BT*) are:

$$BT=\left[-D\alpha\phi_k\frac{\partial c}{\partial x}\bigg|^{n+1}-D(1-\alpha)\phi_k\frac{\partial c}{\partial x}\bigg|^{\xi}\right]_{\Gamma} \tag{2.11}$$

where Γ represents the inflow and outflow boundaries.

At this stage, choices need to be made regarding (a) the location of the heads of the characteristic lines, (b) the strategy for interpolation of concentrations and concentration derivatives at ξ, and (c) the strategy for evaluation of integrals at time n. Most choices will lead to finite-difference analogs of the generic form:

$$\sum_{j=l_1}^{l_2} L_j c\,(i+j, n+1) = \sum_{j=r_1}^{r_2} H_j c\,(i-K+j, n) \tag{2.12}$$

where L_j and H_j are the coefficients associated with the concentration at time n+1 and node i+j, and the concentration at time n and node i-K+j, respectively. K is defined in Table 2.1. for all methods. The pointers l_1, l_2, r_1 and r_2 specify the nodes involved in the contribution of element i to the weighted residual statement.

Localized Adjoint formulation

By contrast with the previous formulation, ELLAMs start with the Eulerian form of the transport equation:

$$L(c) = \frac{\partial c}{\partial t} + u\frac{\partial c}{\partial x} - D\frac{\partial^2 c}{\partial x^2} = 0 \tag{2.13}$$

A time-space finite element technique is used, the weighted residual statement being defined as:

$$\int_{t^n}^{t^{n+1}} \int_{\Omega} wL(c)\,dxdt = 0 \tag{2.14}$$

The weighting function w is defined by setting the adjoint operator associated with L to zero in each element, i.e.:

$$L^{\Psi} = -\frac{\partial w}{\partial t} - u\frac{\partial w}{\partial x} - D\frac{\partial^2 w}{\partial x^2} = 0 \tag{2.15}$$

The adjoint operator L^{Ψ} associated with the operator L is formally defined as:

$$\int L(c)\, w dx = \int L^{\Psi}(w)\, c dx + Boundary\ \ terms \tag{2.16}$$

which follows from the basic rule of integration by parts in 1D.

Equation (2.15) has several solutions. By choosing to set the problem as:

$$\begin{cases} \dfrac{\partial w}{\partial t} + u\dfrac{\partial w}{\partial x} = 0 \\ D\dfrac{\partial^2 w}{\partial x^2} = 0 \end{cases} \tag{2.17}$$

the concept of characteristic lines becomes linked to the definition of the weighting function (Figure 2.3(a)).

The weak form of Equation (2.14) leads to:

$$\sum_{k=1}^{N_{elems}} \{\Psi_{kj}^{n+1} - \Psi_{kj}^{\xi} + \Phi_{kj} - \delta_{kj}\} + BT = 0 \tag{2.18}$$

with:

$$\Psi_{kj}^{m} = \int_{\Omega_k} c^m w_j dx \tag{2.19}$$

$$\Phi_{kj} = \int_{t^n}^{t^{n+1}} \int_{\Omega_k} D\frac{\partial c}{\partial x}\frac{\partial w_j}{\partial x} dx dt \tag{2.20}$$

$$\delta_{kj} = \int_{t^n}^{t^{n+1}} \int_{\Omega_k} c\,(\frac{\partial w_j}{\partial t} + u\frac{\partial w_j}{\partial x})\, dx dt \tag{2.21}$$

and

$$BT = \int_{t^n}^{t^{n+1}} \left[w_j (uc - D\frac{\partial c}{\partial x}) \right]_{\Gamma} dt \tag{2.22}$$

where Γ represents the inflow and outflow boundaries.

The integral in Equation (2.21) vanishes due to Equation (2.17) (note: this condition may not be strictly true if there are errors in the tracking of the characteristic lines). If the chain rule is applied again to Equation (2.20) and an α-method is selected to approximate the time integration [*Russell*, 1989][2], then Equation (2.18) can be re-written as:

$$\sum_{k=1}^{N_{elems}} \{ \Psi_{kj}^{n+1} - \Psi_{kj}^{\xi} + \Delta t \alpha \Phi_{kj}^{n+1} + \Delta t (1-\alpha) \Phi_{kj}^{\xi} \} + BT = 0 \tag{2.23}$$

with:

$$\Phi_{kj}^{m} = \int_{\Omega_k} D \frac{\partial c}{\partial x} \Big|^{m} \frac{\partial w_j}{\partial x} dx dt \tag{2.24}$$

The comparison of Equations (2.8) and (2.23) shows that, except for the boundary elements, the two generic formulations - ELLAMs and Galerkin ELMs - differ only on the definition of the weighting functions ϕ and w. Since w is constant in time along the characteristic lines, it is enough to select the same weighting function in space for the methods to coincide (for constant coefficients only). For instance, the chapeau function can be used for Galerkin ELMs, and the "chapeau function along the characteristics" [*Celia, et al.*, 1990] for ELLAMs (Figure 2.3).

Specific formulations

Interpolation methods

In this class of ELMs the nodes at time n+1 are tracked backwards, and the concentration and its first derivative at the feet of the characteristic lines are obtained by interpolation with polynomial functions. The interpolated values are then assigned to shape functions that define the initial conditions for the diffusion equation.

---

2. For an alternative approach to the time integration, see *Celia, et al.* [1990]

Two interpolation methods were selected from those analyzed by *Baptista*, 1987. The first method (2P-LI2 in the notation of *Baptista* [1987]) uses information only from the nodes of the element that contains the foot of the characteristic line (compact interpolator). The second method (4P-LR2 in the notation of *Baptista* [1987]) also uses the 2 adjacent nodes (non-compact interpolator). Both methods enforce inter-element continuity but not first derivative continuity (class C^0), and use linear core elements (element that contains the foot of the relevant characteristic line). The 2P-LI2 was selected due to its simplicity and potential low cost, although it presents considerable numerical diffusion. The 4P-LR2 was selected for its accuracy, which bears some overall similarities to the accuracy of a widely used method, the compact interpolator of class C^0 with quadratic elements - 3P-LI3 [*Baptista, et al.*, 1984]. The direct use of the 3P-LI3 in this paper would have been inconvenient, because its propagation errors are different for the corner and the middle nodes, which results in time-dependent errors; the use of linear core elements in the 4P-LR2 guarantees time-independent propagation errors.

The concentration at the feet of characteristic line is defined by a different set of interpolation functions for each interpolation method. The interpolation functions for the 2P-LI2 are linear Lagrangian polynomials, defined by the concentration of the nodes of the core element. Cubic polynomials, defined by concentrations both at the nodes of the core element and the 2 adjacent nodes, are the interpolation functions for the 4P-LR2.

The concentration after the interpolation step for both methods, for a generic position over the element, is defined by linear Lagrangian polynomials:

$$c^{\xi} = \sum_{i=1}^{2} \phi_i c_i^{\xi} \tag{2.25}$$

where c_i^{ξ} is the concentration at the feet of characteristic line of node i and ϕ_i are the shape functions:

$$\begin{cases} \phi_1 = \frac{1}{2}(1-r) \\ \phi_2 = \frac{1}{2}(1+r) \end{cases} \qquad r \in [-1, 1] \tag{2.26}$$

The interpolation methods can be applied either in a Galerkin-ELM or an ELLAM framework. In the first case, the initial conditions for the diffusion step (Equation (2.25)) are defined over the element at time $n+1$. For the ELLAM approach, the concentration after advection does not need to be transported along the characteristic lines since the weighting functions are defined at time n (Figure 2.3). For constant coefficients, the interpolation Galerkin-ELMs coincide with the interpolation ELLAMs.

The finite difference analogs for the 2P-LI2 and the 4P-LR2 are presented in Table 2.1..

Piecewise Integration methods

These methods are based on the exact evaluation of the integrals at the feet of the characteristic lines. In a Galerkin-ELM framework, this is accomplished through the backward tracking of the nodes, followed by the forward tracking of the nodes and other notable points found between two consecutive feet of characteristic lines [*Yeh, et al.*, 1992]. As a consequence, the initial conditions for the diffusion equation have discontinuous first derivative in each element. In order to evaluate the integrals exactly, either numerically or analytically, elements are split in pieces where the first derivative is continuous.

In the original piecewise integration method, proposed by *Yeh, et al.*, 1992, the concentration at the forward-tracked points is corrected by adding a compensation factor, after the solution of the diffusion equation. This compensation factor is a function of the difference between the concentrations before and after the diffusion step, at the nodes of the element that contains the notable point. This way, the final concentration in an element becomes a piecewise function, defined by the nodes and by the forward-tracked points (notable points). This technique is theoretically very attractive, but may lead to very high

computational costs for practical applications. The number of notable points necessary to define the concentration inside one element will increase rapidly with time, and so will the computational cost.

We propose a simpler implementation of the piecewise integration concept (pi-ELM), which provides a time-step independent cost. The concept of notable points is eliminated and the initial conditions for the diffusion equation are solely defined by the concentration at the backward and forward nodes (Figure 2.2(c)). For a constant velocity problem, since only one node is found between two consecutive feet of characteristic lines, the concentration after advection is defined as (in local coordinates):

$$c^{\xi}(r) = \begin{cases} \dfrac{c_{int}-c_1}{r_{int}+1}r + c_1 + \dfrac{c_{int}-c_1}{r_{int}+1}, & r \in [-1, r_{int}] \\ \dfrac{c_{int}-c_2}{r_{int}-1}r + c_2 - \dfrac{c_{int}-c_2}{r_{int}-1}, & r \in [r_{int}, 1] \end{cases} \tag{2.27}$$

where c_1 and c_2 are the concentrations at the feet of characteristic lines of the back-tracked nodes and c_{int} and r_{int} are, respectively, the concentration and location at time n+1 of the forward-tracked node.

The concentration corrections after the diffusion equation are also eliminated, the final concentration in an element being solely defined by polynomial shape functions supported by the concentrations at the nodes.

In an ELLAM framework, the piecewise integration method does not require the forward tracking of the nodes found between two consecutive feet of characteristic lines, since the weight function is defined at time n. Therefore, fewer characteristic lines need to be tracked, and an ELLAM implementation of the piecewise integration may be less expensive than its Galerkin ELM counterpart. For constant coefficients, the piecewise integration concept applied to each framework - Galerkin ELM or ELLAM - leads to the same finite difference analog (Table 2.1.).

Quadrature methods

The quadrature methods (qu-ELMs) propose the evaluation of the integrals at the feet of characteristic lines through numerical integration [*Russell*, 1985, *Hasbani, et al.*, 1983].

In a Galerkin ELM framework, quadrature points, rather than nodes, are back-tracked from n+1 to n. Once the concentration and its first derivative at the feet of the characteristic lines of the quadrature points are interpolated, the evaluation of the integrals at time n becomes trivial:

$$\Phi_{kj}^{\xi} = \int_{\Omega_k} (1-\alpha) D \frac{\partial \phi_j}{\partial r} \frac{\partial c}{\partial r}\Big|^{\xi} dr = (1-\alpha) D \sum_{i=1}^{nqp} w_i \frac{\partial c_i}{\partial r} \frac{\partial \phi_j}{\partial r}(r_i)$$
$$\Psi_{kj}^{\xi} = \int_{\Omega_k} \phi_j \frac{c^{\xi}}{\Delta t} dr = \frac{1}{\Delta t} \sum_{i=1}^{nqp} w_i c_i^{\xi} \phi_j(r_i) \tag{2.28}$$

where c_i^{ξ} and $\partial c_i/\partial r$ are the concentration and its first derivative at the feet of the characteristic line for quadrature point i, r_i and w_i are the location (at time n+1) and weight of point i, $\phi_j(r_i)$ is the value of the weight function at quadrature point i and nqp is the number of quadrature points.

In this paper, we selected two quadrature integration methods - Gauss and Lobatto quadrature [*Hasbani, et al.*, 1983, *Russell*, 1985]. For n quadrature points, the Gauss approach leads to the highest order of integration: indeed, the Lobatto quadrature integrates exactly polynomials of order up to $2n$-3, while Gauss quadrature can integrate exactly polynomials of order $2n$-1. The Lobatto method minimizes the number of tracking operations. The finite difference analog for a generic quadrature method is presented in Table 2.1..

As opposed to the previous methods, the "numerical integration" concept presented for Galerkin ELMs cannot be implemented in an ELLAM framework, since the element at time n is defined by the characteristic lines of the nodes. However, a numerical

integration can be used to evaluate the integrals, through the definition of quadrature points between the feet of the characteristic lines of the nodes (element at time n). The concentration at these quadrature points is interpolated, rather than the concentration at the feet of the characteristic lines of the nodes. The evaluation of the integrals is still straightforward, and the computational cost of the method can be smaller than for the quadrature Galerkin-ELM, since the number of characteristic lines to be tracked can be smaller.

For constant coefficients, the quadrature Galerkin-ELMs coincide with ELLAMs with numerical integration.

Formal analysis

The accuracy and stability of the methods are characterized through the analysis of propagation and truncation errors. Fourier analysis is used to study the influence of both the Courant number and the dimensionless wavelength on these numerical properties, for specific diffusion numbers. A truncation error analysis completes the previous study, by examining the influence of the diffusion number and the Courant number.

Fourier analysis

Methodology

The exact solution of the advection-diffusion equation can be written as a summation of Fourier components:

$$c(x,t) = \sum_{m=-\infty}^{+\infty} c_m(x,t) \tag{2.29}$$

with:

$$c_m(x,t) = A_m^n exp\{I\frac{2\pi}{L_m}(x-ut)\} \tag{2.30}$$

where $I = \sqrt{-1}$, A_m^n are problem-related coefficients and L_m is the wavelength of the m^{th} Fourier component.

In an uniform space-time grid, c_m becomes:

$$c_m(i,n) = A_m^n exp\left(I\lambda_m(i-n\beta)\right) \tag{2.31}$$

where λ_m is the dimensionless wavenumber and β is the Courant number:

$$\lambda_m = \frac{2\pi\Delta x}{L_m} \qquad \beta = \frac{u\Delta t}{\Delta x} \tag{2.32}$$

and:

$$i = \frac{x}{\Delta x} \qquad n = \frac{t}{\Delta t} \tag{2.33}$$

The error introduced by a numerical solution (G_m) can be defined as:

$$G_m = \frac{\tilde{c}_m(i,n+1)}{c_m(i,n)} exp\left(\beta\lambda_m I\right) \tag{2.34}$$

where $\tilde{c}_m(i,n+1)$ is the concentration given by the numerical algorithm.

The numerical concentration associated with the generic finite difference analogs (Equation (2.12)) can be described as:

$$\tilde{c}_m(i,n+1) = P\sum_{j=r_1}^{r_2} H_j c(i-K+j,n) \tag{2.35}$$

with P defined as:

$$P = \left[\frac{4}{6} + 2\alpha D + 2\left(\frac{1}{6} - \alpha D\right)\cos\lambda_m\right]^{-1} \tag{2.36}$$

where D is the diffusion number ($D = D\frac{\Delta t}{\Delta x^2}$).

By substituting Equations (2.31) and (2.35) into Equation (2.34), amplification factors and phase errors are defined as:

$$|G_m| = \mu\sqrt{(Re^2(G_m) + Imag^2(G_m))} \tag{2.37}$$

$$arg(G_m) = arctg\left(\frac{Imag(G_m)}{Re(G_m)}\right) \tag{2.38}$$

with:

$$\begin{aligned} Re(G_m) &= P\sum_{j=r_1}^{r_2} H_j \cos((\beta - K + j)\lambda_m) \\ Imag(G_m) &= P\sum_{j=r_1}^{r_2} H_j \sin((\beta - K + j)\lambda_m) \end{aligned} \tag{2.39}$$

and the physical diffusion of the exact solution (μ) defined as [*Baptista*, 1986]:

$$\mu = \frac{A_m^n}{A_m^{n+1}} = exp(D\lambda_m^2) \tag{2.40}$$

The stability condition is:

$$|G_m| < exp(D\lambda_m^2) \tag{2.41}$$

which reduces, for pure advection, to the more familiar form:

$$|G_m| < 1 \tag{2.42}$$

Since all methods have linear core elements, the propagation error is time-independent [*Baptista*, 1987]. Therefore, it is enough to compare the errors after a single time step.

Analysis of propagation errors

In this section we study the accuracy and stability of the methods through the analysis of the amplification factors and phase errors per time step as functions of the Courant number, diffusion number and dimensionless wavelength ($L_m/\Delta x$).

We selected two cases with diffusion numbers ($\boldsymbol{D}$) of 0 and 0.01 respectively. For both cases, propagation errors were analyzed for a range of Courant numbers (β) from 0 to 1, and dimensionless wavelength from 2 to 34. The values of β were limited to 1 because the errors per time step in ELMs with linear core elements are only dependent on the fractional part of β (Figure 2.4). The amplification factors are presented in Figs. 2.5-2.11 ($\boldsymbol{D}$ = 0) and in Figs. 2.12-2.14 ($\boldsymbol{D}$ = 0.01). Phase errors for $\boldsymbol{D}$ = 0 are plotted in Figs. 2.15-2.19.

Our discussion of propagation errors will focus first on stability, and then on accuracy. While the analysis of stability is based on the amplification factors only, both amplification factors and phase errors are necessary to characterize accuracy.

Amplification factors for pure advection show that the pi-ELM, the 2P-LI2 and the 4P-LR2 are unconditionally stable (Figs. 2.5, 2.10 and 2.11); however, the qu-ELM with 3 and 6 points is unstable for some ranges of β, for both Gauss and Lobatto quadratures (Figs. 2.6-2.9). Figs. 2.6-2.9 suggest that the number of instability regions is related to the number of quadrature points. To further investigate this hypothesis, the amplification factor was plotted against the Courant number for a wider range of quadrature points and, for both types of quadrature, for a specific dimensionless wavelength (Figure 2.20). Figs. 2.20(a) and 2.20(b) indicate that the number of quadrature points generally corresponds to the number of maxima. For the Gauss quadrature, it also corresponds to the number of instability zones. We will formally quantify the relationship between the number and location of the quadrature points and the number and location of the instability zones later in the context of the truncation errors analysis.

The instability of the qu-ELM can be eliminated by introducing a small amount of diffusion, which depends both on the type and number of quadrature points used. Since the

maxima and minima of the amplification factors decrease as the number of quadrature points increases (Figs. 2.6-2.9, Figure 2.20), so does the amount of diffusion necessary to guarantee stability. This is illustrated in Figs. 2.12 and 2.13, where a diffusion number of 0.01 is enough to stabilize the qu-ELM with 4 Gauss points, but not the qu-ELM with 3 Gauss points. The use of a specific type of quadrature also determines the D required for stability, as shown in Figs. 2.12 and 2.14. For the same number of quadrature points, the stability of the qu-ELM requires a larger value of D for the Lobatto than for the Gauss quadrature. The diffusion number necessary to stabilize the qu-ELM for both Gauss and Lobatto points, for a wide range of quadrature points, will be evaluated in the truncation error section.

The accuracy analysis of a method usually requires the study of both amplification and phase errors. However, earlier work [*Baptista*, 1987] showed that the amplification factors are dominant over the phase errors for ELMs with linear core element and centered interpolators (i.e., when the core element is centered within the region that defines the interpolator). Figs. 2.15-2.19 confirm that phase errors are very small for all methods.

In order to illustrate the relative importance of amplification and phase errors, a Gauss hill problem is simulated (Figure 2.21). The frequency, amplitude and phase of each Fourier component that defines the initial conditions for the Gauss hill were evaluated through Fourier decomposition. Each of these components was then propagated, and the concentration field after 100 time steps was evaluated through harmonic synthesis of the concentrations of each component. Amplification factors and/or phase errors were applied to each of these Fourier components, thus defining solutions with amplification and/or phase errors. The dominance of amplification factors over phase errors for the integration ELMs is shown in Figure 2.21: the numerical solution without amplification factors almost coincides with the exact solution, while the numerical solution without phase errors is indistinguishable from the complete solution. Therefore, our comparative analysis of the accuracy of the methods can be done on the basis of amplification factors alone.

In order to make the comparison between methods easier, we plotted the amplification factor against β, for all methods, for $L_m/\Delta x = 15$ and $D = 0$ (Figure 2.22). The pi-ELM shows a very small error for the entire range of β. For all other methods, the amplification factor depends strongly on β, although in distinct ways. For the 2P-LI2 and 4P-LR2, this error has a single minimum at $\beta = 0.5$; for the qu-ELM, the dependence of the error on β is related to the number and type (Gauss, Lobatto) of quadrature points. For instance, a small number of points (3) can lead to errors as large as the 4P-LR2's, or as small as the pi-ELM's (Figure 2.22(a)).

The comparison between the accuracy of qu-ELMs with different types of quadrature points can be based on several criteria. Two criteria were selected: identical number of points and identical number of tracked points per element. Note that, since the extreme Lobatto points coincide with the nodes, only m-1 points are back-tracked, for a m quadrature points run. For the first criterion (Figs. 2.20 and 2.22), the use of Gauss points leads to more accurate results than the qu-ELM with Lobatto points. The second criterion is inconclusive: while the 3 Gauss points method is less diffusive than the 4 Lobatto points, the 4 Gauss points has larger amplification factor than the 5 Lobatto points (Figure 2.22(b)).

In order to compare the methods in a β-independent perspective, we averaged the amplification factors over the entire range of the Courant number. The mean amplification factors and the mean plus and minus the standard deviation of the amplification factors are presented in Figure 2.23. It is important to include the standard deviation, since a large standard deviation may lead to a wiggly behavior [*Baptista* 1987]. If the amplification factor depends strongly on β, consecutive nodes may have very different errors. This can lead to the generation of spurious oscillations that would give rise to both accuracy and stability problems.

Figure 2.23(a) shows that the mean amplification factors are similar and close to 1, for both the qu-ELM with 6 Gauss points and the pi-ELM. The qu-ELM with 3 quadrature points is unstable for most values of $L_m/\Delta x$: while amplification factors for 3 Lobatto

points are well above 1, the use of 3 Gauss points leads only to a very mild instability, with amplification factors very close to 1.

Figs. 2.23(b) and 2.23(c) show that the qu-ELM has a considerably larger standard deviation than the pi-ELM's. The standard deviation increases as the number of quadrature points decreases and it is larger for Lobatto than for Gauss points. Therefore, unless a large number of quadrature points is used, the accuracy of the qu-ELM is more sensitive to non-constant flow fields. On the other hand, as all upper limiting curves (mean plus standard deviation) for the qu-ELM are above 1, for $L_m/\Delta x$ larger than 4, the method will probably be unstable even under a non-constant velocity field (where the effect of unstable Courant numbers can be compensated). Thus, the performance of the pi-ELM in a real case is expected to be better than the qu-ELM's, for the same conditions.

Both interpolation methods present mean amplification factors indicating larger numerical damping than the integration methods (Figure 2.23(a)). The standard deviation for the 4P-LR2 is very small, but it is considerably large for the 2P-LI2 (Figure 2.23(c)). However this large standard deviation will not lead to the problems stated above, because the 2P-LI2 is extremely dissipative (Figure 2.23(a)).

The Fourier analysis showed that the pi-ELM is the only integration method that provides both unconditional stability and a considerable accuracy improvement over the interpolation methods. The qu-ELM can be also more accurate than the interpolation methods (for a large number of points), but is only conditionally stable. This analysis showed that the qu-ELM's instability can be eliminated by a small amount of diffusion.

Truncation error analysis

Methodology

If each term of its finite differences analog is expanded in Taylor series, a generic numerical approximation of the 1D transport equation becomes:

$$\frac{\partial c}{\partial t} + (u+\eta)\frac{\partial c}{\partial x} - (D+\tau)\frac{\partial^2 c}{\partial x^2} + higher\ \ order\ \ terms\ =\ 0 \qquad (2.43)$$

where η and τ represent the phase error and numerical diffusion associated with the lowest order derivatives.

In order to analyze the influence of the dimensionless numbers on the accuracy and stability of the methods, it is convenient to define the *effective diffusion number* (Υ), associated with the second derivative of concentration:

$$\Upsilon(\beta, \boldsymbol{D}) \ =\ \frac{\Delta t}{\Delta x^2}(D+\tau) \qquad (2.44)$$

where $\boldsymbol{D}$ is the diffusion number. A method will be stable for positive values of Υ, and unstable otherwise. The expressions for Υ, for each method, are presented in Table 2.2.

In the following section, we will compare the effective diffusion number, for the pi-ELM, qu-ELM and 2P-LI2. As the truncation error for the 4P-LR2 is independent of the second derivative of concentration, this method will not be analyzed.

Comparative analysis of effective diffusion

The effective diffusion number was plotted for a range of β from 0 to 1 and $\boldsymbol{D}$ from 0 to 0.1 (Figs. 2.24-2.29). In order to study the importance of both the number and type of quadrature points in further detail, Υ was plotted against β, for $\boldsymbol{D} = 0$, for 3 and 6 quadrature points, using both Gauss and Lobatto quadratures (Figure 2.30).

Figs. 2.24-2.29 confirm both the unconditional stability of the pi-ELM and 2P-LI2, and the conditional stability of the qu-ELM. As suggested by the Fourier analysis, the number of quadrature points is related to the number of instability zones. Figure 2.30 shows that the number of local minima in Υ is equal to the number of quadrature points. It also shows that the first derivative of Υ is continuous everywhere, except at the local minima. Since an instability region must include a minimum of Υ, the definition of a first

derivative discontinuity will identify a *potentially* unstable region. By examining the Υ expression for the qu-ELM (Table 2.2), one easily recognizes that these discontinuities are generated by the sub-function of Υ that identifies the element which contains the foot of the characteristic line of each quadrature point:

$$K_i = int(\beta - \frac{r_i}{2} - \frac{1}{2}) + 1 \tag{2.45}$$

where r_i is the location of the quadrature point i. Thus, the first derivative of Υ has a discontinuity when K is increased by one. The correspondent Courant number is given by:

$$fractional(\beta_i - \frac{r_i}{2} - 0.5) = 0 \quad \Rightarrow \quad \beta_i = \frac{r_i}{2} + 0.5 + n \quad (\forall n \in \mathrm{N}) \tag{2.46}$$

Equation (2.46) shows that a minimum in Υ will occur when the foot of the characteristic line of any quadrature point coincides with a node (Figure 2.31).

Each type of quadrature will lead to a different relationship between the number of unstable zones and the number of minima (and quadrature points). The extreme Lobatto points that coincide with the grid nodes identify the integer Courant numbers only as minima, not as unstable zones (Figure 2.30). Since ELMs are exact for integer Courant numbers [*Baptista*, 1987], the Lobatto quadrature will have m-2 unstable zones, for m quadrature points. As the location of all Gauss points falls in the interior of each element, the number of unstable zones coincides with the number of minima and with the number of quadrature points (Figure 2.30).

Figs. 2.25-2.28 show that the conditional stability of the qu-ELMs can be eliminated by a very small amount of diffusion. The minimum diffusion number that leads to a positive effective diffusion is plotted against the number of quadrature points, for both types of quadrature, in Figure 2.32. This figure shows that D decreases as the number of quadrature points increases for both types of quadrature points. For the same number of points, the minimum D is smaller for Gauss than for Lobatto quadrature points. The identical number of tracked points per element criterion does not provide any conclusion, since

the type of quadrature that requires smaller minimum ***D*** depends on the number of points selected.

Regardless of the type and number of quadrature points, the amount of diffusion to stabilize the qu-ELM is considerably smaller than the dispersion coefficients currently used in numerical simulations. To illustrate this point, consider a spatial discretization of 100 m, a Δt of 1800 s and a diffusion number of 0.02, which is enough to stabilize the qu-ELM with 3 or more Gauss points and 4 or more Lobatto points. This will lead to a diffusion coefficient of 0.11 m^2/s, which is well below the dispersion coefficients used in most simulations.

The truncation error analysis confirmed the conditional stability of the qu-ELM and established the relationship between the number and location of the quadrature points and the number and location of unstable zones. It also showed that the conditional stability of the qu-ELM can be eliminated with a very small amount of diffusion, that usually exists in real systems.

Numerical Tests

This section provides a complementary analysis of the properties of the integration methods. It is divided in two main parts. In the first part, the performance of the integration methods is analyzed for a set of tests extracted from the Convection-Diffusion (CD) forum [*Baptista, et al.*, 1986, *Adams, et al.*, 1993]. Tests from this benchmark were selected for two reasons. First, the CD forum problems were specially designed to characterize the properties of numerical techniques for the solution of the transport equation; therefore they provide a good testing to the integration methods. Secondly, as the CD forum tests are part of a reference framework in which many numerical techniques were studied, they provide grounds for comparison with other methods that were not included in this paper.

In the second part, we extend the previous experimentation, by examining the influence of three parameters - Courant number, diffusion coefficient and dimensionless source length - on the performance of the integration methods. Two error measures were selected among those presented by *Baptista, et al.*, 1984: the Integral Measure of Global Mass conservation and the Discrete L2-norm, normalized by the total mass (Table 2.3).

We are aware that the study of mass conservation proposed here is rather incomplete, since the major sources of mass imbalances - tracking errors and flow mass imbalances - cannot be included in our constant coefficients study. Nevertheless, these simple tests allow for a first characterization of the mass properties of the integration methods, which had not been done.

As in the formal analysis, the compact and the non-compact interpolators will be used as references, throughout this numerical experimentation.

The initial conditions for all tests are defined on a nodal basis, i.e., the initial concentration is defined as a piecewise linear function.

Convection-Diffusion forum

Two 1D problems were proposed in the CD forum: the first problem concerns the transport of a Gauss hill subject to advection and diffusion, under an uniform flow. In the second problem, the concentration field is imposed by a constant mass flux, specified through the upstream concentration (advancing front).

We selected some representative cases from both problems. The parameters for these cases are presented in Table 2.4, and the boundary and initial conditions are specified in Table 2.5. The plots of concentration for the Gauss hill, at time 9600 s, are presented in Figs. 2.33-2.35. For the advancing front, the concentration plots are shown in Figs. 2.36-2.39.

Several important features arise from the concentration plots for the Gauss hill problem. Figs. 2.33-2.35 show that pi-ELM provides very accurate solutions, with the peaks being much better preserved than in the reference solutions. The increase of the fractional part of β, from 0.24 (Figure 2.33) to 0.48 (Figure 2.35) does not bring major differences in this method's performance, as the above formal analysis had already shown. In contrast, the qu-ELM's performance changes dramatically with β: the 3-Gauss points presents either a stable and reasonably accurate solution (Figure 2.33) or an unstable behavior (Figure 2.35). Both runs confirm the β-dependent behavior of the qu-ELM, discussed in the previous sections.

The increase of diffusion (Figure 2.34) leads to a considerable increase of accuracy for all methods, although the 2P-LI2 still presents a large damping. This increase of accuracy is achieved through an increase of peak preservation for all methods, and an elimination of the regions of negative concentrations for the pi-ELM, the qu-ELM and the 4P-LR2.

The advancing front problem tests the ability of the methods to handle poorly discretized concentration gradients. As in the previous problem, the pi-ELM and the qu-ELM provide accurate solutions (Figs. 2.36-2.39). However, they show some sensitivity to the sharp slopes (Figure 2.36), by presenting artificial oscillations that are not present in the reference solutions. These oscillations have larger amplitude for the pi-ELM than for the qu-ELMs, but they lead to the qu-ELM's instability when the fractional part of β reaches one of the unstable zones previously defined in the formal analysis (Figure 2.39).

The small amount of diffusion introduced in test 3B allows for the reduction of the artificial oscillations of the integration methods, and it improves considerably the performance of all methods (Figure 2.37). Figure 2.38 shows that the performance of all methods is further improved by a much larger value of D, in the range of low Peclet numbers (Pe=2).

In order to illustrate the differences between the pi-ELM and the original algorithm proposed by Yeh, we present the concentrations for Problem 3A for Yeh's method, extracted from *Yeh, et al.*, 1992 (Figure 2.40). The comparison between Figure 2.40 and Figure 2.36 shows that Yeh's method does not present any artificial oscillations, being more accurate than the pi-ELM. However, this increase of accuracy is achieved through the introduction of a large number of notable points.

The Convection-Diffusion test cases demonstrated the excellent performance of the pi-ELM as well as the conditional stability of the qu-ELM.

Analysis of the influence of selected parameters

Courant number

In this section, we examine the stability and overall accuracy of the integration FE-ELMs as a function of the Courant number.

Since the formal analysis showed that the accuracy of the methods per time step is independent of the integer part of β, our tests concentrate on the influence of the fractional part of β only. The advancing front case from the CD forum, was selected for these tests because it was the most stringent in the previous analysis. The integer part of β was set to 2 and several fractional parts were obtained by varying the velocity. All other parameters were extracted from the CD forum problem 3A (Table 2.4). Figure 2.41 shows the L2-norm and the mass ratio against the Courant number.

The accuracy and stability patterns defined in the previous formal analysis are clearly shown in Figure 2.41. Figure 2.41(a) confirms both the excellent performance of the pi-ELM and the large damping of the 2P-LI2, for all values of β. This is in sharp contrast with the qu-ELM's performance, which is strongly dependent on β. It can either be as accurate as the pi-ELM (Figure 2.41(b)) or be unstable (Figure 2.41(a)). The unstable runs, that can be identified by the extremely large values of the L2-norm, occur in the ranges of β predicted by the Fourier analysis: Courant numbers of 2.11, 2.51 and 2.91 fall

in the instability zones of the 3 Gauss points, as a β of 2.51 falls in the 3 Lobatto points's instability zone (Figure 2.20).

The above results show that the comparative study of the methods could hardly have been supported by numerical experimentation alone. The numerical experimentation can only simulate specific cases; therefore the global behavior of the methods with a strong dependance on one parameter cannot be well understood. Since the study of a method is traditionally based on a few tests only, an incorrect evaluation of the performance of the qu-ELM could result from an analysis based only on numerical experimentation.

The formal analysis is a very useful tool to fully understand the behavior of the methods and to compare them in an unbiased form. It identified the dependency of the formal properties of the integration methods on β in a complete way, allowing us to select representative cases for the numerical experimentation.

In contrast with the L2-norm results, the ability to preserve mass is similar for all methods and presents a strong dependency on the fractional part of β (Figure 2.41(c)). The relative mass errors after the 100 time steps vary for all methods from a minimum of 0.01%, up to a common maximum of 0.3 to 0.5%.

Although these mass errors are not excessive, they are still higher than would be expected for very simple tests. They may be the result of under-discretized high frequencies, which are generated by the steep gradients of the advancing front problem. The energy associated with these Fourier components is then folded to the zero-frequency [*Baptista*, 1987]. We were not able to identify these errors in the Fourier analysis, since the amplification factors for the zero-frequency component are very close to one.

Even though these results suggest that all methods preserve mass relatively well, it must be noted that there are major sources of mass conservation failure that are not present in the simple tests performed here. In a non-constant velocity field, both the failure to pre-

serve mass in the flow model and the errors in the evaluation of the characteristic lines may lead to considerable mass conservation errors.

We have shown that a comparative performance of the methods cannot be made for a specific β, due to the qu-ELM's strong dependence on this parameter. Therefore, the following sections must be regarded, not in a comparative sense, but as an evaluation of each method's characteristics.

Diffusion coefficient

Diffusion smooths gradients of concentration, and, therefore, should improve the accuracy of the methods. However, it also introduces additional errors that are associated with time and space discretization of the diffusion equation [*Baptista*, 1987]. The influence of the time step is especially important, since the errors associated with the advective step decrease when the time step decreases while the errors due to diffusion increase with the time step.

Earlier studies of interpolation ELMs [*Baptista*, 1987] showed that these two different types of errors lead to an optimal time step that depends on several parameters. The integration methods present a similar behavior, which is illustrated in Figure 2.42. The L2-norm is presented against the time step, for a Peclet number of 1, for both integration and interpolation methods. This figure shows the integration methods lead to smaller optimal time steps, and to an increase of the accuracy.

In this section, we study the influence of the diffusion in the properties of the integration ELMs for a range of Peclet numbers from infinite to 2, and for a constant time step of 96 s.

The analysis is done for a Gauss hill problem, borrowing the parameters from CD forum test 1A (Table 2.4), and for an advancing front, starting with the parameters from

test 3A (Table 2.4). Several diffusion coefficients were selected in a range from 0 to 50 m^2/s.

Since we want to study the effect of diffusion, the choice of the time discretization weight (α) may condition the performance of the methods. A sensitivity analysis of α was performed for the pi-ELM and the qu-ELM (3 Gauss points). The amplification factor was plotted against the Courant number (Figure 2.43), for $\alpha = 0.0$, 0.5 and 1.0, for $\boldsymbol{D} = 0.5$ and $L_m/\Delta x = 15$. Figure 2.43 shows that $\alpha = 0.5$ leads to the most accurate results for both the pi-ELM and the qu-ELM.

The error measures versus the diffusion coefficient are presented in Figure 2.44 for the Gauss hill, and in Figure 2.45 for the advancing front. The increase of the diffusion coefficient leads to a decrease of the L2-norm, for all methods, for the Gauss hill and the advancing front. The rate of decrease of the L2-norm with D is similar for all methods, being slightly higher for the 4P-LR2 and the pi-ELM. For the Gauss hill, the pi-ELM and the qu-ELM with 6 quadrature points present the smaller values of L2-norm. The presence of oscillations in the advancing front problem decreases the accuracy of the integration methods, the best performance being achieved by the non-compact method.

The mass ratio results are rather distinct for the Gauss hill and for the advancing front tests. The mass is almost perfectly preserved in the Gauss hill test, for all methods, and the diffusion coefficient has little influence on it (Figure 2.44(b)). For the advancing front (Figure 2.45(b)), the integration methods present a notable gain of mass as the diffusion coefficient increases. The interpolation methods present a similar but more pronounced behavior for small diffusion coefficients, but with a much larger rate of increase. For large diffusion coefficients, the interpolation methods present an opposite pattern, the mass ratio decreasing as D increases.

The order of magnitude of the mass ratio is another important distinction between the two problems: while the mass ratio for the Gauss hill is very close to 1 for all methods,

the mass gain/lost in the advancing front can be as large as 2% of the exact mass, after 100 time steps.

Dimensionless source length

In this section, we investigate the importance of the dimensionless source length ($\sigma/\Delta x$) for a Gauss hill, on the performance of the integration methods.

A set of runs was defined, starting from the parameters of the CD forum test 1A. Several standard deviations (σ) were selected, from 200 to 400. The error measures versus $\sigma/\Delta x$ are presented in Figure 2.46.

The L2-norm decreases as $\sigma/\Delta x$ increases, for all methods, since the plume becomes better discretized. The accuracy patterns defined in the formal analysis are shown in Figure 2.46(a): the pi-ELM presents a considerable improvement over the reference methods and the qu-ELM's performance is highly dependent on the number and type of quadrature points.

As in the diffusion analysis, the mass conservation analysis shows that all methods tend to conserve global mass very well for a Gauss hill perturbation. The increase of the discretization ratio does not lead to any significative differences in the mass ratio (Figure 2.46(b)).

Conclusions

The main goal of this paper was to clarify and consolidate current knowledge on ELMs. This was achieved by:

- describing the historical evolution of the ELMs,
- introducing a classification of FE-ELMs that accounts for differences in the definition of the initial conditions for the Lagrangian form of the diffusion equation. Two distinct classes were identified: the *integration* methods, that take advantage of the finite element formulation, and recognize the evaluation of the integrals at

the feet of the characteristic lines as the operation that has ultimately to be dealt with; the *interpolation* methods, which "ignore" the piecewise shape of the concentration between the feet of the characteristic lines, and specify the initial conditions for diffusion as polynomial functions supported only by the concentration at the feet of the characteristic lines.

- showing that the above classification can be applied either in a Galerkin ELM framework or in the more recent general ELM formulation proposed by Celia and co-workers - the ELLAMs. In particular, it was shown that, for constant coefficients and inside the domain, both generic frameworks - Galerkin ELMs and ELLAMs - coincide,
- studying in detail the formal properties (accuracy and stability) of two integration ELMs, in a 1D, constant coefficient context: the *quadrature* ELMs [*Hasbani, et al.*, 1983, *Russell*, 1985], based on a numerical integration at the feet of the characteristic lines, and a *piecewise* ELM, which evaluate the integrals exactly. The piecewise ELM proposed here, is a simplified, yet accurate, implementation of the original piecewise integration method [*Yeh, et al.*, 1992],
- systematically comparing both piecewise and quadrature integration methods with two representative, well studied, interpolation ELMs. This comparison was done through a combination of formal analysis of propagation and truncation errors, and numerical experimentation.

While none of the methods could be recognized as optimal, several important patterns are revealed. The pi-ELM proved to be unconditionally stable. The conditional stability of the qu-ELMs was confirmed and the stability criteria were defined as functions of the Courant number, diffusion number as well as type and number of quadrature points. In particular, the truncation error analysis allowed us to quantify the amount of diffusion necessary to stabilize the quadrature methods.

The integration ELMs can provide a considerable improvement of the accuracy, over the reference interpolation methods. The piecewise ELM is much more accurate than the reference methods, on an equal number of nodes basis, except when the presence of very strong gradients of concentration leads to a weakly wiggly behavior. The accuracy of the qu-ELM is strongly dependent on the Courant number and on the type and number of quadrature points.

This study showed that the integration methods constitute a new direction in the search for more accurate ELMs. Also, in sharp contrast with other very accurate ELMs proposed in the past (e.g. non-compact interpolation methods), the integration methods pose no conceptual difficulties for implementation in multiple dimensions, even for unstructured grids. Therefore, they constitute a potential alternative to the ELMs currently used in application oriented models.

The extension of our results to more complex cases and to multiple dimensions has to be handled with care. Although the implementation of the integration ELMs in multiple dimensions does not pose a major challenge, the risk of unattractive costs is possible. Computational cost is a major issue and it should be carefully estimated before extending these sophisticated methods to higher dimensions. For instance, both the use of a very large number of quadrature points or an exact integration in 2 or 3D problems, can lead to very high computational costs.

While a new direction for better accuracy was established, mass conservation remains a major issue in ELMs: it may compromise long term simulations and the precise results needed to handle complex transformations. Thus, new ideas are needed to address this problem.

References

Adams, E. E., A. M. Baptista, and P. Gresho, Benchmarks for the Transport Equation: the Convection-Diffusion forum and Beyond, 1993, *in preparation.*

Baptista, A. M., E. E. Adams, and K. D. Stolzenbach, Eulerian- Lagrangian analysis of pollutant transport in shallow water, *Technical Report no. 296*, MIT R.M. Parsons Laboratory, Cambridge, Mass, 1984.

Baptista, A. M., Accurate Numerical Modeling of Advection-Dominated Transport of Passive Scalars: A contribution, Laboratório Nacional de Engenharia Civil, Lisbon, Portugal, 1986.

Baptista, A. M., E. E. Adams, and P. Gresho, Reference Problems for the Convection-Diffusion forum, 1987, unpublished.

Baptista, A. M., Solution of Advection-Dominated Transport by Eulerian-Lagrangian Methods using the Backwards Method of Characteristics, Ph.D. Dissertation, Massachusetts Institute of Technology, Cambridge, Mass, 1987.

Celia, M. A., T. F. Russell, I. Herrera, R. E. Ewing, An Eulerian-Lagrangian Localized Adjoint Method for the Advection-Diffusion Equation, *Advances in Water Resources, 13*(4), pp. 187-206, 1990.

Cheng, R. T., V. Casulli, and S. N. Milford, Eulerian-Lagrangian Solution of the Convection-Dispersion Equation in natural Coordinates, *Water Resources Research, 20*(7), pp. 944-952, 1984.

Daubert, O., *Programme HYP1 - Rapport C41/74/12*, Laboratoire National D'Hydraulique, Chatou, France, 1974.

Dimou, K., 3-D Hybrid Eulerian-Lagrangian / Particle Tracking Model for Simulating Mass Transport in Coastal Water Bodies, Ph.D. Dissertation, Massachusetts Institute of Technology, Cambridge, Mass, 1992.

Glass, J. and W. Rodi, A Higher Order Numerical Scheme for Scalar Transport, *Comp. Meth. in Appl. Mech. and Eng., 31*, pp. 337-358, 1982.

Hasbani, Y., E. Livne, and M. Bercovier, Finite Elements and Characteristics Applied to Advection-Diffusion Equations, *Computers and Fluids, 11*, pp. 71-83, 1983.

Hauguel, A., Numerical Modelling of Complex Industrian and Environmental Flows, *Proceedings of the International Symposium on Refined Flow Modelling and Turbulence Measurements, I*, Iowa, 1989

Holly, F. M. and A. Preissmann, Accurate Calculation of Transport in Two Dimensions, *Journal of the Hydraulics Division, ASCE, 103*, pp. 1259-1278, 1977.

Leigh, C. E., Numerical Simulation of the Earth's Atmosphere, *Methods in Computational Physics, 4*, pp. 1-28, 1965.

Morton, K. W., A. Priestley, and E. Suli, Stability of the Lagrange-Galerkin Method with Non-exact Integration, *Mathematical Modelling and Numerical Analysis, 22*(4), pp. 625-653, 1988.

Neuman, S. P., A Eulerian-Lagrangian Numerical Scheme for the Dispersion-Convection Equation Using Conjugate Space-Time Grids, *Journal of Computational Physics, 41*, pp. 270-294, 1981.

Neuman, S. P., Adaptive Eulerian-Lagrangian Finite Element Method for Advection-Dispersion, *International Journal for Numerical Methods in Engineering, 20*, pp. 321-337, 1984.

Roache, P., *Computational Fluid Dynamics*, Hermosa Publ., 1982.

Russell, T. F., Time Stepping along characteristic with incomplete iteration for a Galerkin approximation of Miscible Displacement in Porous Media, *SIAM J. of Numerical Analysis, 22*(5), pp. 970-1013, 1985.

Russell, T. F., Eulerian-Lagrangian Localized Adjoint Methods for Advection-Dominated Problems, *Proceedings of the 13th Biennial Conference on Numerical Analysis*, Pitman, Dundee, Scotland, 1989.

Varoglu, E. and W. D. Liam Finn, Utilization of the Method of Characteristics to solve accurately Two-Dimensional Transport Problems by Finite Elements, *International Journal for Numerical Methods in Fluids, 2*, pp. 173-184, 1982.

Wang, J. D., S. V. Cofer-Shabica, and J. Chin Fatt, Finite Element Characteristic Advection Model, *Journal of Hydraulic Engineering, ASCE, 114*, pp. 1098-1114, 1988.

Wood, T. M. and A. M. Baptista, A model for Diagnostic Analysis of Estuarine Geochemistry, *Water Resources Research, 29*(1), pp. 51-71, 1993.

Yeh, G. T., J. R. Chang, and T. E. Short, An Exact Peak Capturing and Oscillation-Free Scheme to Solve Advection-Dispersion Transport Equations, *Water Resources Research, 28*(11), pp. 2937-2951, 1992.

Zisman, S., Simulation of Contaminant Transport in Groundwater Systems using Eulerian-Lagrangian Localized Adjoint Methods, M.S. Thesis, Massachusetts Institute of Technology, Cambridge, Mass, 1990

Table 2.1. Finite difference analogs.

pi-ELM	$\frac{1}{6}(c_{j-1}^{n+1}+4c_j^{n+1}+c_{j+1}^{n+1})-\alpha D(c_{j-1}^{n+1}-2c_j^{n+1}+c_{j+1}^{n+1})=$ $\left[\frac{(1-\upsilon)}{48}\{\frac{1}{r+1}(-2r^3-6r^2+6r-2)+3r^2+6r+3\}+\frac{(1-\upsilon)}{2}D(1-\alpha)\right]c_{j-int\beta-2}^{n}$ $+\left[\frac{1}{24}\{\frac{1-\upsilon}{r+1}(2r^3+3r^2-1)+\frac{1+\upsilon}{r-1}(-r^3+3r-2)+\frac{3r^2}{2}(-1+3\upsilon)+3r(1+\upsilon)+\frac{21}{2}-\frac{15}{2}\upsilon\}-\frac{(1-\upsilon)}{2}D(1-\alpha)\right]c_{j-int\beta-1}^{n}+$ $\left[\frac{1}{24}\{\frac{1-\upsilon}{r+1}(-r^3+3r^2+2)+\frac{1+\upsilon}{r-1}(2r^3-3r^2+1)+\frac{3r^2}{2}(-1-3\upsilon)+3r(-1+\upsilon)+\frac{21}{2}+\frac{15}{2}\upsilon\}+\frac{D(1-\alpha)}{2}(-1-3\upsilon)\right]c_{j-int\beta}^{n}+$ $\left[\frac{(1+\upsilon)}{48}\{\frac{1}{r-1}(-2r^3+6r^2-6r+2)+3r^2-6r+3\}+\frac{(1+\upsilon)}{2}D(1-\alpha)\right]c_{j-int\beta+1}^{n}$
qu-ELM	$\frac{1}{6}(c_{j-1}^{n+1}+4c_j^{n+1}+c_{j+1}^{n+1})-\alpha D(c_{j-1}^{n+1}-2c_j^{n+1}+c_{j+1}^{n+1})=$ $\left[\sum_{i=1}^{nqp}w_i\{\frac{(1+r_i)(1-\upsilon_i)}{8}+\frac{(1-\alpha)D}{2}\}\right]c_{j-int(\beta-r_i/2-0.5)-2}^{n}+$ $\left[\sum_{i=1}^{nqp}w_i\{\frac{(1-r_i)(1-\upsilon_i)}{8}+\frac{(1+r_i)(1+\upsilon_i)}{8}-(1-\alpha)D\}\right]c_{j-int(\beta-r_i/2-0.5)-1}^{n}$ $\left[\sum_{i=1}^{nqp}w_i\{\frac{(1-r_i)(1+\upsilon_i)}{8}+\frac{(1-\alpha)D}{2}\}\right]c_{j-int(\beta-r_i/2-0.5)}^{n}$
2P-LI2	$\frac{1}{6}(c_{j-1}^{n+1}+4c_j^{n+1}+c_{j+1}^{n+1})-\alpha D(c_{j-1}^{n+1}-2c_j^{n+1}+c_{j+1}^{n+1})=$ $\frac{(1-\upsilon)}{2}(\frac{1}{6}-(1-\alpha)D)c_{j-int\beta-2}^{n}+\left[\frac{1}{6}(\frac{5}{2}-\frac{3}{2}\upsilon)-(1-\alpha)D(-\frac{1}{2}+\frac{3}{2}\upsilon)\right]c_{j-int\beta-1}^{n}$ $+\left[\frac{1}{6}(\frac{5}{2}+\frac{3}{2}\upsilon)-(1-\alpha)D(-\frac{1}{2}-\frac{3}{2}\upsilon)\right]c_{j-int\beta}^{n}+(\frac{1}{6}-(1-\alpha)D)\frac{(1+\upsilon)}{2}c_{j-int\beta+1}^{n}$
4P-LR2	$\frac{1}{6}(c_{j-1}^{n+1}+4c_j^{n+1}+c_{j+1}^{n+1})-\alpha D(c_{j-1}^{n+1}-2c_j^{n+1}+c_{j+1}^{n+1})=$ $\left[(-\frac{7}{360})\frac{(1-\upsilon)}{2}\right]c_{j-int\beta-3}^{n}+\left[(\frac{29}{180}-(1-\alpha)D)\frac{1-\upsilon}{2}+(-\frac{7}{360})\frac{(1+\upsilon)}{2}\right]c_{j-int\beta-2}^{n}$ $+\left[(\frac{43}{60}+2(1-\alpha)D)\frac{1-\upsilon}{2}+(\frac{29}{180}-(1-\alpha)D)\frac{(1+\upsilon)}{2}\right]c_{j-int\beta-1}^{n}+$ $\left[(\frac{43}{60}+2(1-\alpha)D)\frac{1+\upsilon}{2}+(\frac{29}{180}-(1-\alpha)D)\frac{(1-\upsilon)}{2}\right]c_{j-int\beta}^{n}+$ $\left[(\frac{29}{180}-(1-\alpha)D)\frac{1+\upsilon}{2}+(-\frac{7}{360})\frac{(1-\upsilon)}{2}\right]c_{j-int\beta+1}^{n}+\left[(-\frac{7}{360})\frac{(1+\upsilon)}{2}\right]c_{j-int\beta+2}^{n}$

υ - distance between node j and the feet of the characteristic lines in local coordinates (see Figure 2.2(a)).

Table 2.2 Truncation error - Effective Diffusion number

Υ

qu-ELM	$\sum_{i=1}^{nqp}\left[\frac{w_i}{2}\left(\frac{2K^2+1}{4}-\frac{K\upsilon_i}{2}\right)-\frac{w_i r_i}{8}(2K-\upsilon_i)\right]-\left(\frac{\beta^2}{2}+\frac{1}{6}\right)+D$
pi-ELM	$\frac{int^2\beta}{2}+\frac{1}{48}[int\beta(2k_1-(k_2+k_3+k_4)\upsilon+3k_2+k_3-k_4)+D+$ $k_1+k_2\left(-\frac{3}{2}\upsilon+\frac{5}{2}\right)+\left(\frac{1}{2}-\frac{1}{2}\upsilon\right)k_3+k_4\left(\frac{\upsilon}{2}+\frac{1}{2}\right)]-\frac{\beta^2}{2}-\frac{1}{6}$
2P-LI2	$\frac{1}{12}(-6int^2\beta-6int\beta+6\beta+12\beta int\beta)-\frac{\beta^2}{2}+D$
	Auxiliary constants
k_1	$\frac{1}{r_{int}+1}(2r_{int}^3+6r_{int}^2+6r_{int}+2)+\frac{1}{r_{int}-1}(-2r_{int}^3+6r_{int}-4)$
k_2	$\frac{1}{r_{int}+1}(-2r_{int}^3-6r_{int}^2-6r_{int}-2)+3r_{int}^2+6r_{int}+3$
k_3	$\frac{1}{r_{int}+1}(2r_{int}^3-6r_{int}-4)+\frac{1}{r_{int}-1}(2r_{int}^3-6r_{int}+4)-6r_{int}^2+18$
k_4	$\frac{1}{r_{int}-1}(-2r_{int}^3+6r_{int}^2-6r_{int}+2)+3r_{int}^2-6r_{int}+3$
K_i	$int\left(\beta-\frac{r_i}{2}-\frac{1}{2}\right)+1 \;\; if \;\; \beta-\frac{r_i}{2}-\frac{1}{2}>0$ $0 \quad otherwise$

Table 2.3 Error measures [*Baptista, et al.*, 1984]

Discrete L2-norm	$L2(t)=\frac{1}{m^*(t)}\left\{\left[\sum_i (c_i^{num^*}(x,t)-c^{ex^*}(x,t))\right]^{1/2}\right\}$
Measure of Global Mass	$Mass(t)=\frac{1}{m(t)}\int_\Omega c^{num}(x,t)\,dx$

* c^{num} - numerical solution, c^{ex} - exact solution, m - total mass

Table 2.4 Parameters for selected tests from problem 1 and 3 of the Convection-Diffusion forum

Case	u(m/s)	D(m2/s)	Type *	σ(m)	Δt(s)	#time steps
1-A	0.5	0	GH	264	96	100
1-C	0.5	50	GH	264	96	100
1-K	0.5	0	GH	264	192	50
3-A	0.5	0	AF	-	96	100
3-B	0.5	2	AF	-	96	100
3-C	0.5	50	AF	-	96	100
3-F	0.5	0	AF	-	48	200

* GH - Gauss hill, AF - advancing front

Table 2.5 Initial and boundary conditions

Problem	Initial conditions	Upstream B.C.	Downstream B.C.
1	$c_0(x) = exp\left(-\frac{(x-x_0)^2}{2\sigma_0^2}\right)^*$	$c = 0$	$c = c_{advection}$
3	$c = 0$	$c = 1$	$c = c_{advection}$

* x_0 - center of mass of the initial conditions, σ_0 - standard deviation of the initial concentration field

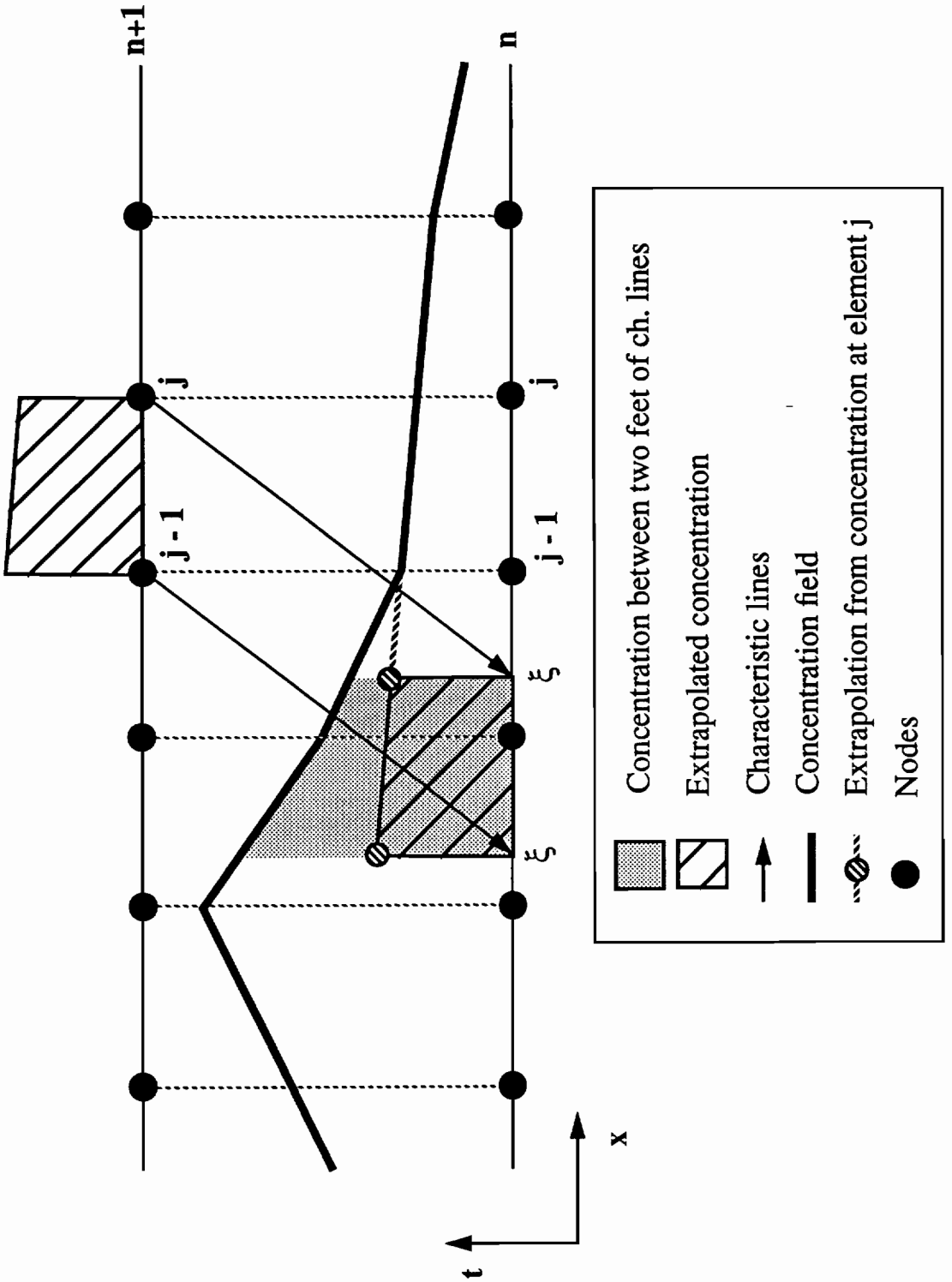

Figure 2.1(a) Extrapolation of the concentration at the feet of the characteristic lines.

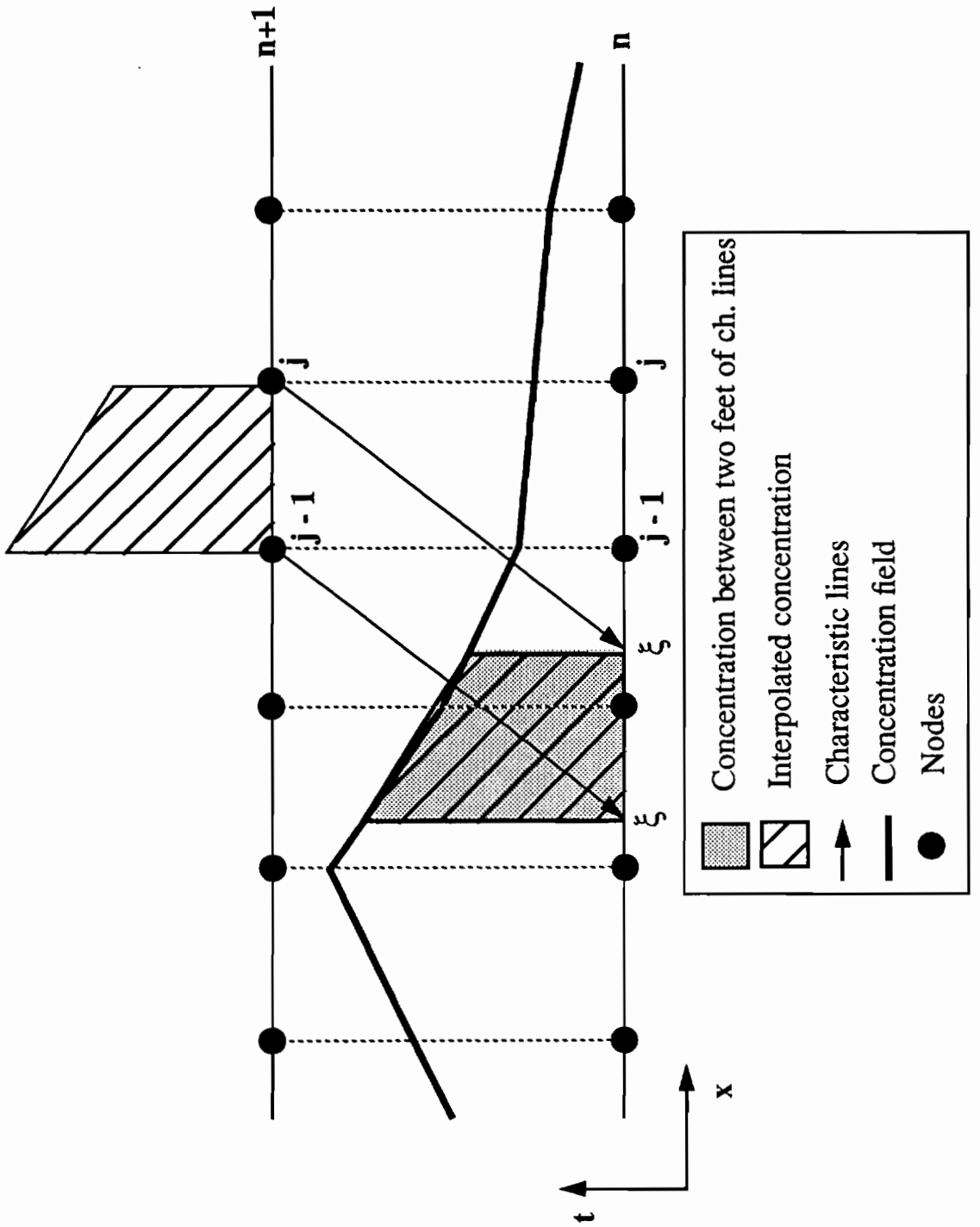

Figure 2.1(b) Interpolation of the concentration at the feet of the characteristic lines.

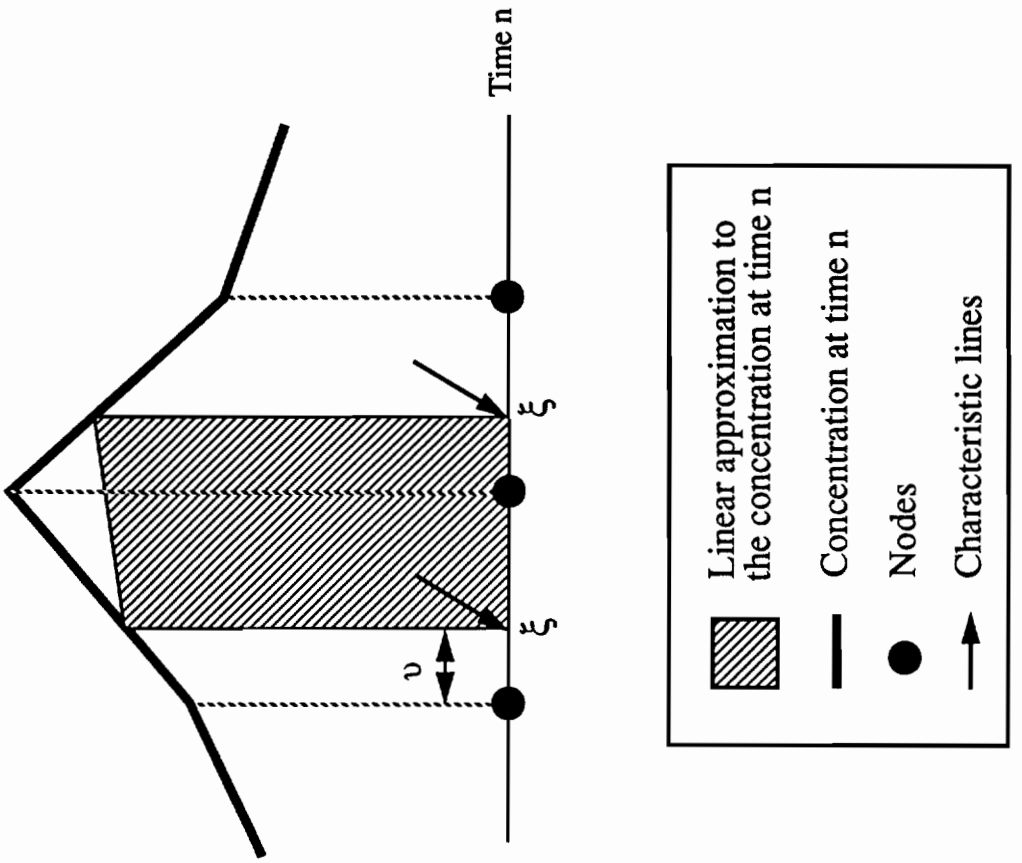

Figure 2.2(a) Evaluation of the integrals at the feet of the characteristic lines: interpolation ELM.

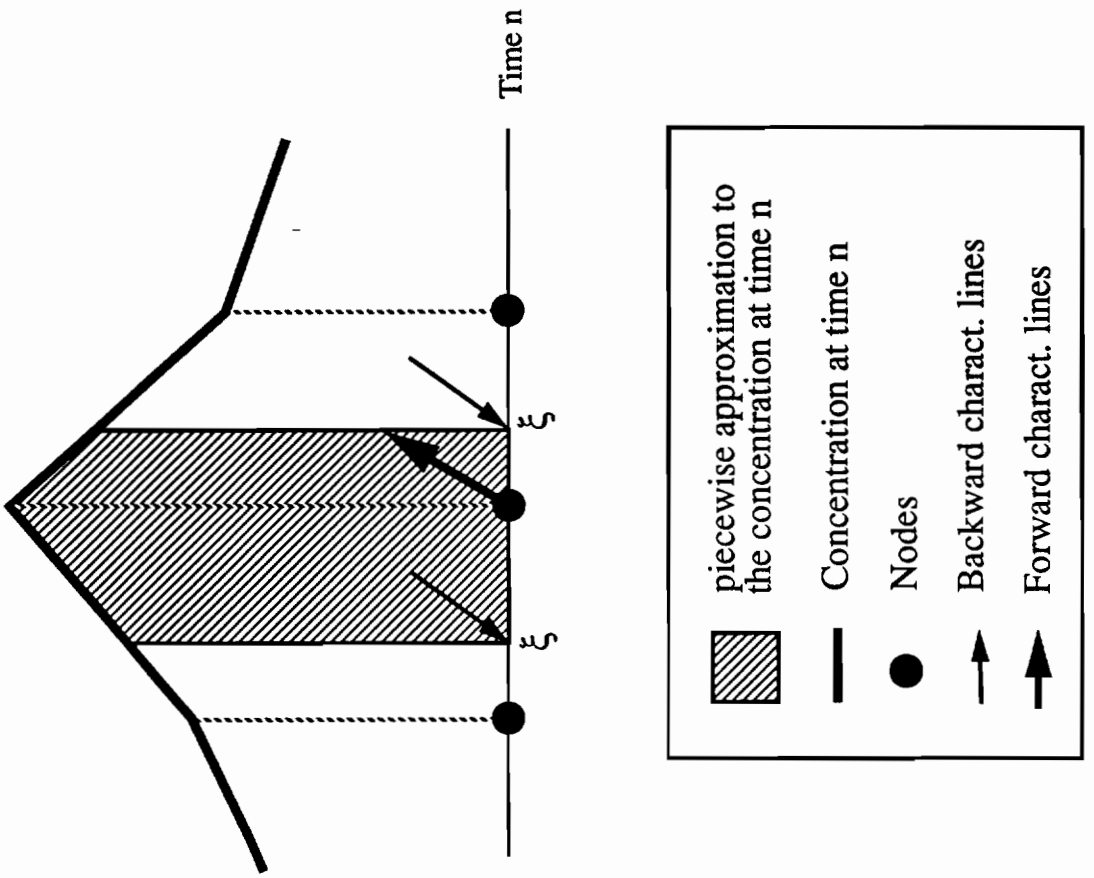

Figure 2.2(b) Evaluation of the integrals at the feet of the characteristic lines: piecewise ELM.

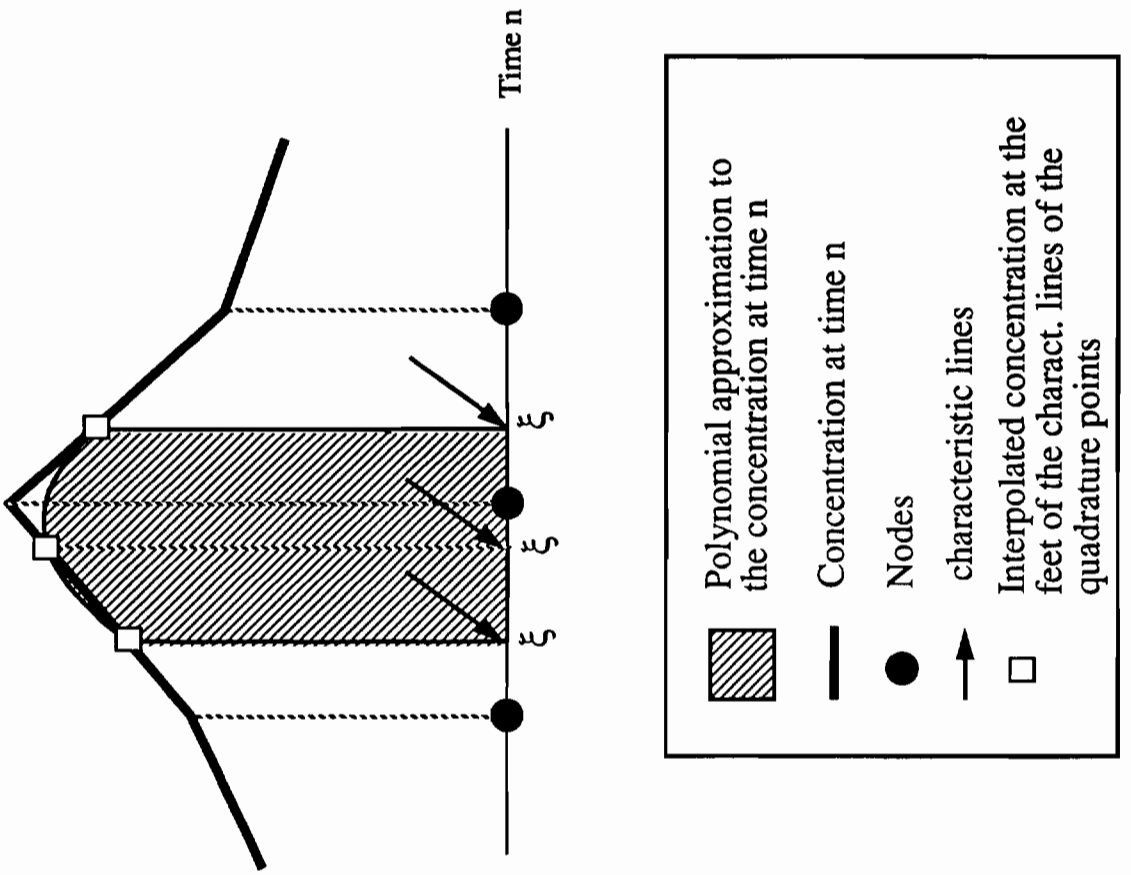

Figure 2.2(c) Evaluation of the integrals at the feet of the characteristic lines: quadrature ELM.

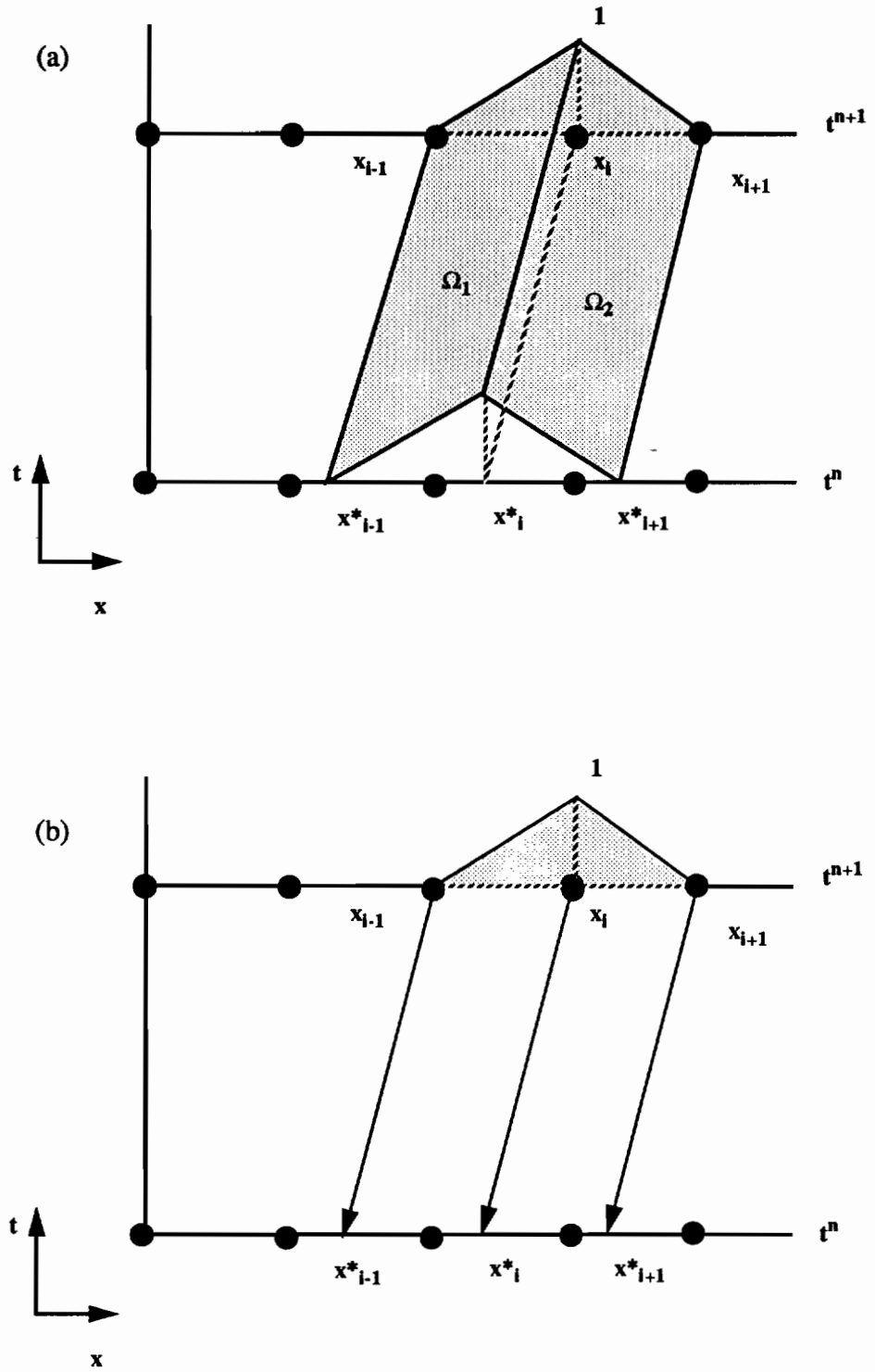

Figure 2.3 Comparison of weight functions: (a) ELLAMs; (b) ELMs.

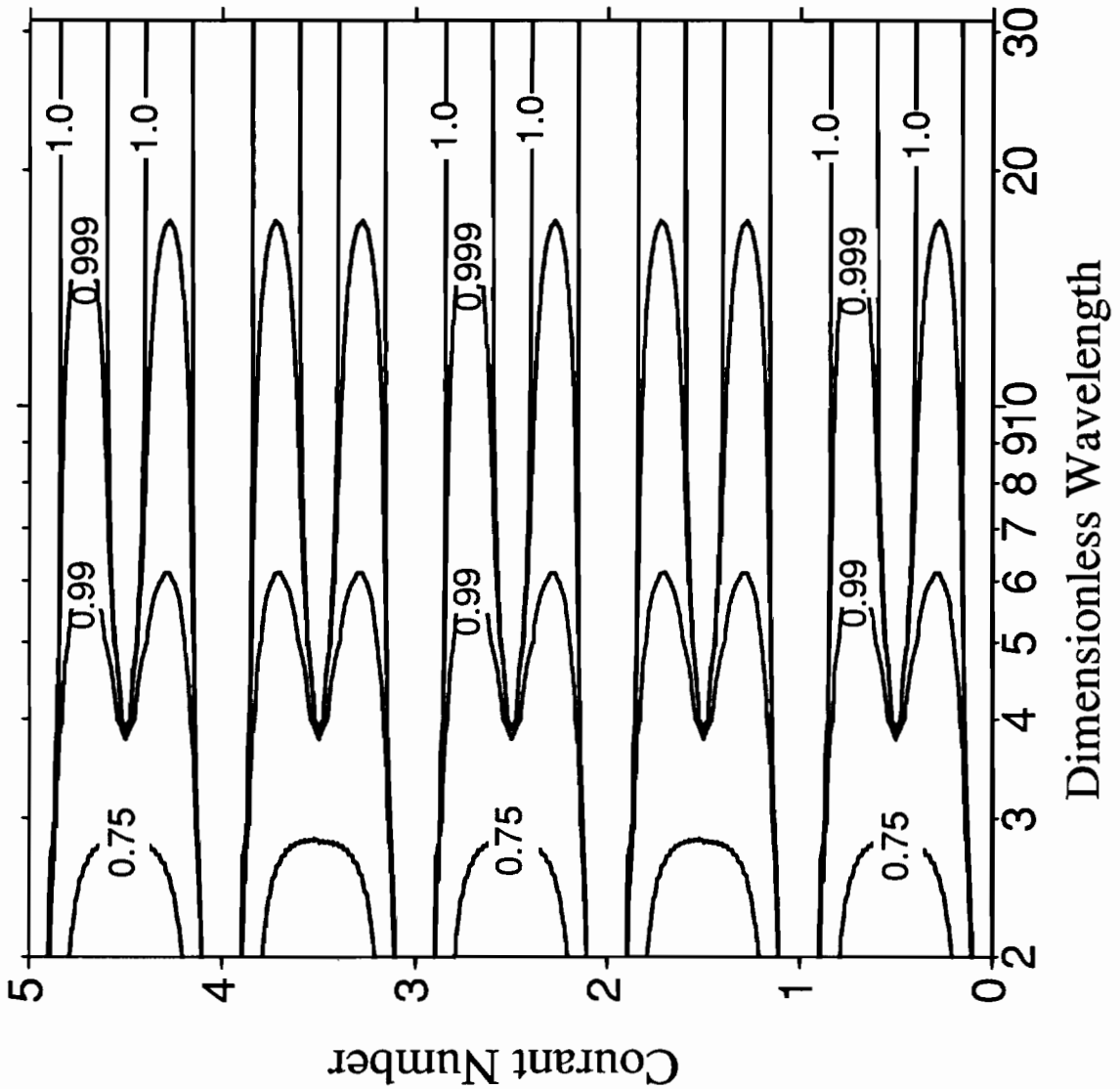

Figure 2.4 Amplification factor for the qu-ELM with 3 Gauss points (pure advection).

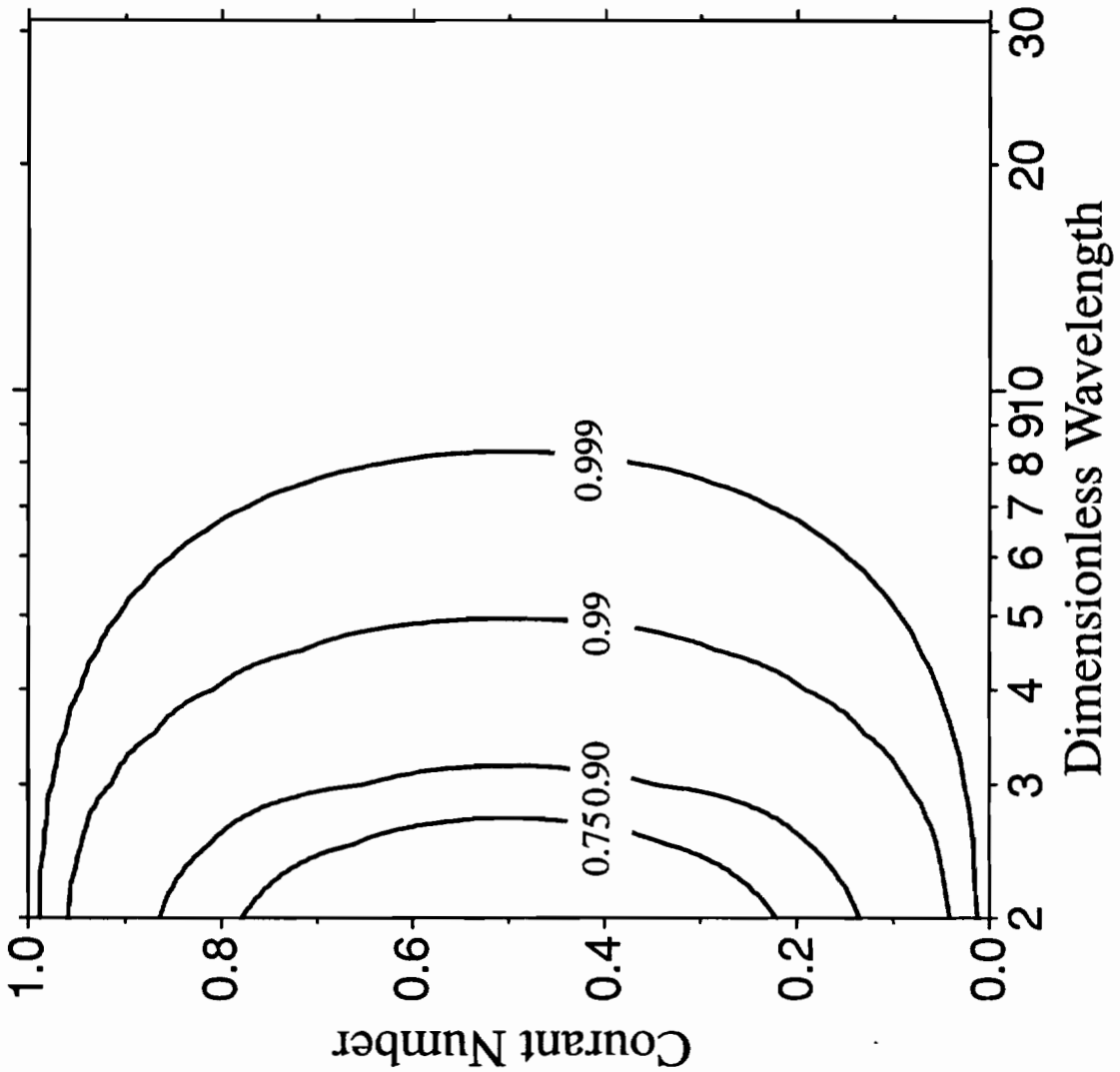

Figure 2.5 Amplification factor for the pi-ELM (pure advection).

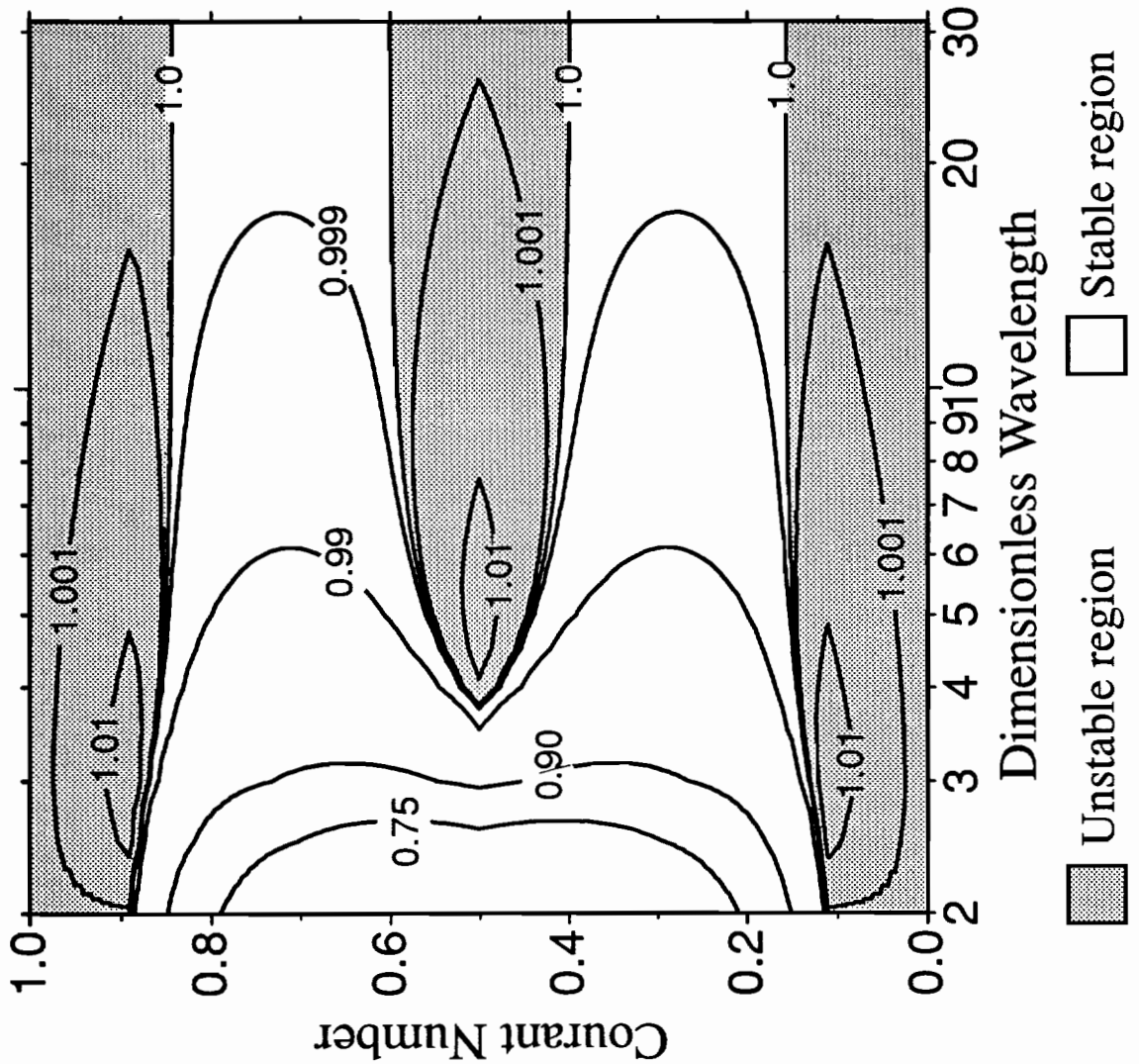

Figure 2.6 Amplification factor for the qu-ELM with 3 Gauss points (pure advection).

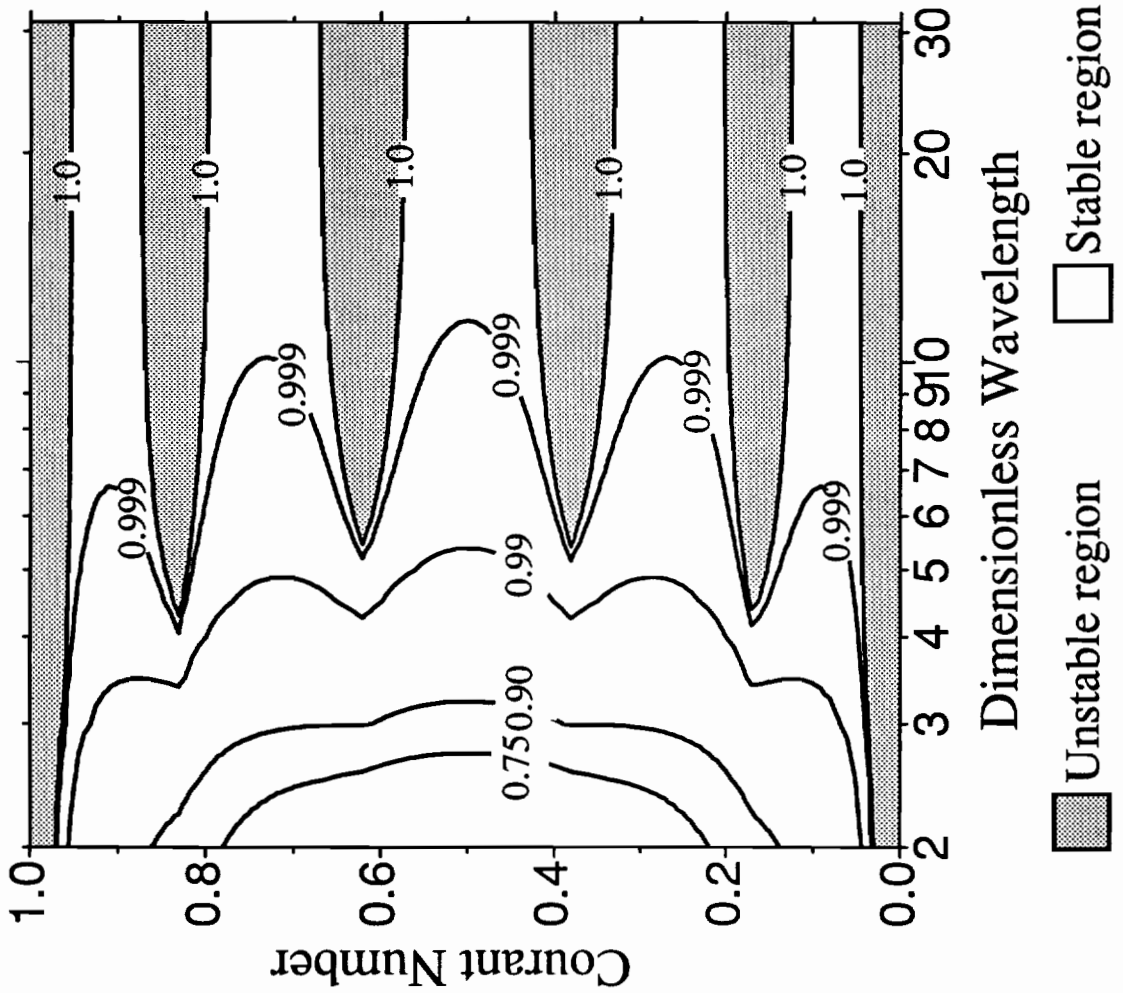

Figure 2.7 Amplification factor for the qu-ELM with 6 Gauss points (pure advection).

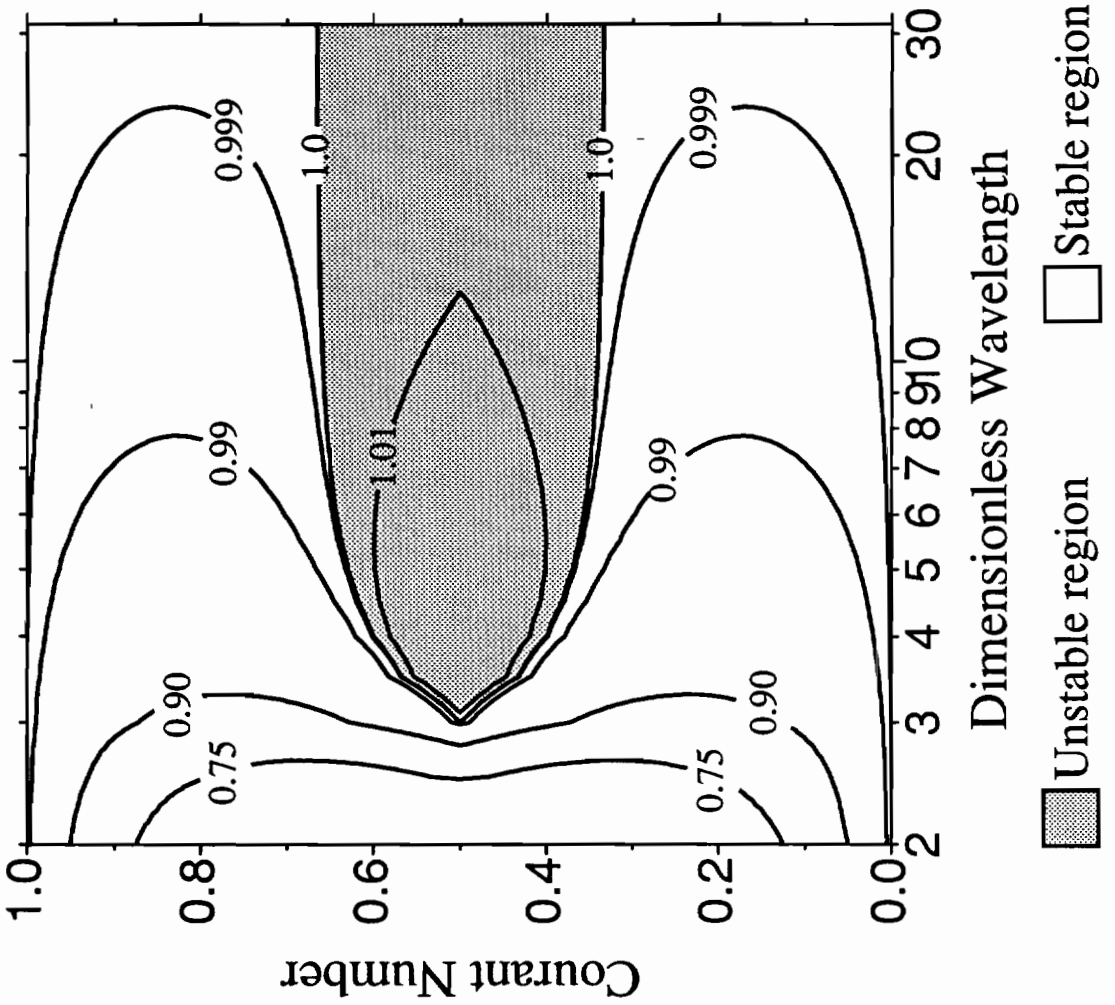

Figure 2.8 Amplification factor for the qu-ELM with 3 Lobatto points (pure advection).

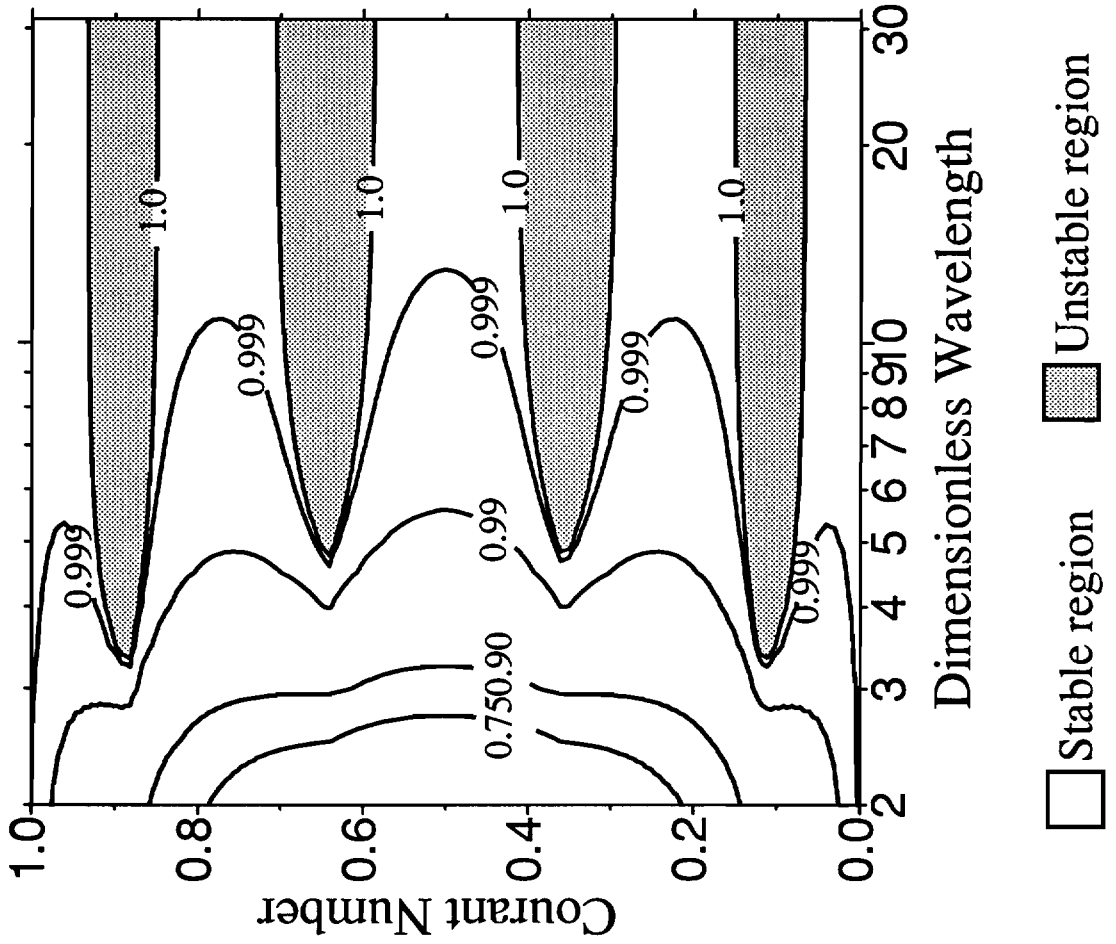

Figure 2.9 Amplification factor for the qu-ELM with 6 Lobatto points (pure advection).

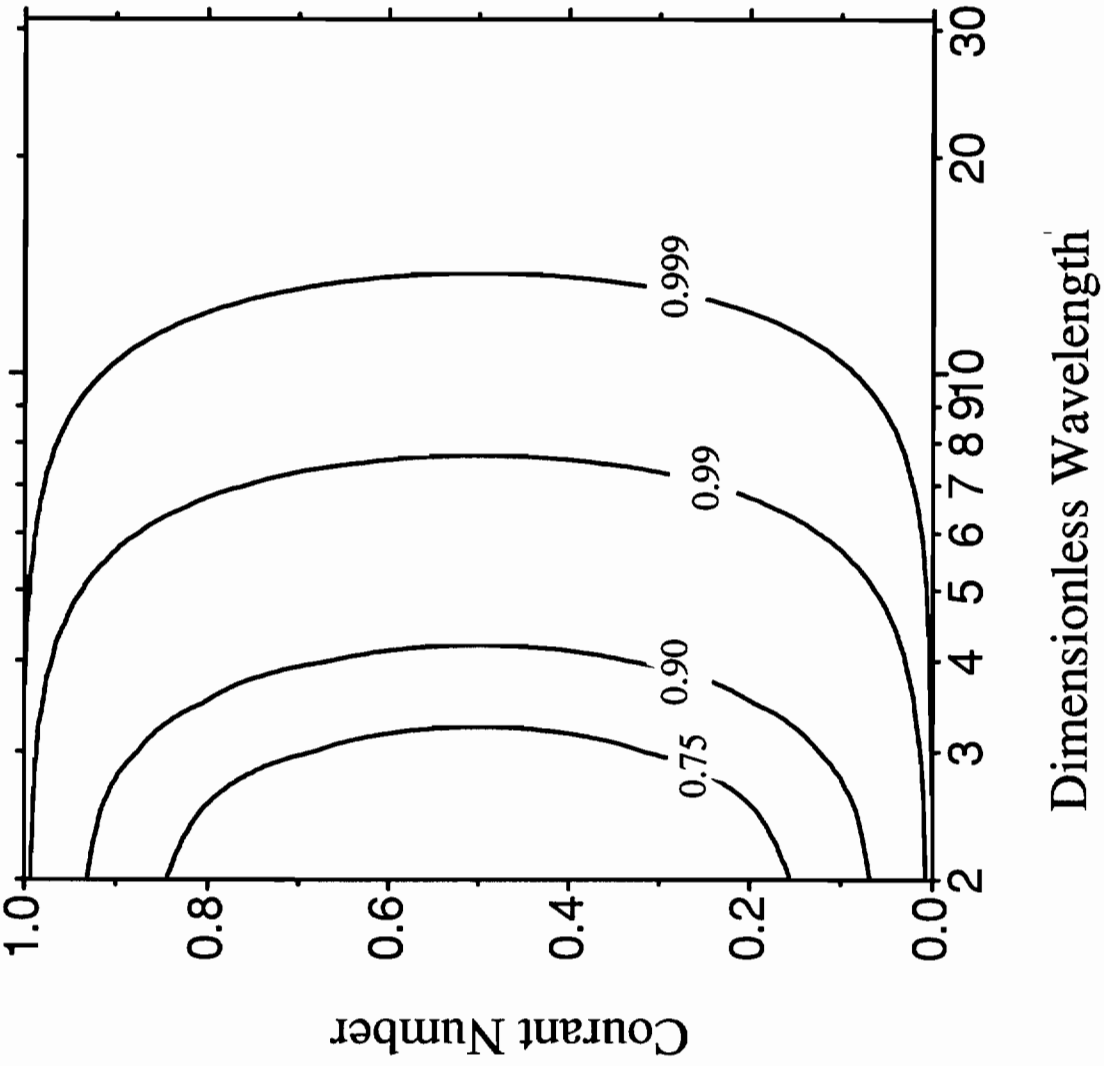

Figure 2.10 Amplification factor for the 4P-LR2 (pure advection).

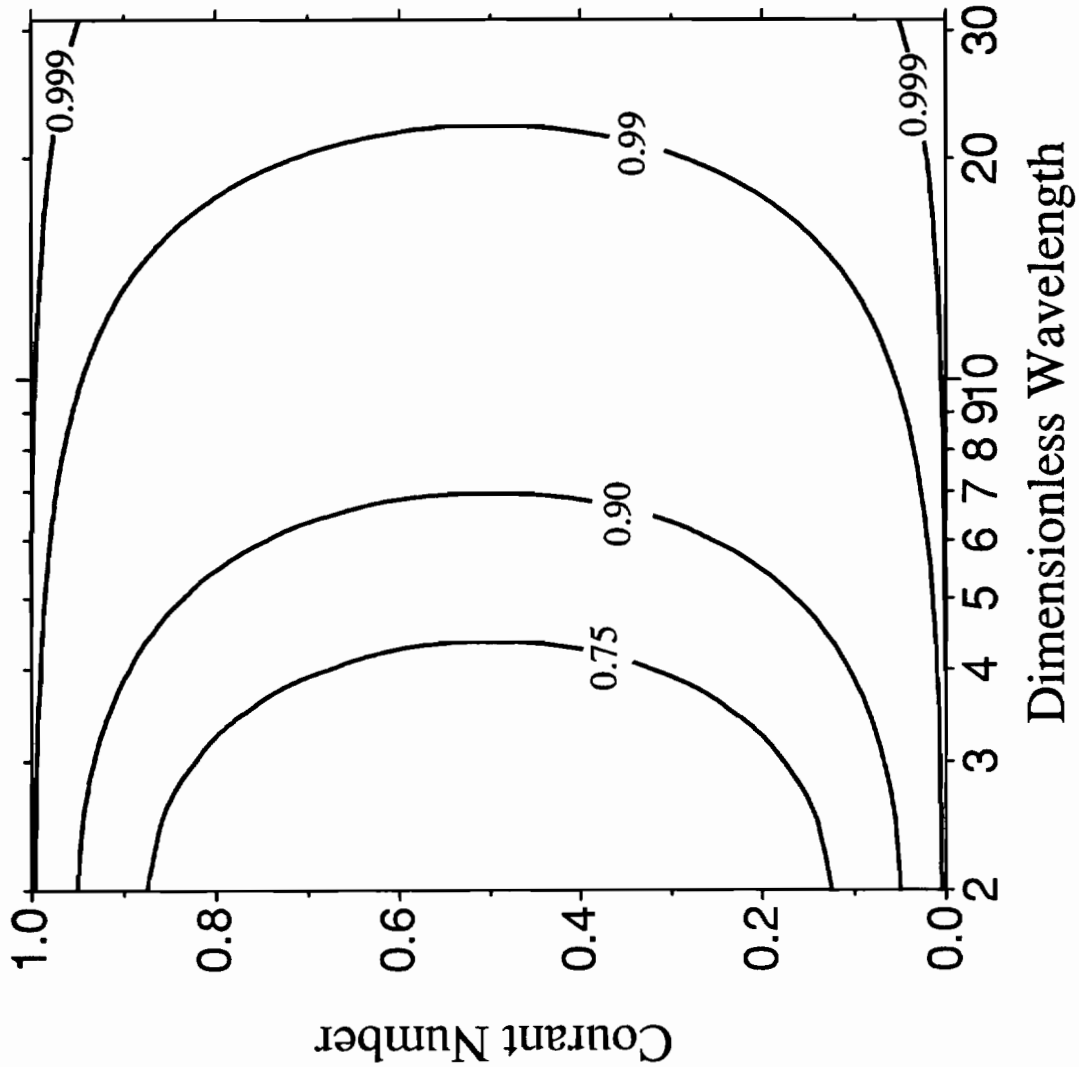

Figure 2.11 Amplification factor for the 2P-LI2 (pure advection).

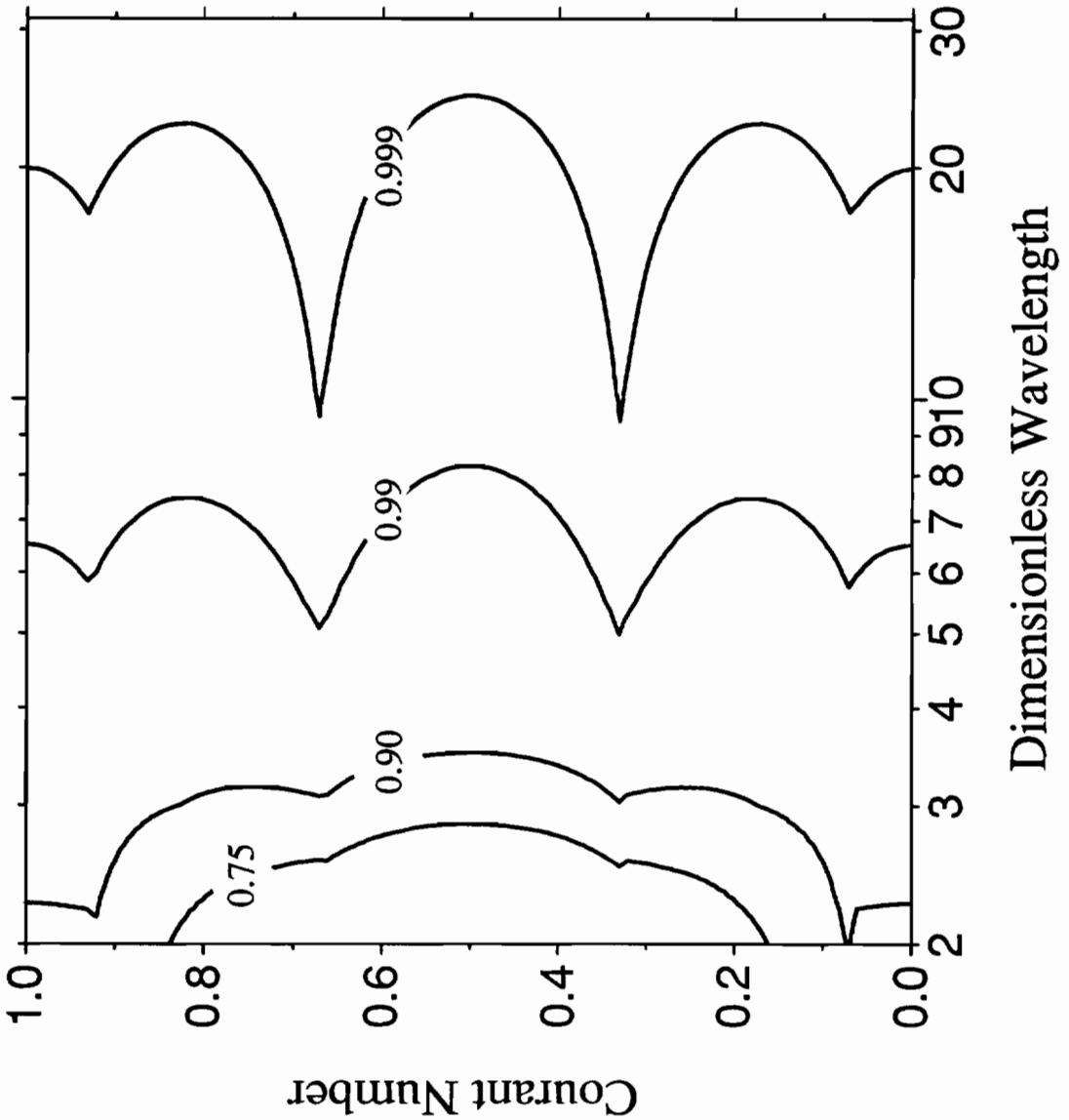

Figure 2.12 Amplification factor for the qu-ELM with 4 Gauss points ($D = 0.01$).

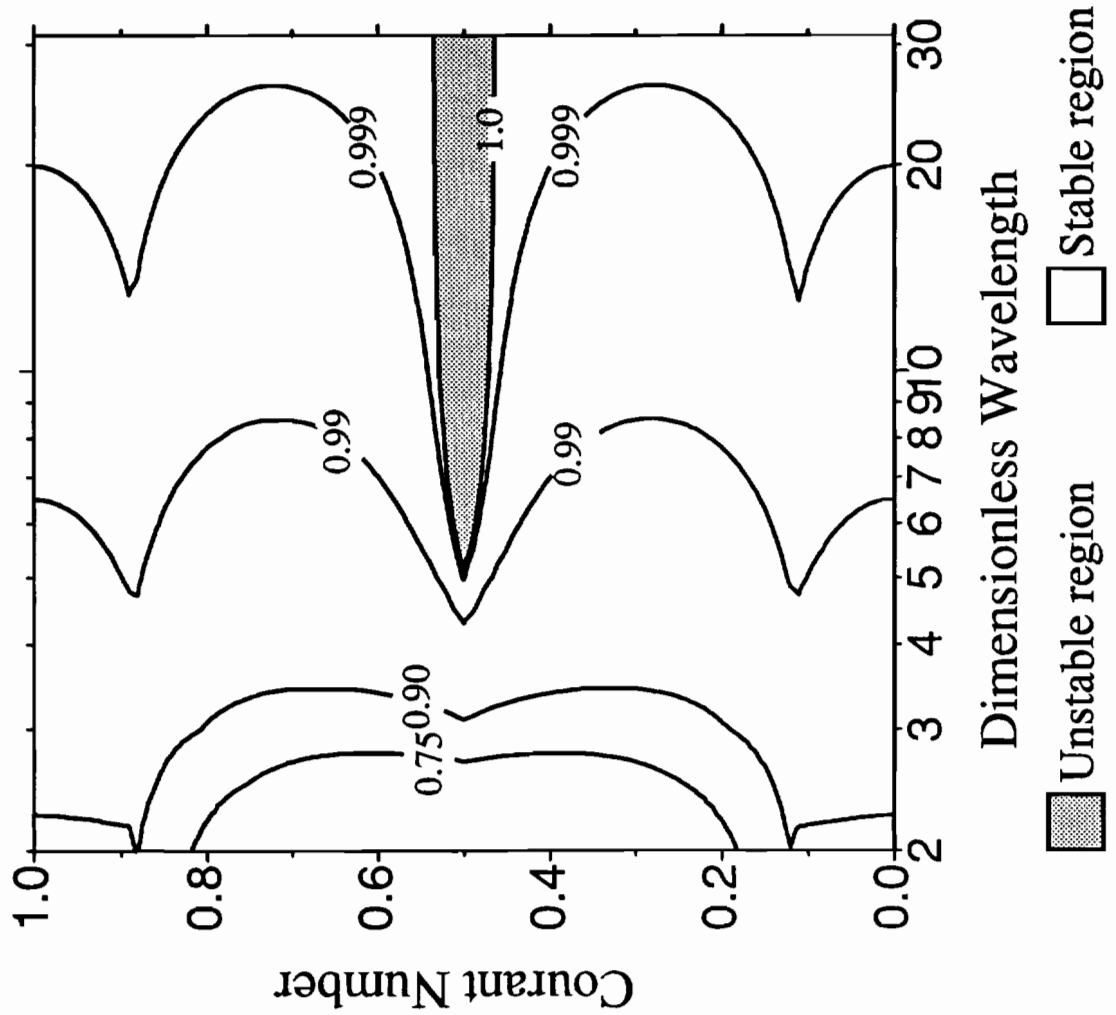

Figure 2.13 Amplification factor for the qu-ELM with 3 Gauss points ($D = 0.01$).

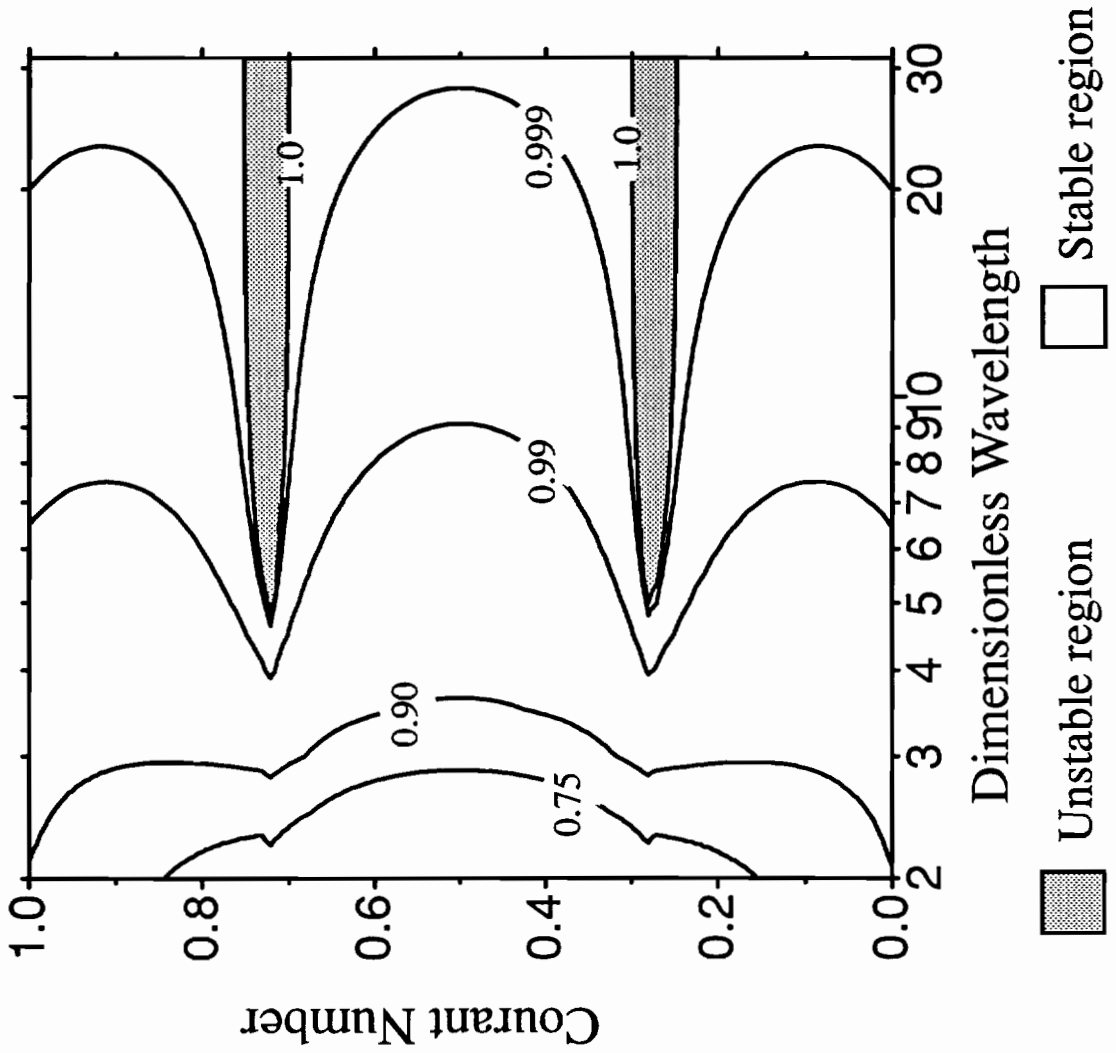

Figure 2.14 Amplification factor for the qu-ELM with 4 Lobatto points ($D = 0.01$).

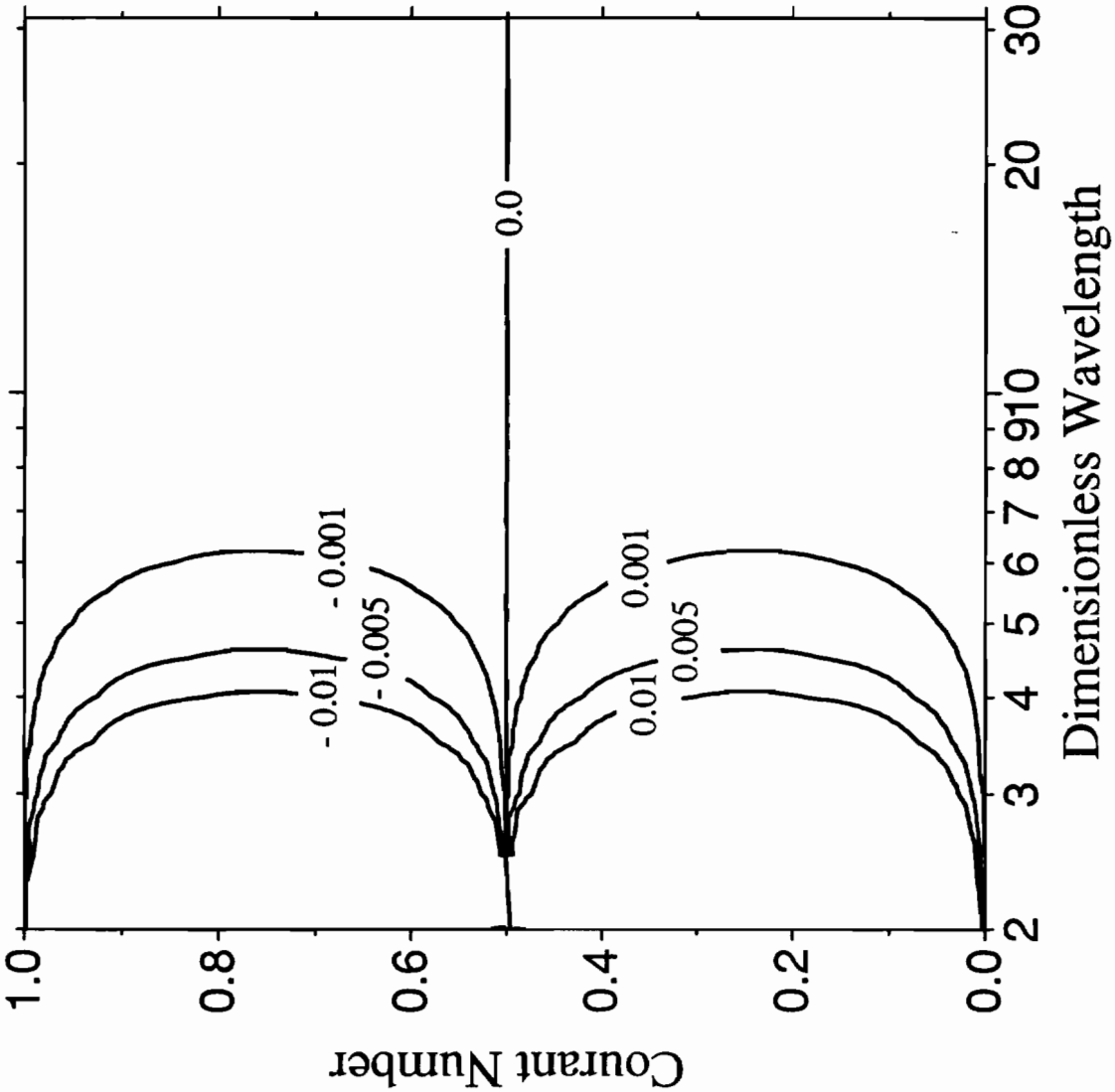

Figure 2.15 Phase error for the pi-ELM (pure advection).

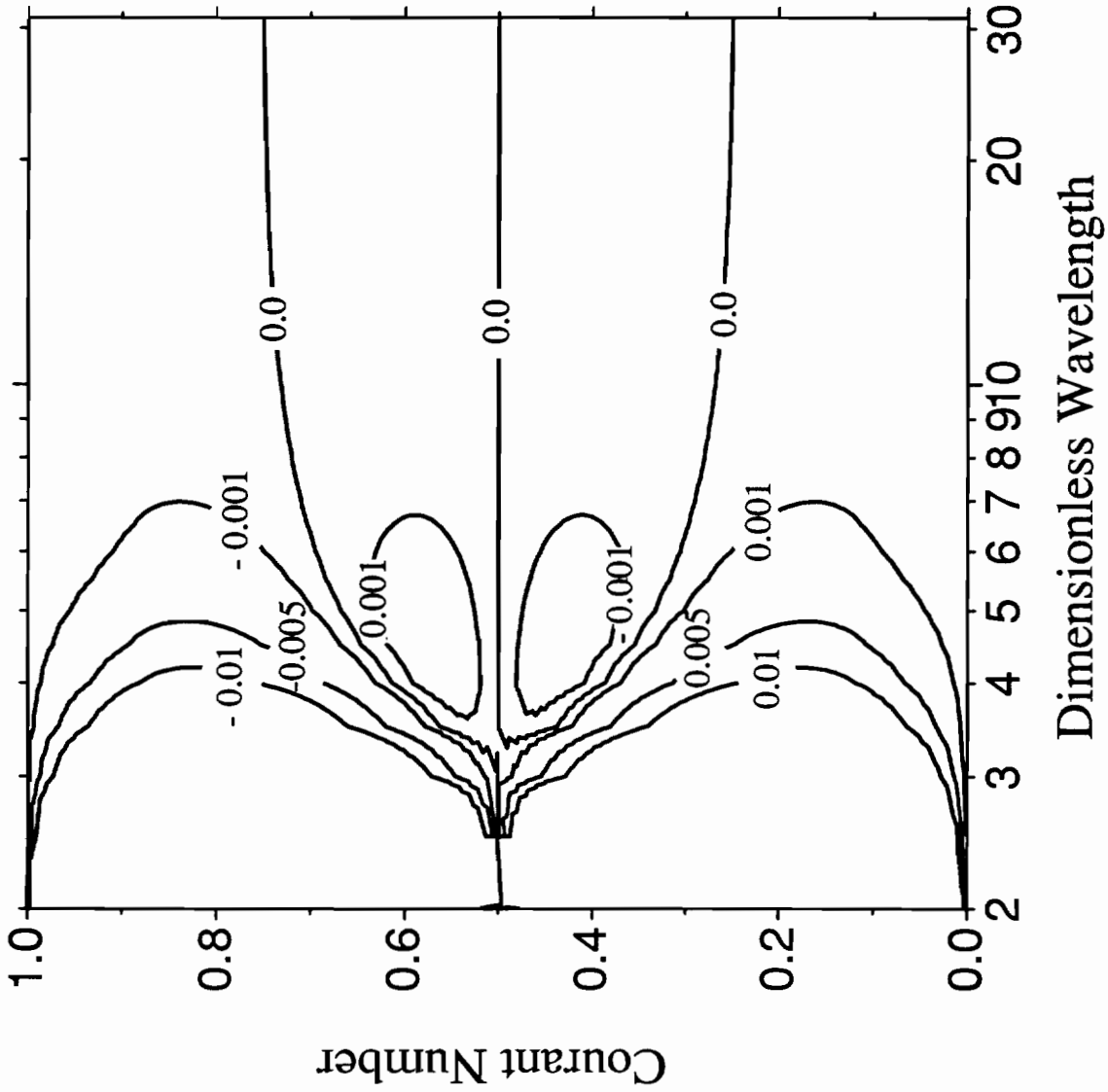

Figure 2.16 Phase error for the qu-ELM with 3 Gauss points (pure advection).

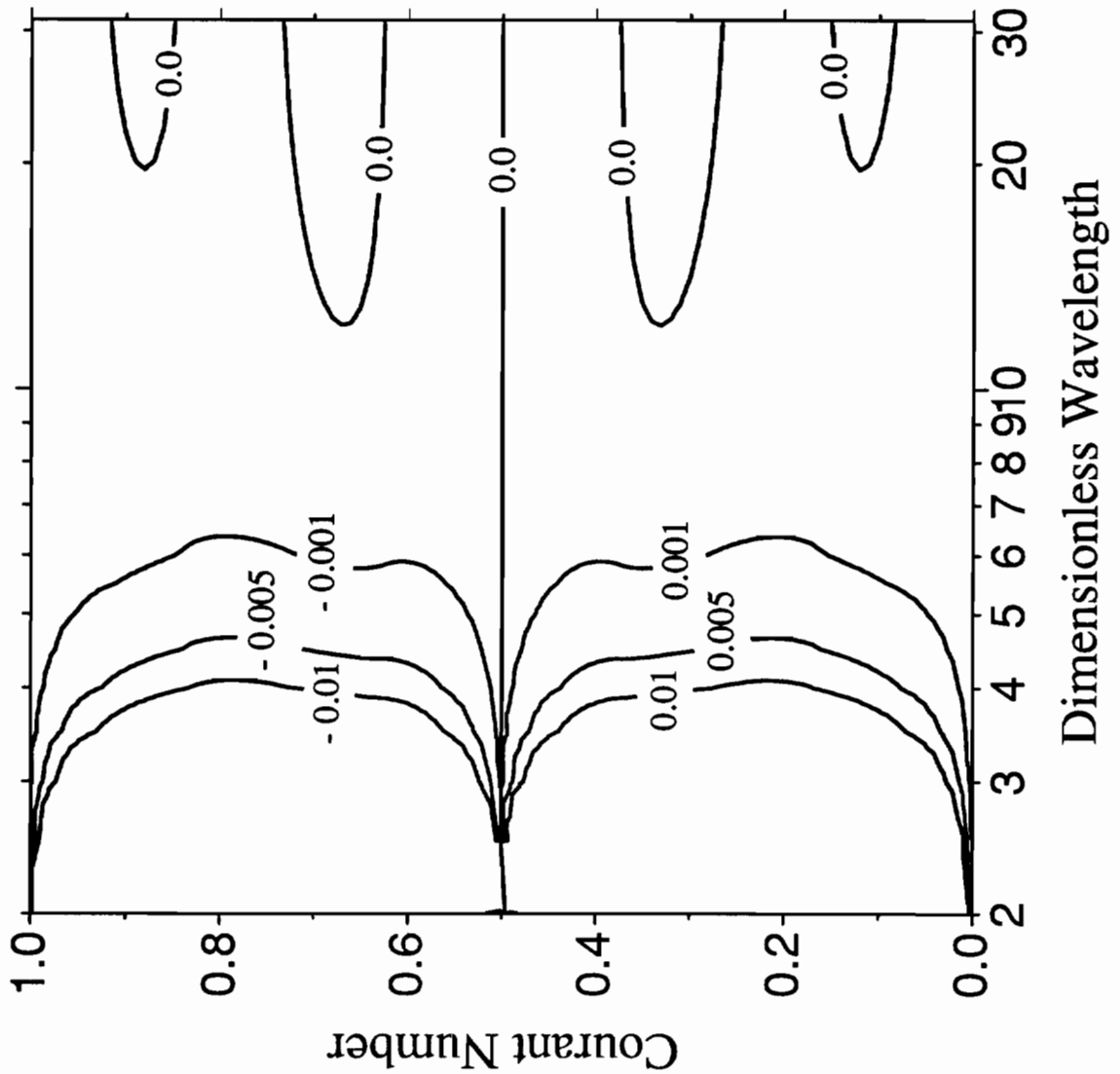

Figure 2.17 Phase error for the qu-ELM with 6 Gauss points (pure advection).

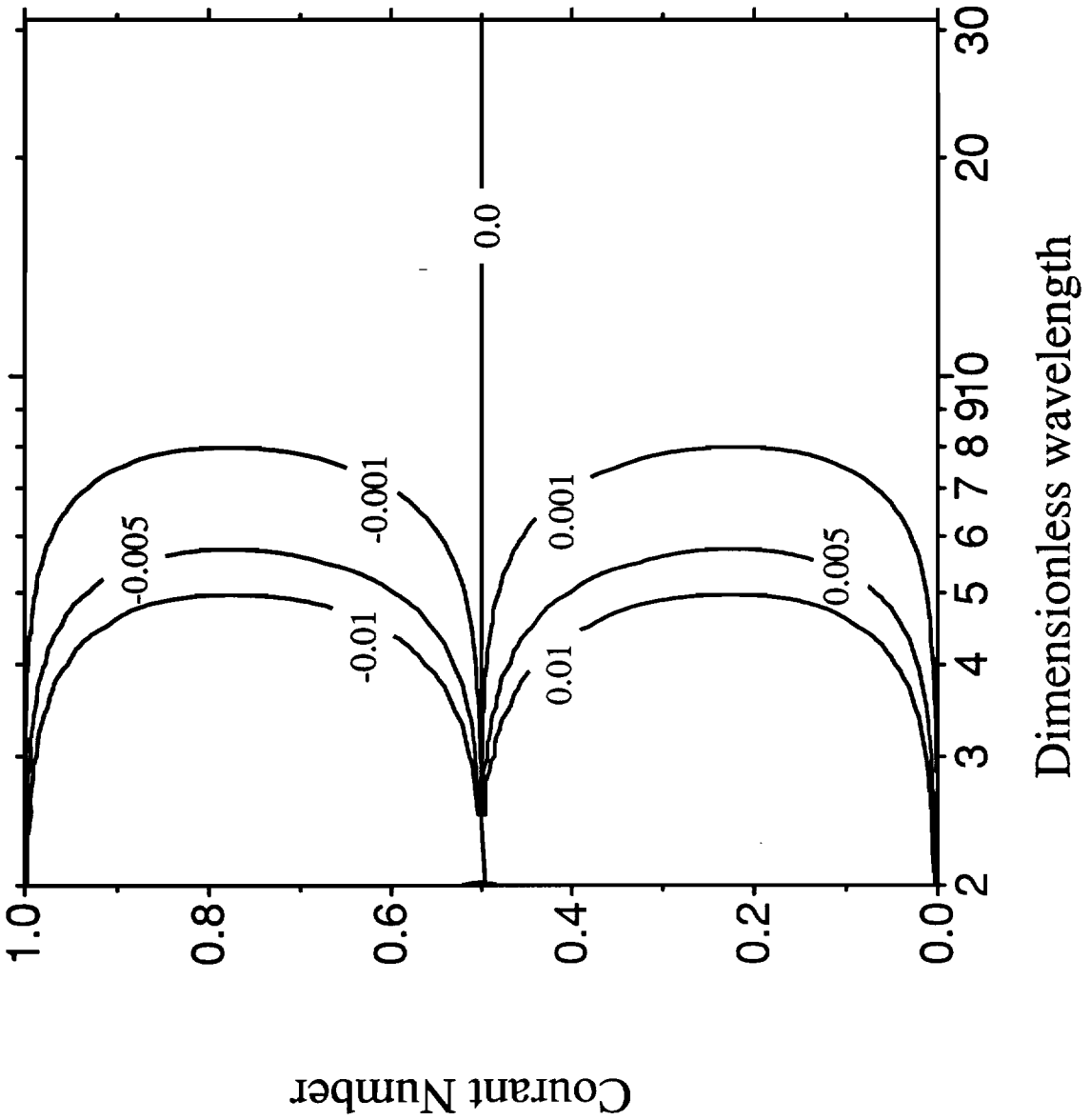

Figure 2.18 Phase error for the 4P-LR2 (pure advection).

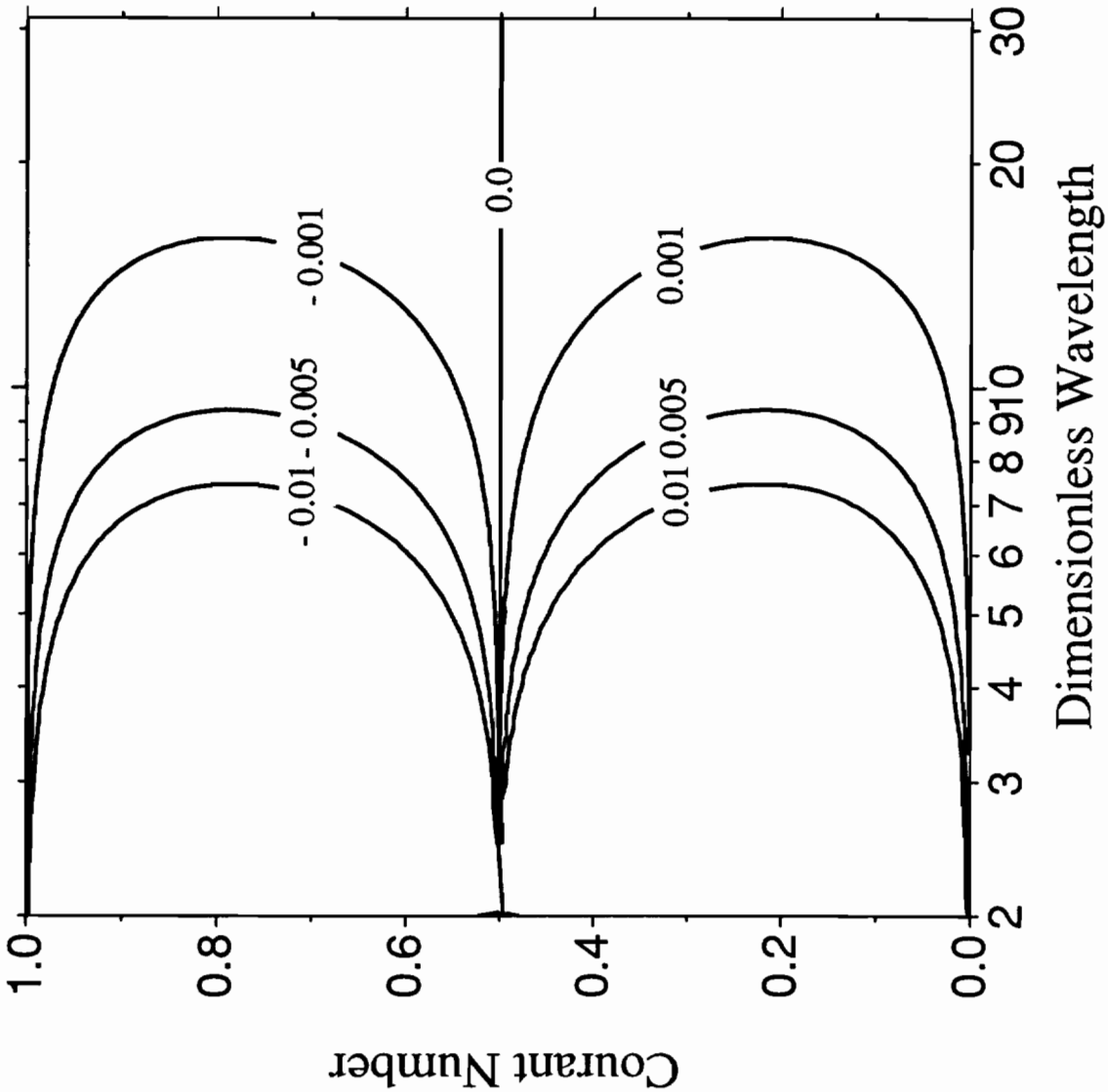

Figure 2.19 Phase error for the 2P-LI2 (pure advection).

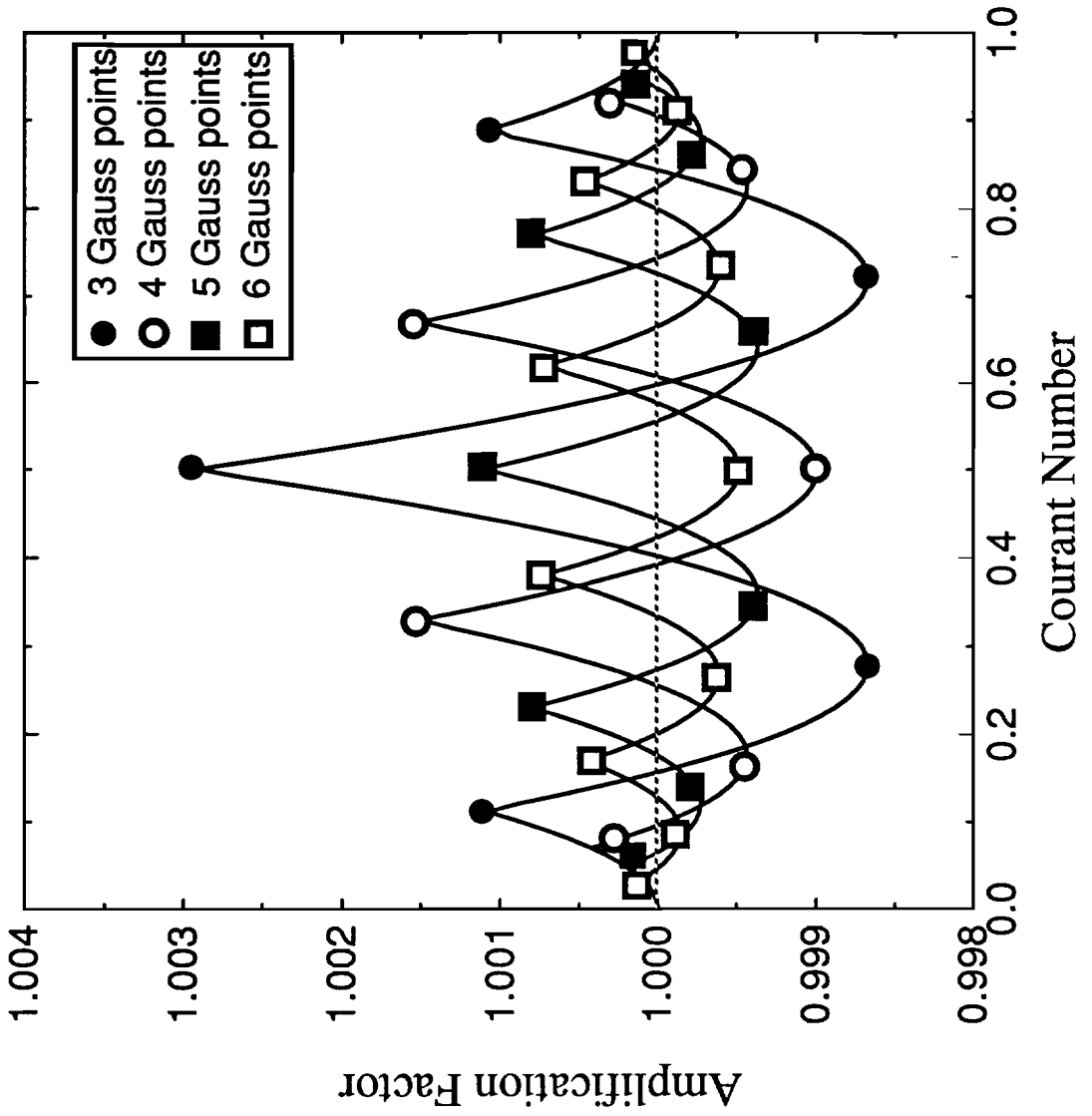

Figure 2.20(a) Comparison of amplification factors for the qu-ELM, with $L_m/\Delta x = 15$: Gauss quadrature points.

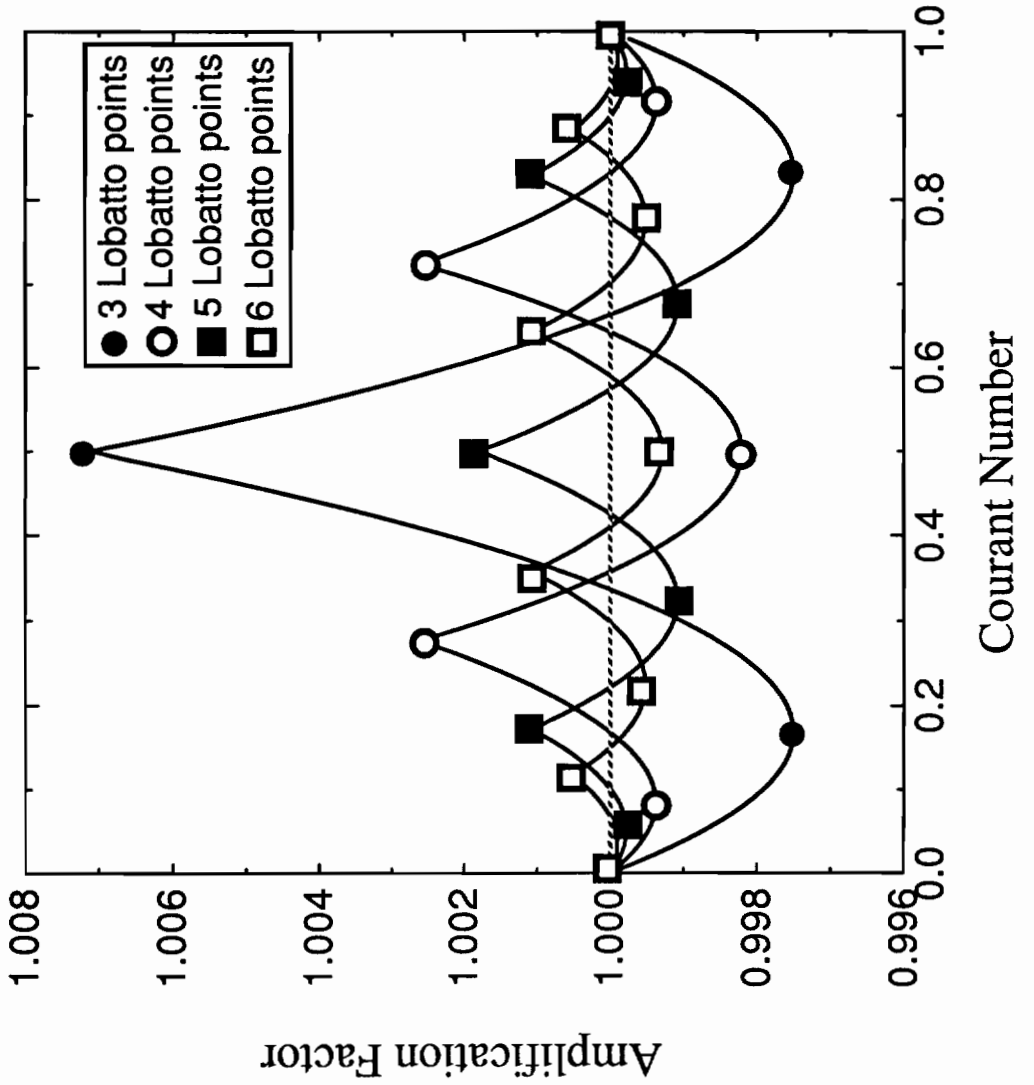

Figure 2.20(b) Comparison of amplification factors for the qu-ELM, with $L_m/\Delta x = 15$: Lobatto quadrature points.

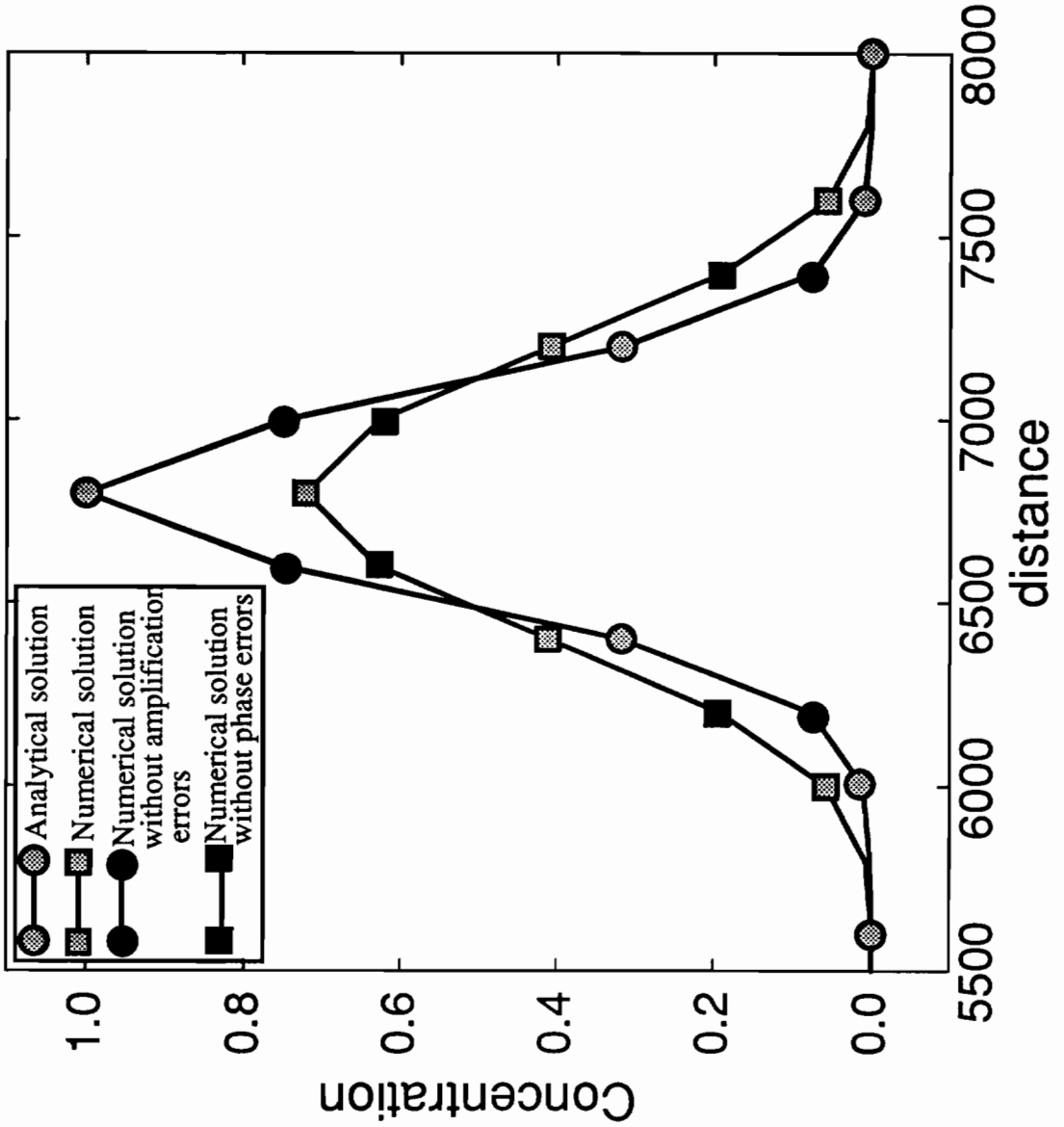

Figure 2.21 Comparison of the relative importance of amplification factors and phase errors, for the qu-ELM with 3 Gauss points.

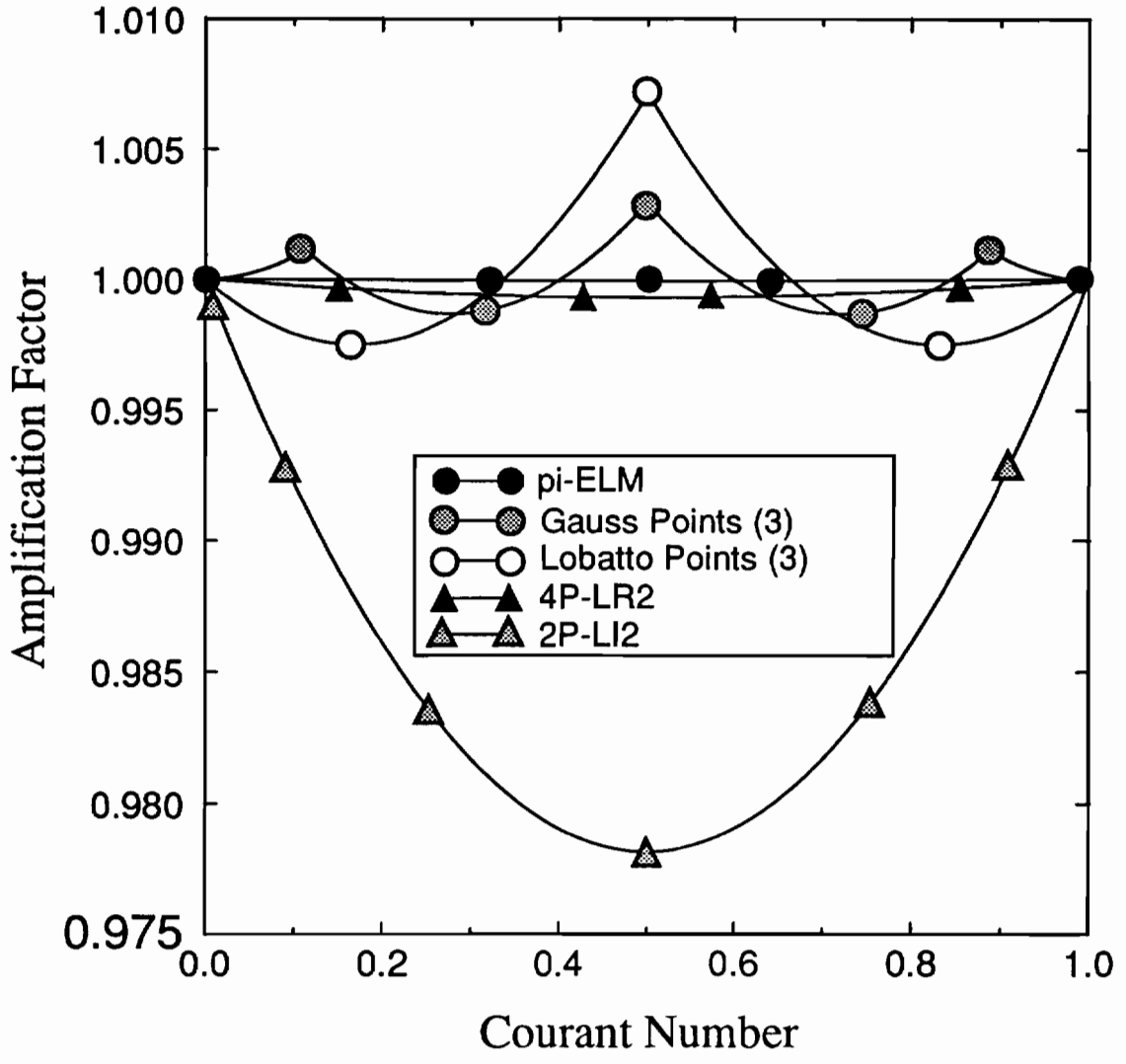

Figure 2.22(a) Comparison of amplification factors for $L_m/\Delta x = 15$: pi-ELM, qu-ELM with 3 Gauss Points, qu-ELM with 3 Lobatto Points, 4P-LR2 and 2P-LI2.

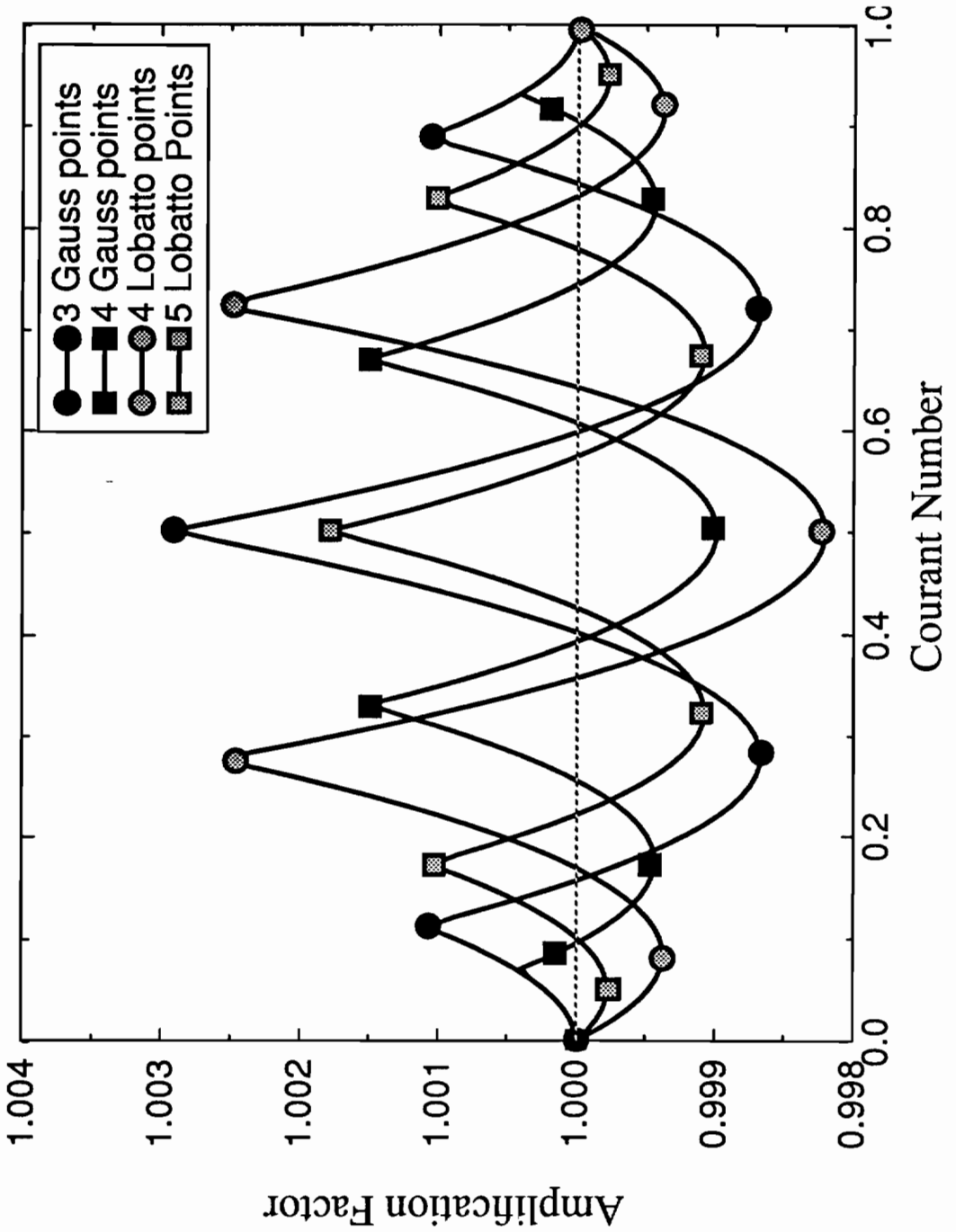

Figure 2.22(b) Comparison of amplification factors for $L_m/\Delta x = 15$: qu-ELM with 3 and 4 Gauss Points,qu-ELM with 4 and 5 Lobatto Points.

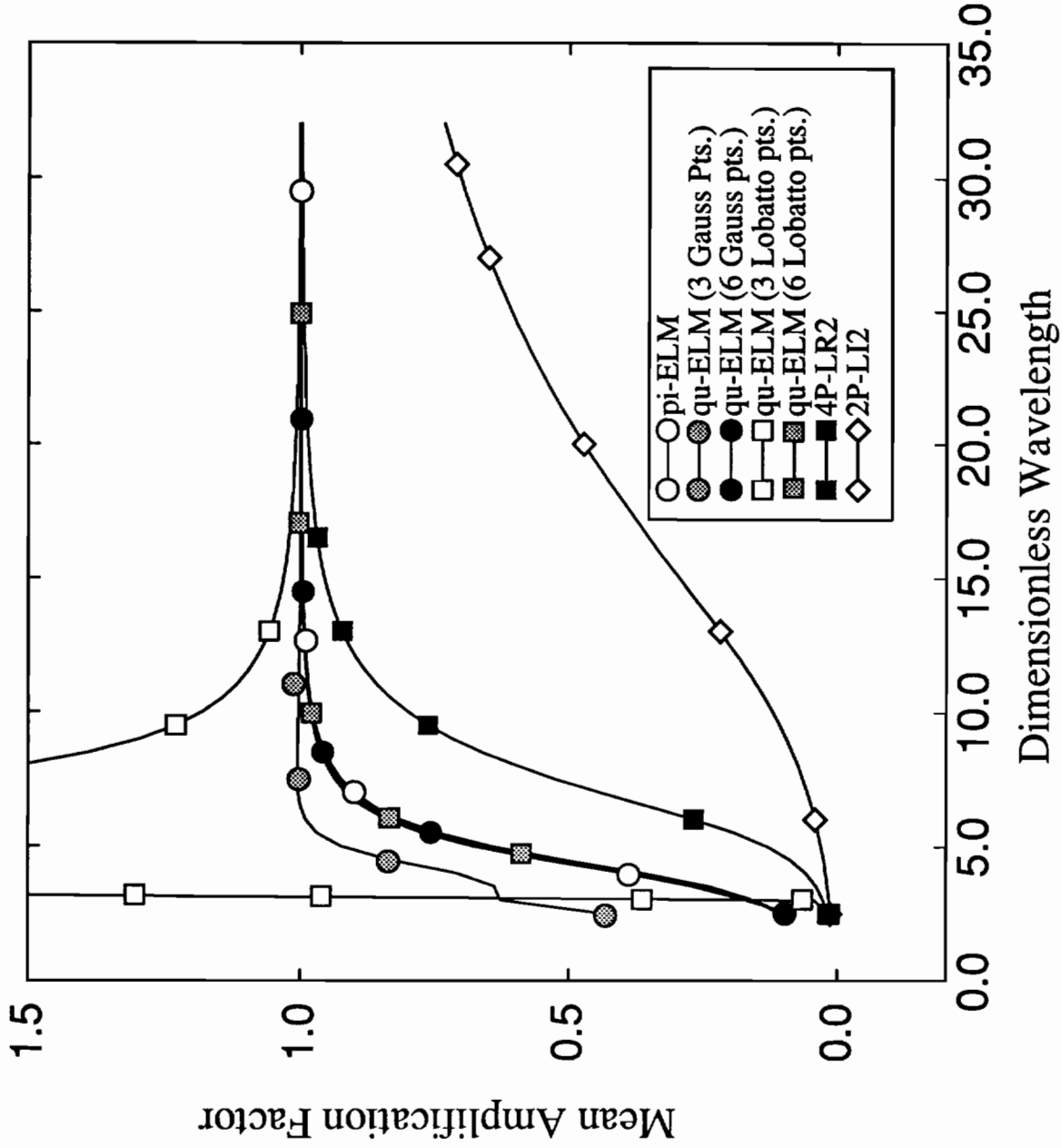

Figure 2.23(a) Comparison of mean amplification factors for all methods.

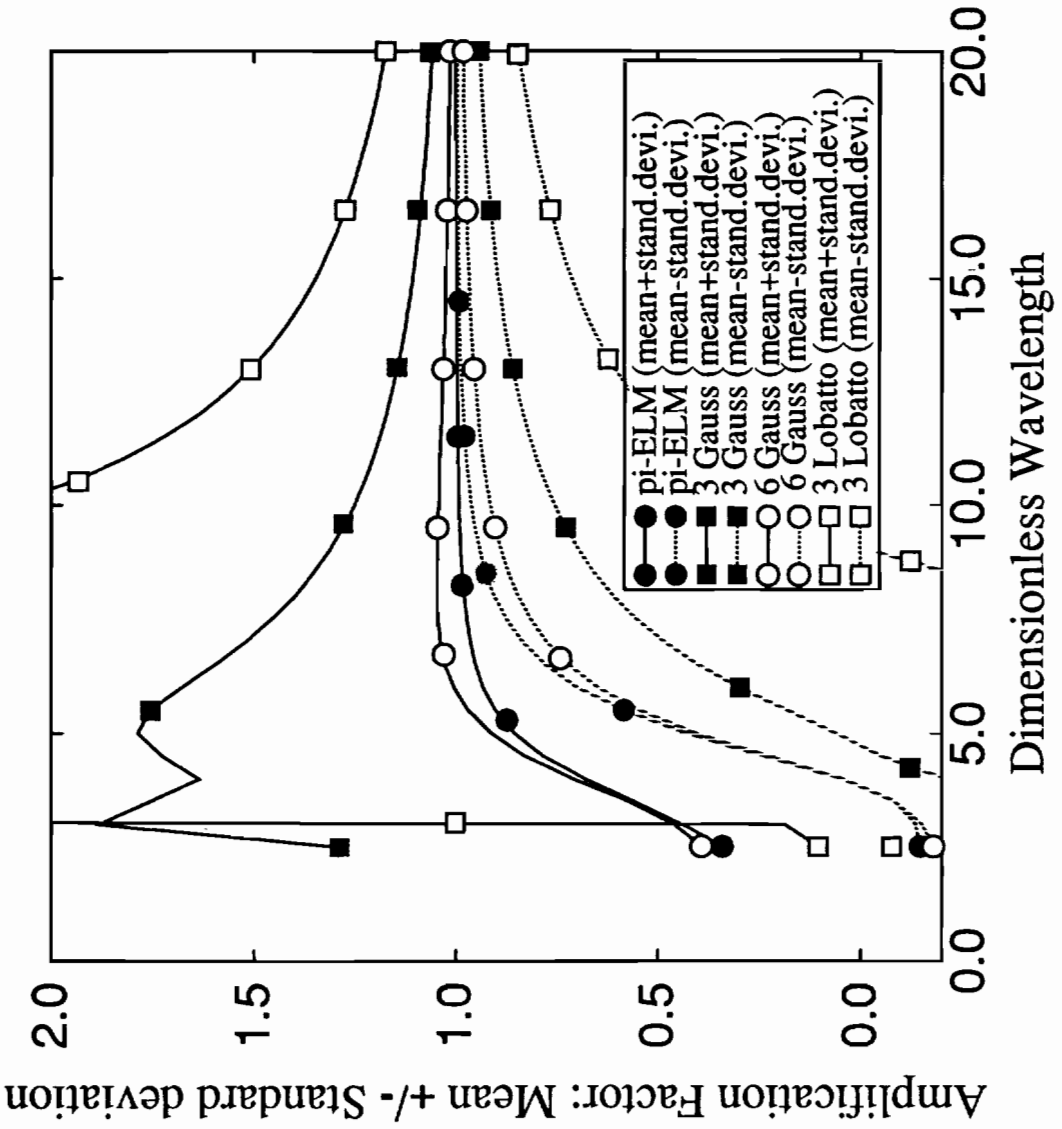

Figure 2.23(b) Comparison of amplification factors statistics for all methods: range limited by mean+standard deviation and mean-standard deviation, for the pi-ELM and qu-ELM (3 and 6 Gauss points, 3 Lobatto points).

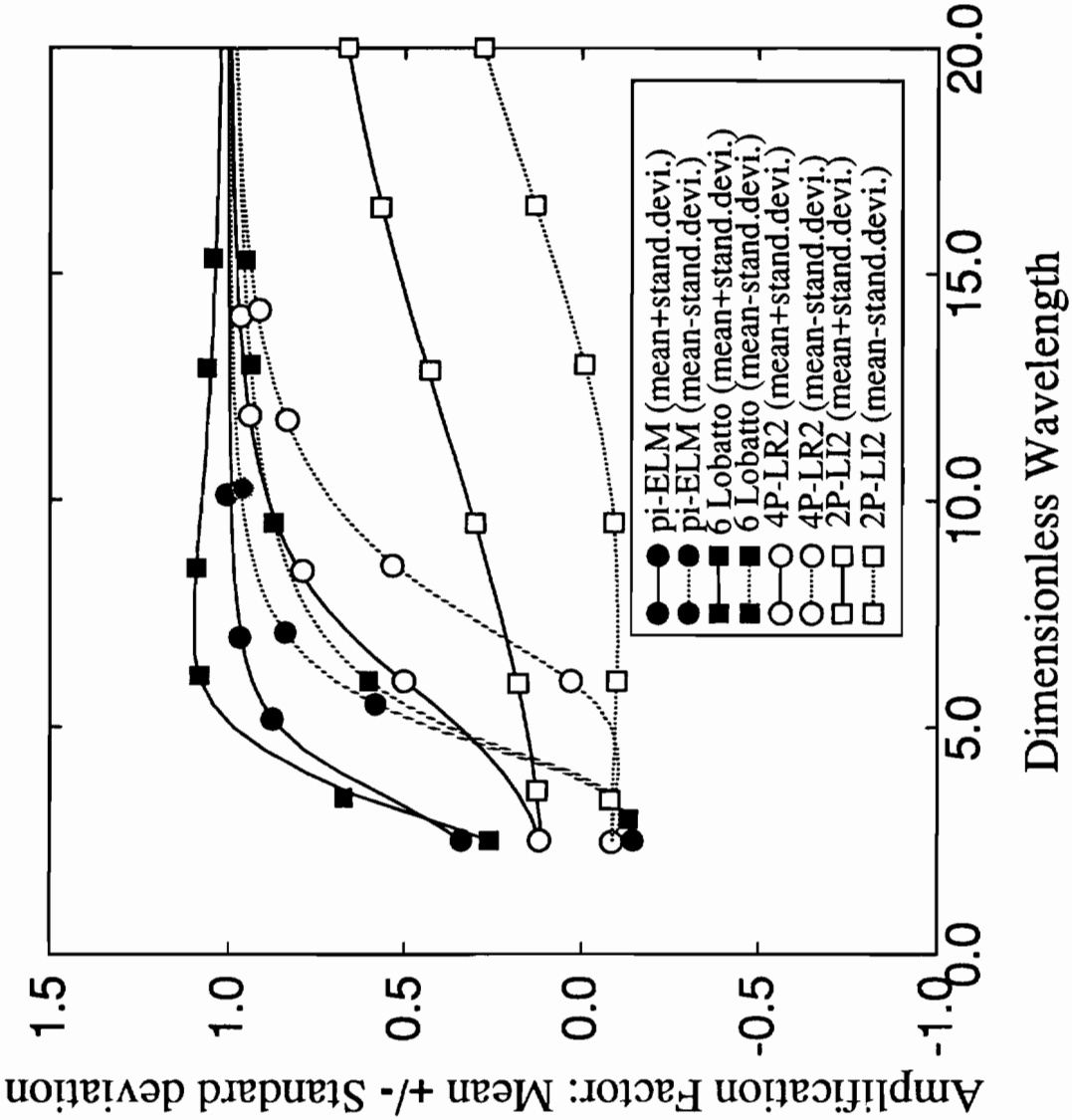

Figure 2.23(c) Comparison of amplification factors statistics for all methods: range limited by mean+standard deviation and mean-standard deviation, for the pi-ELM, qu-ELM(6 Lobatto points), 4P-LR2 and 2P-LI2.

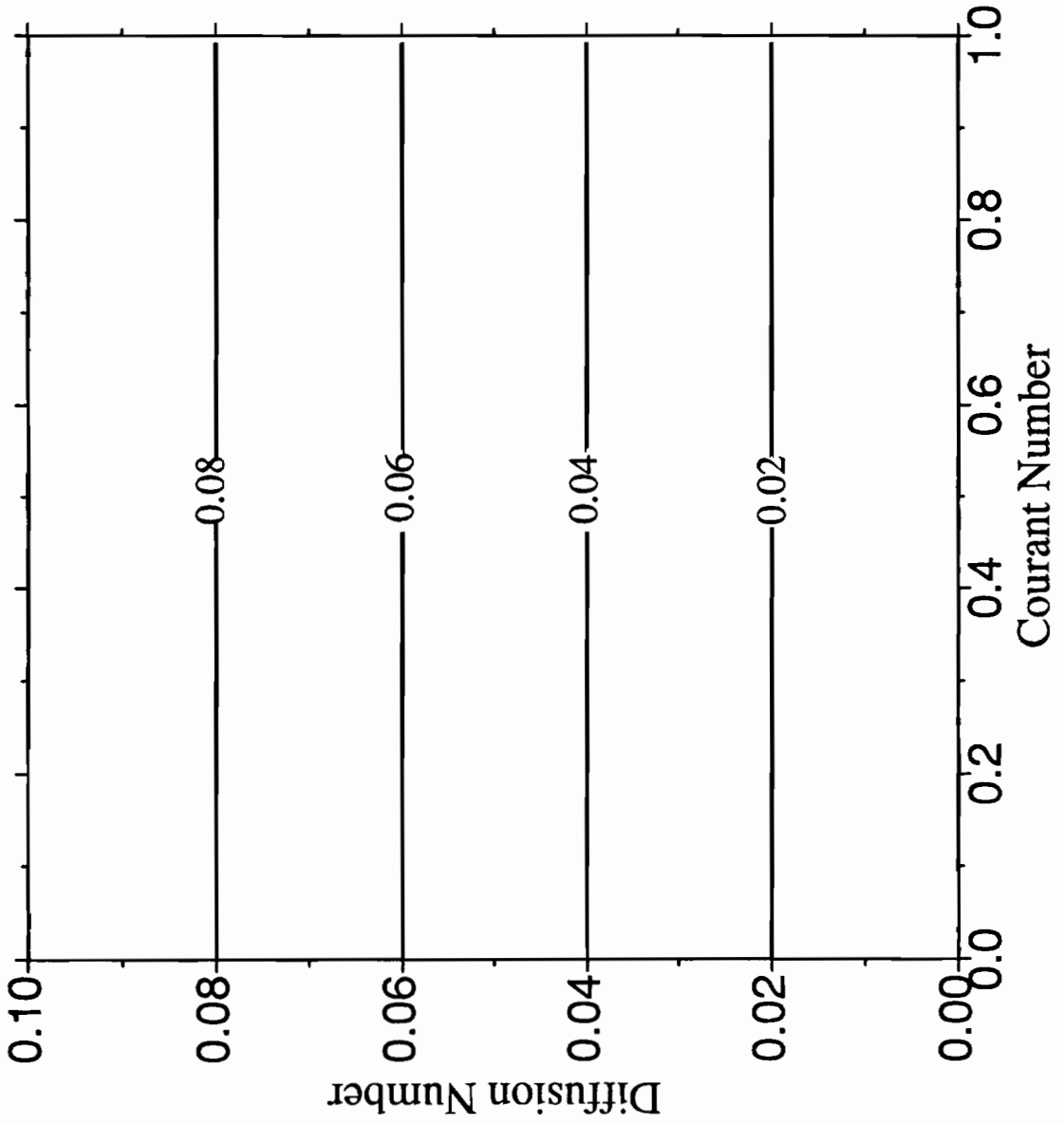

Figure 2.24 Truncation error - effective diffusion number for the pi-ELM.

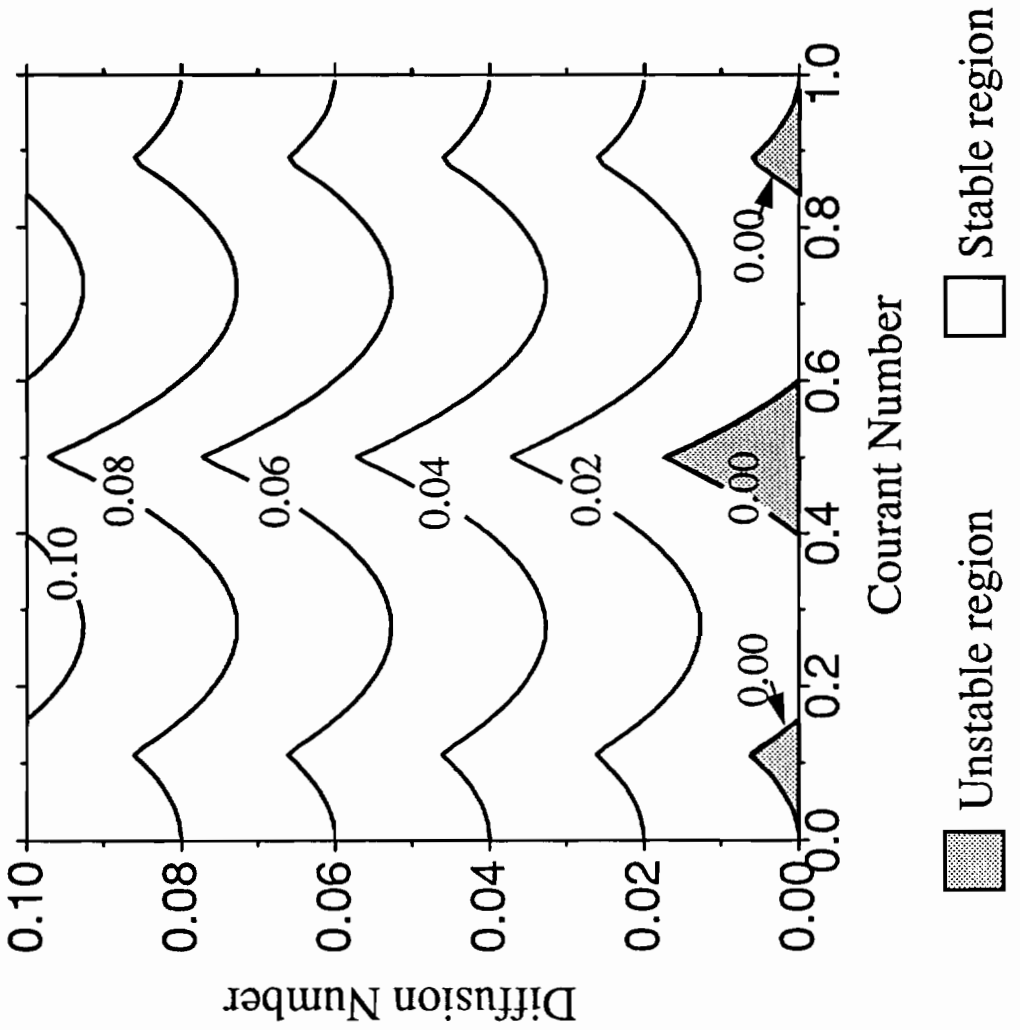

Figure 2.25 Truncation error - effective diffusion number for the qu-ELM with 3 Gauss Points.

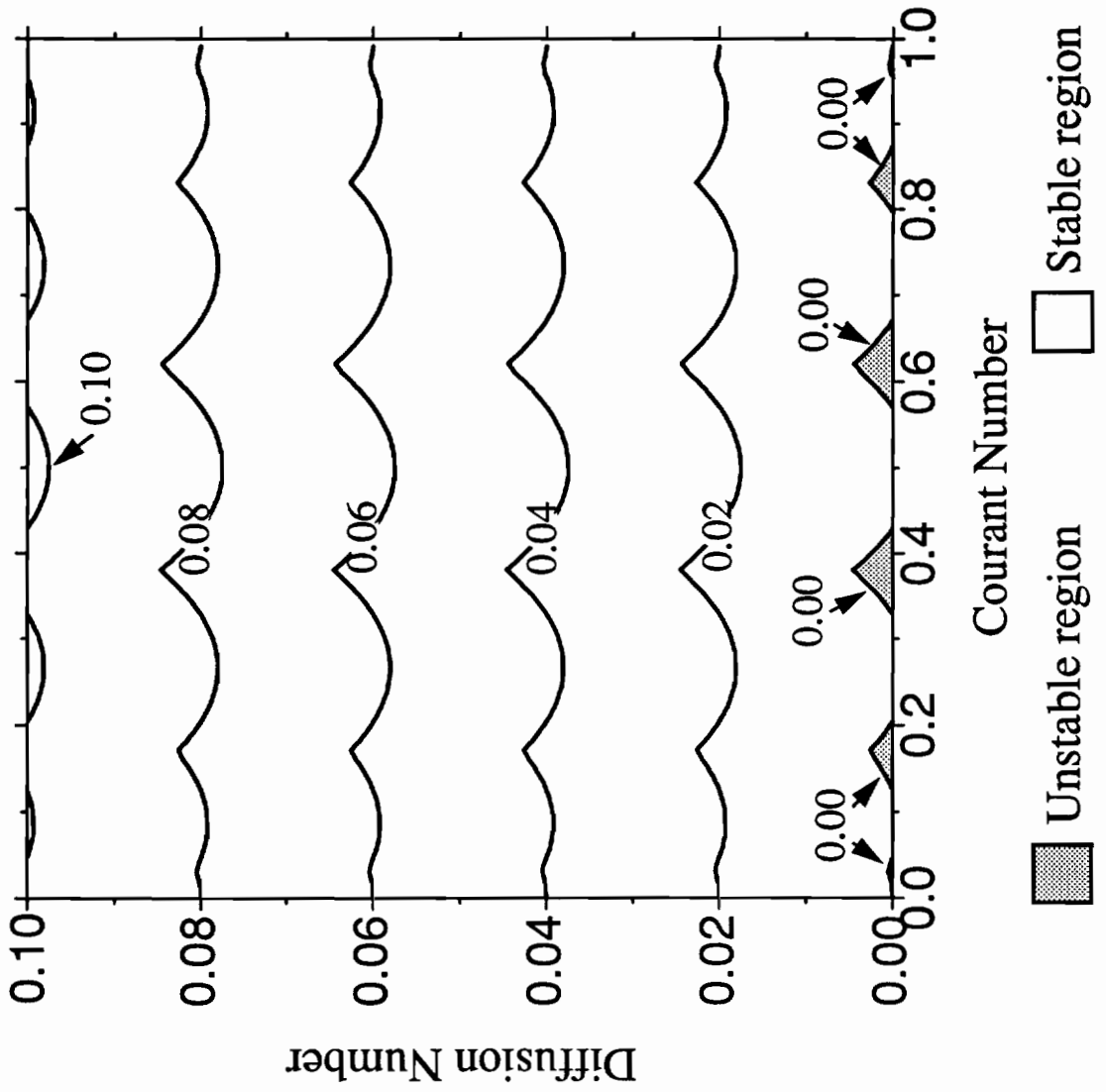

Figure 2.26 Truncation error - effective diffusion number for the qu-ELM with 6 Gauss Points.

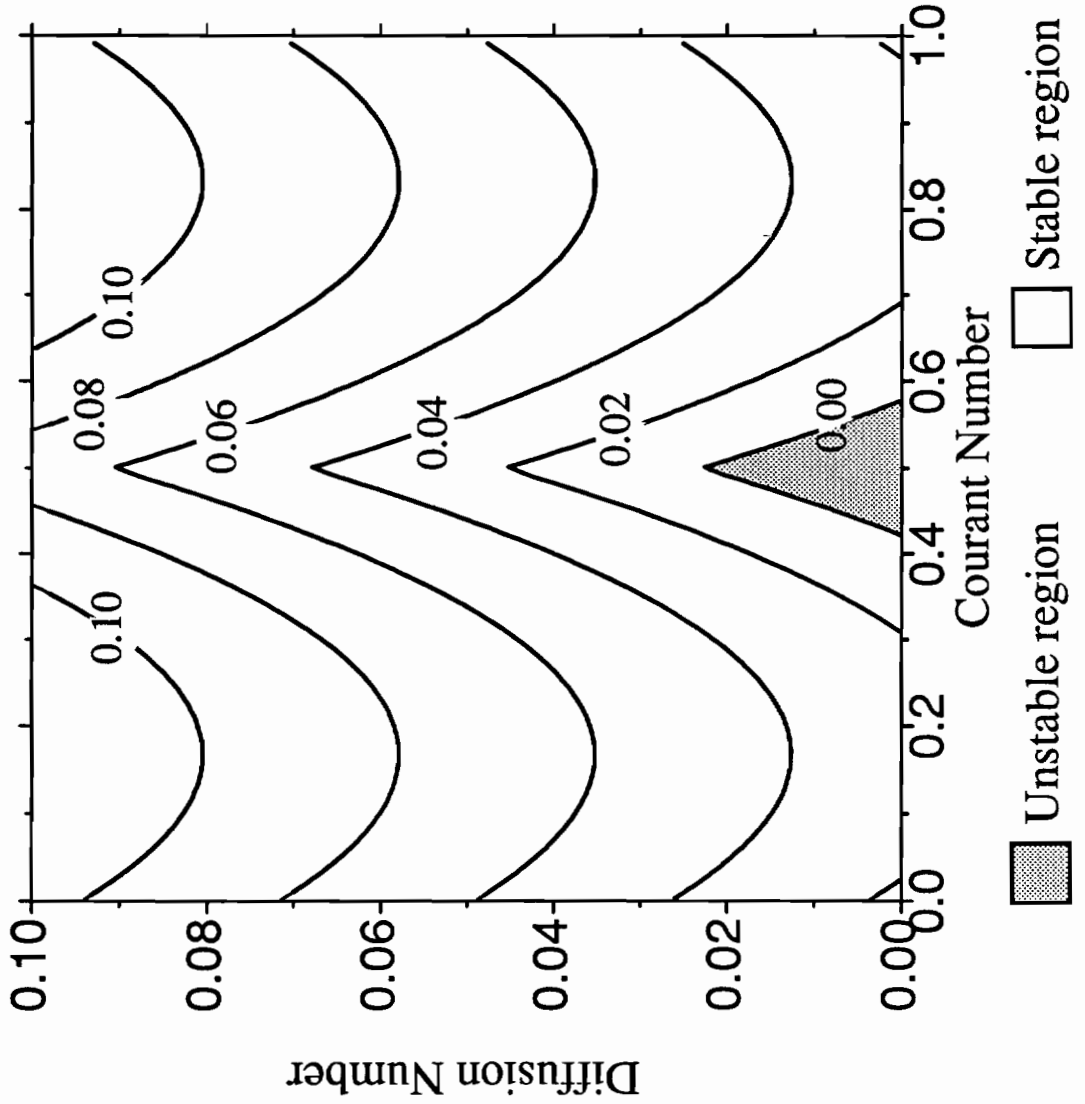

Figure 2.27 Truncation error - effective diffusion number for the qu-ELM with 3 Lobatto Points.

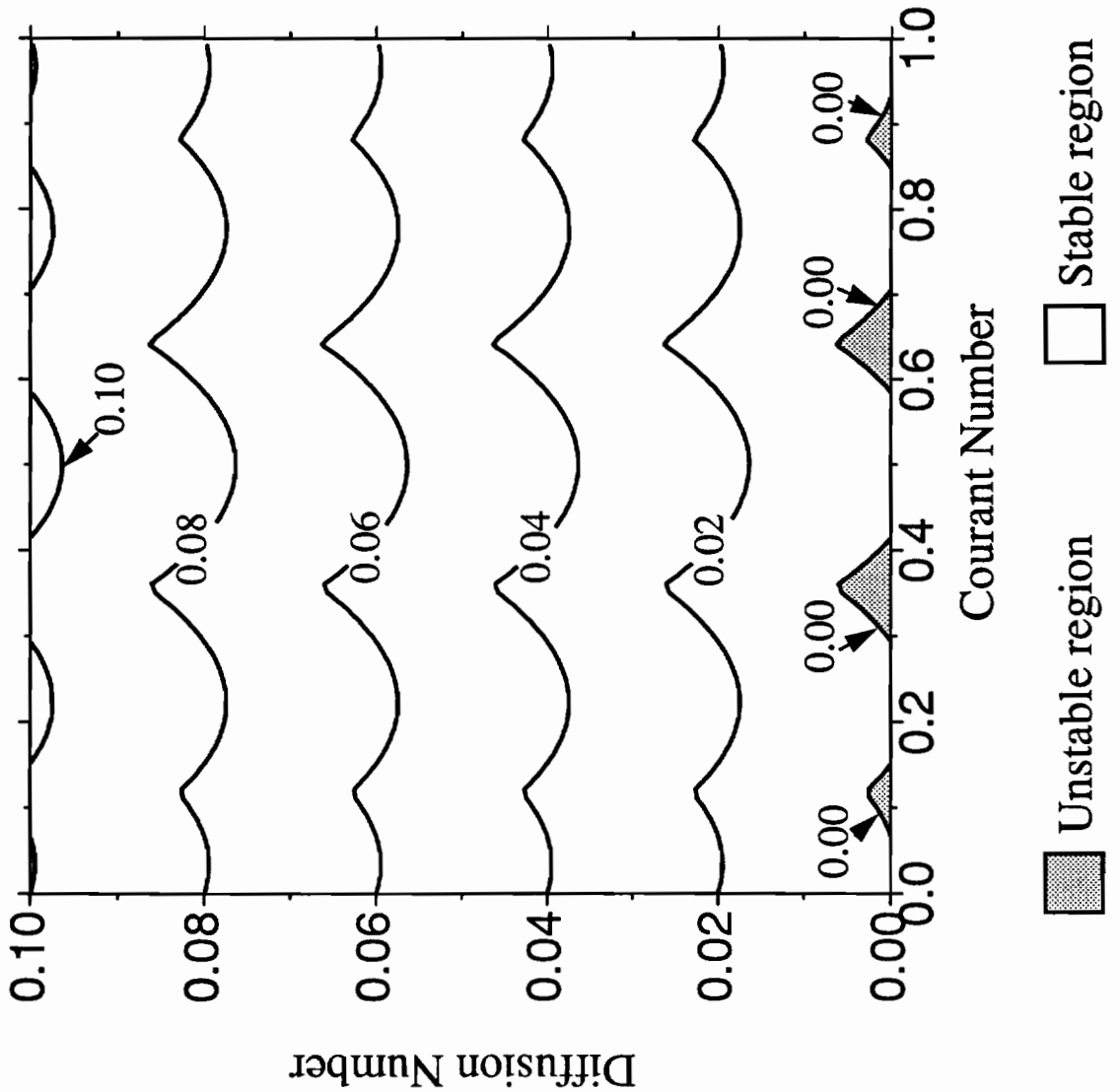

Figure 2.28 Truncation error - effective diffusion number for the qu-ELM with 6 Lobatto Points.

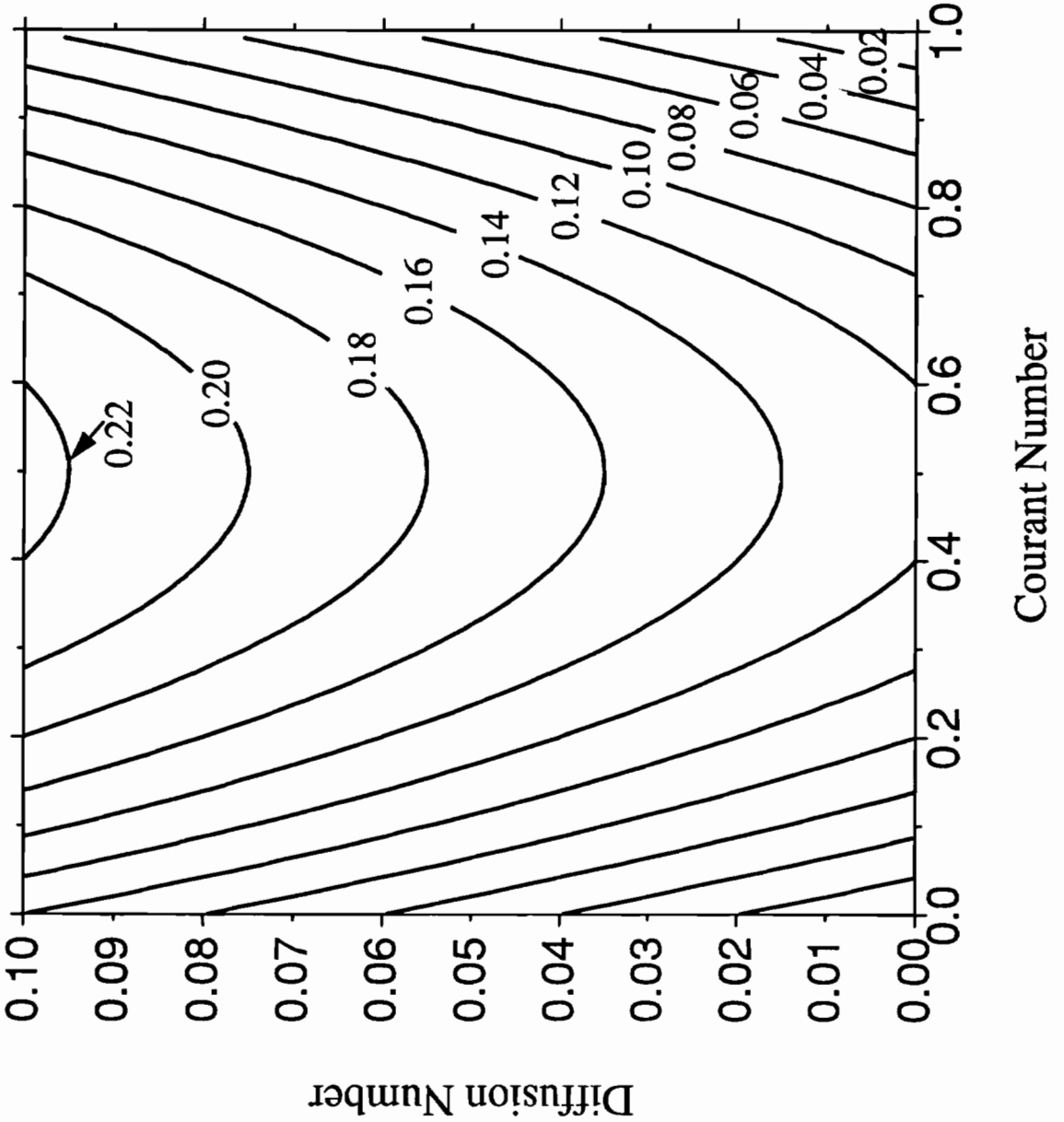

Figure 2.29 Truncation error - effective diffusion number for the 2P-LI2.

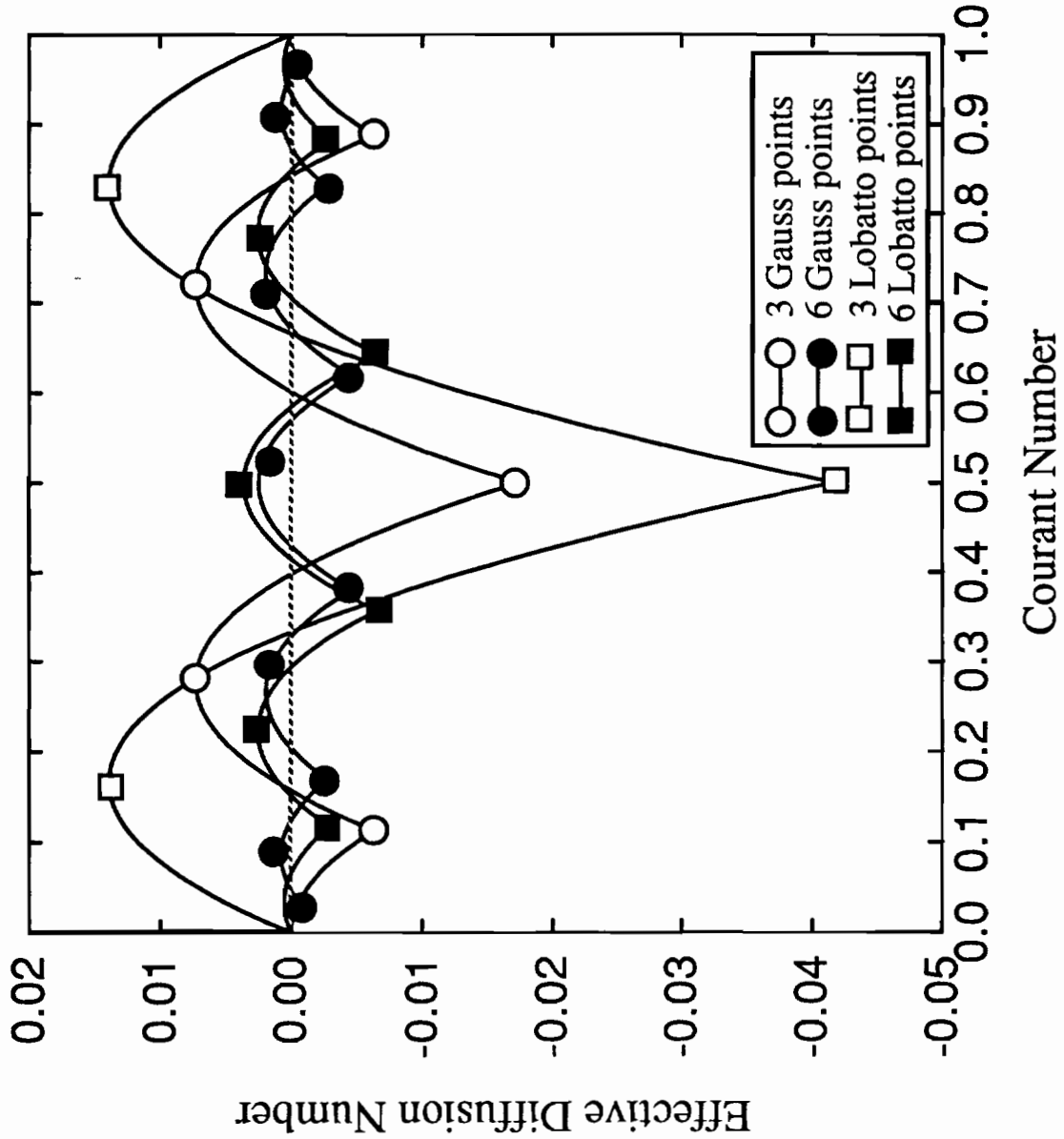

Figure 2.30 Comparison of the effective diffusion number for alternative qu-ELM, for $D = 0$.

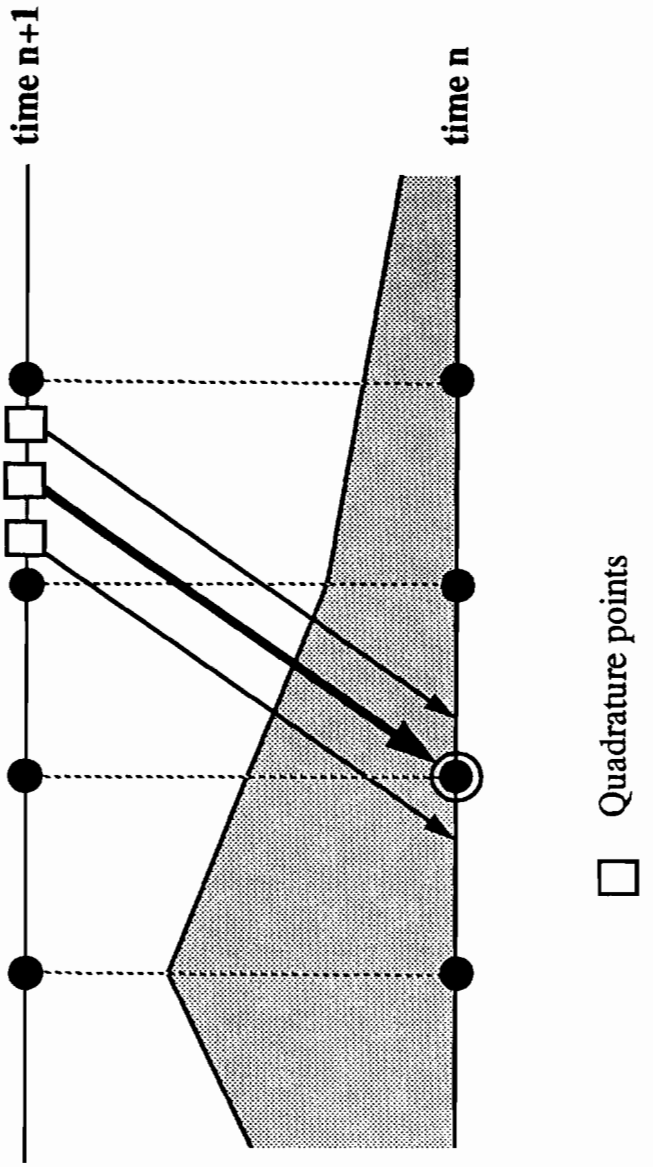

Figure 2.31 Instability of the qu-ELMs: a maximum of negative effective diffusion number occurs when the foot of the characteristic line of a quadrature point coincides with a node.

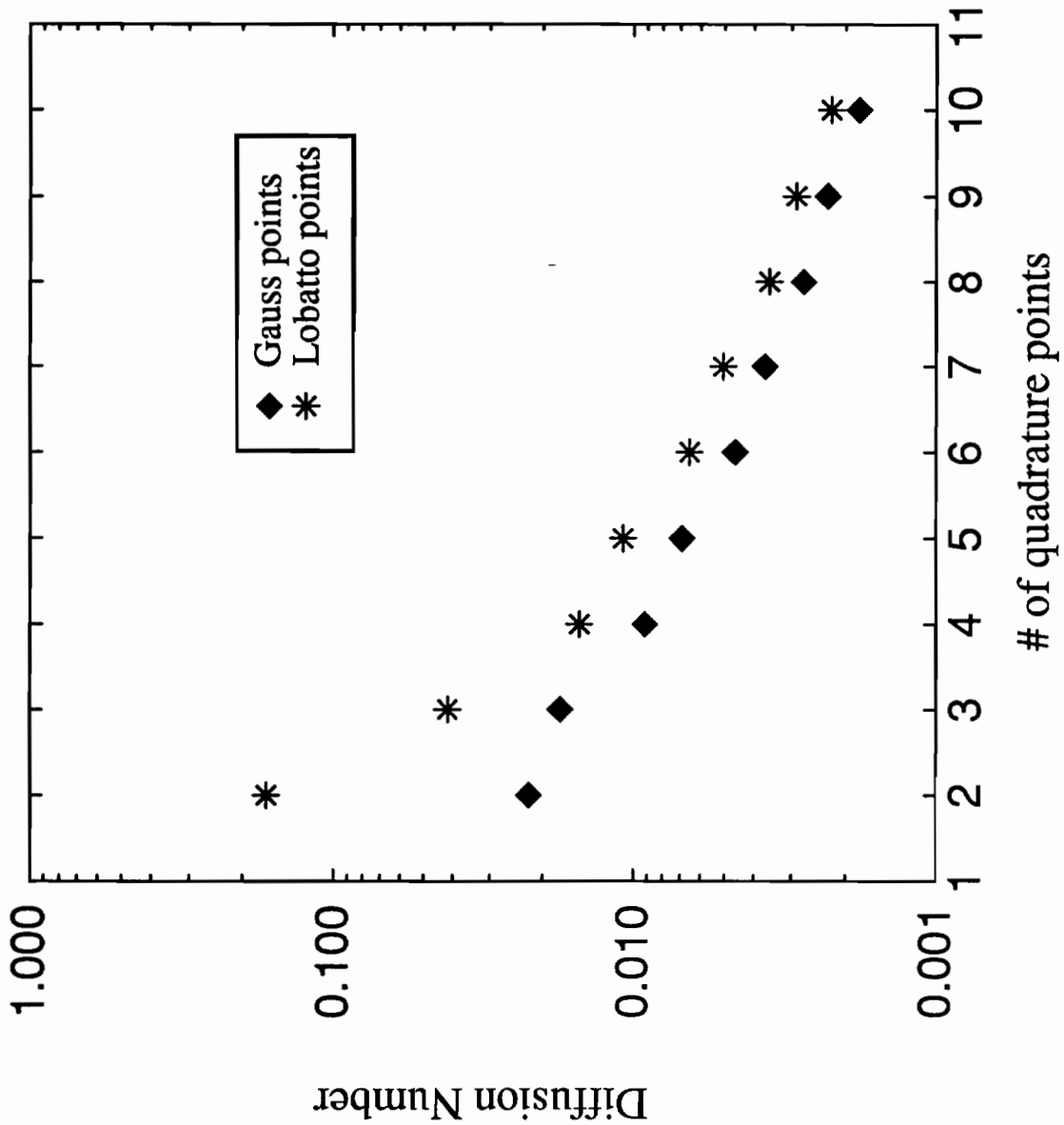

Figure 2.32 Comparison of the Diffusion numbers required to stabilize the qu-ELM with Gauss and Lobatto points, for several numbers of quadrature points.

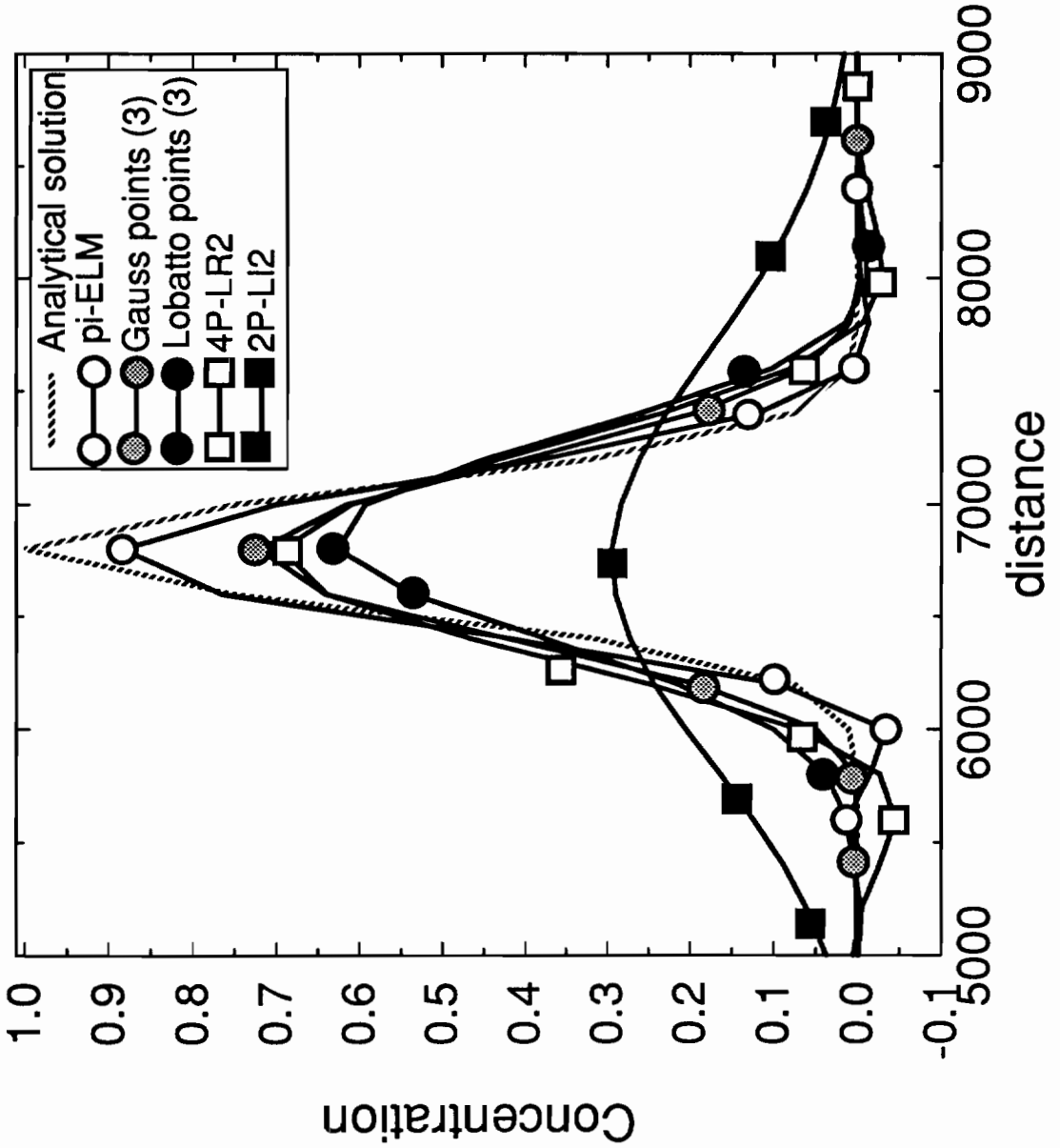

Figure 2.33 Convection-Diffusion forum - case 1A.

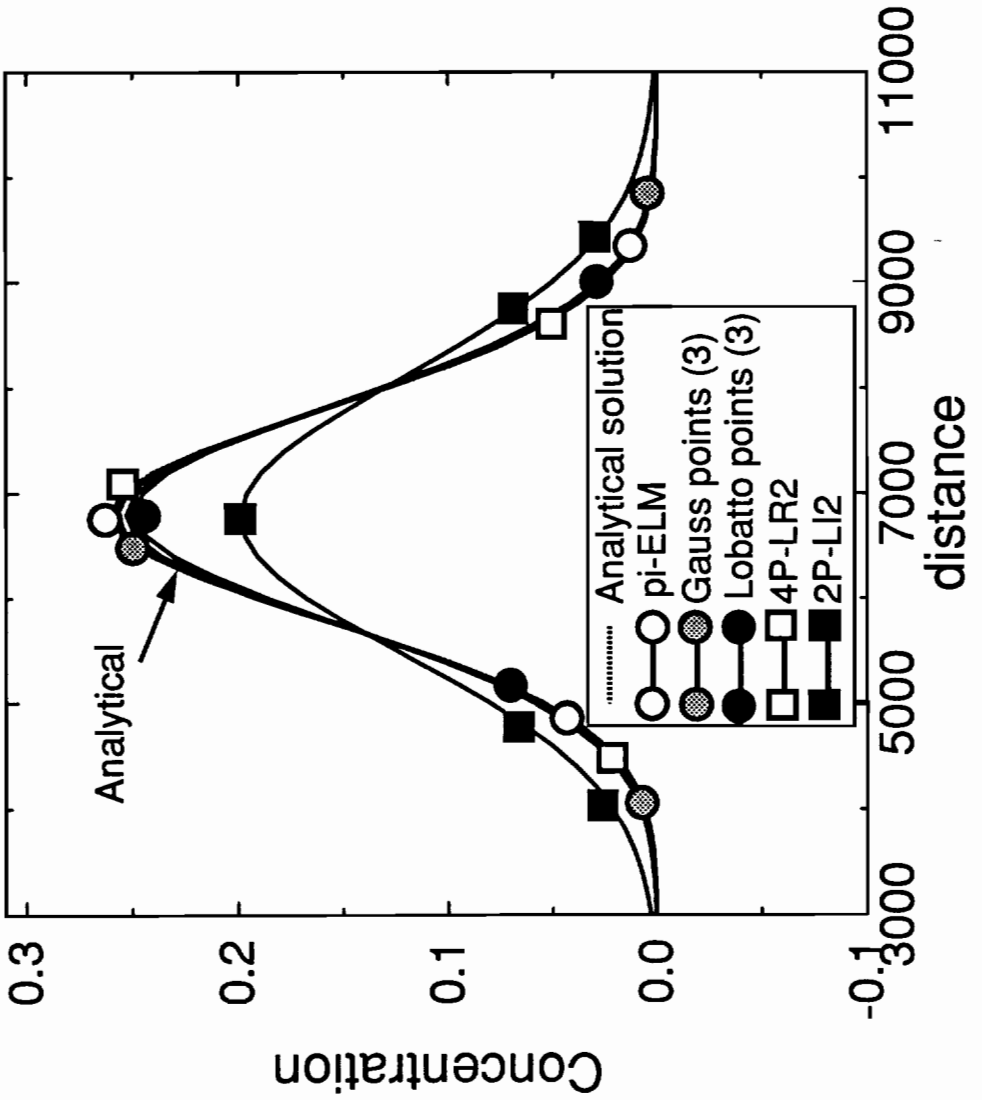

Figure 2.34 Convection-Diffusion forum - case 1C.

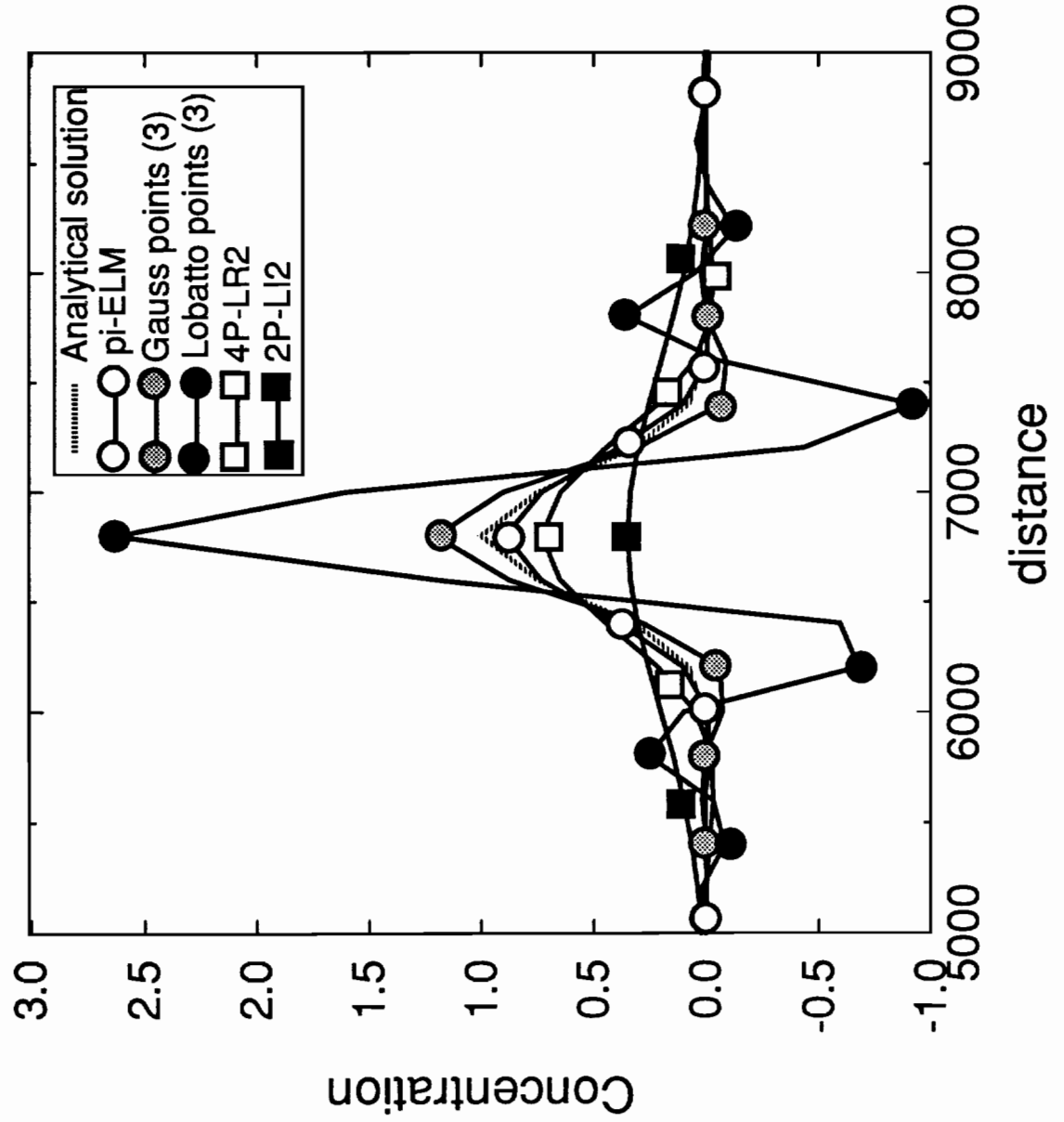

Figure 2.35 Convection-Diffusion forum - case 1K.

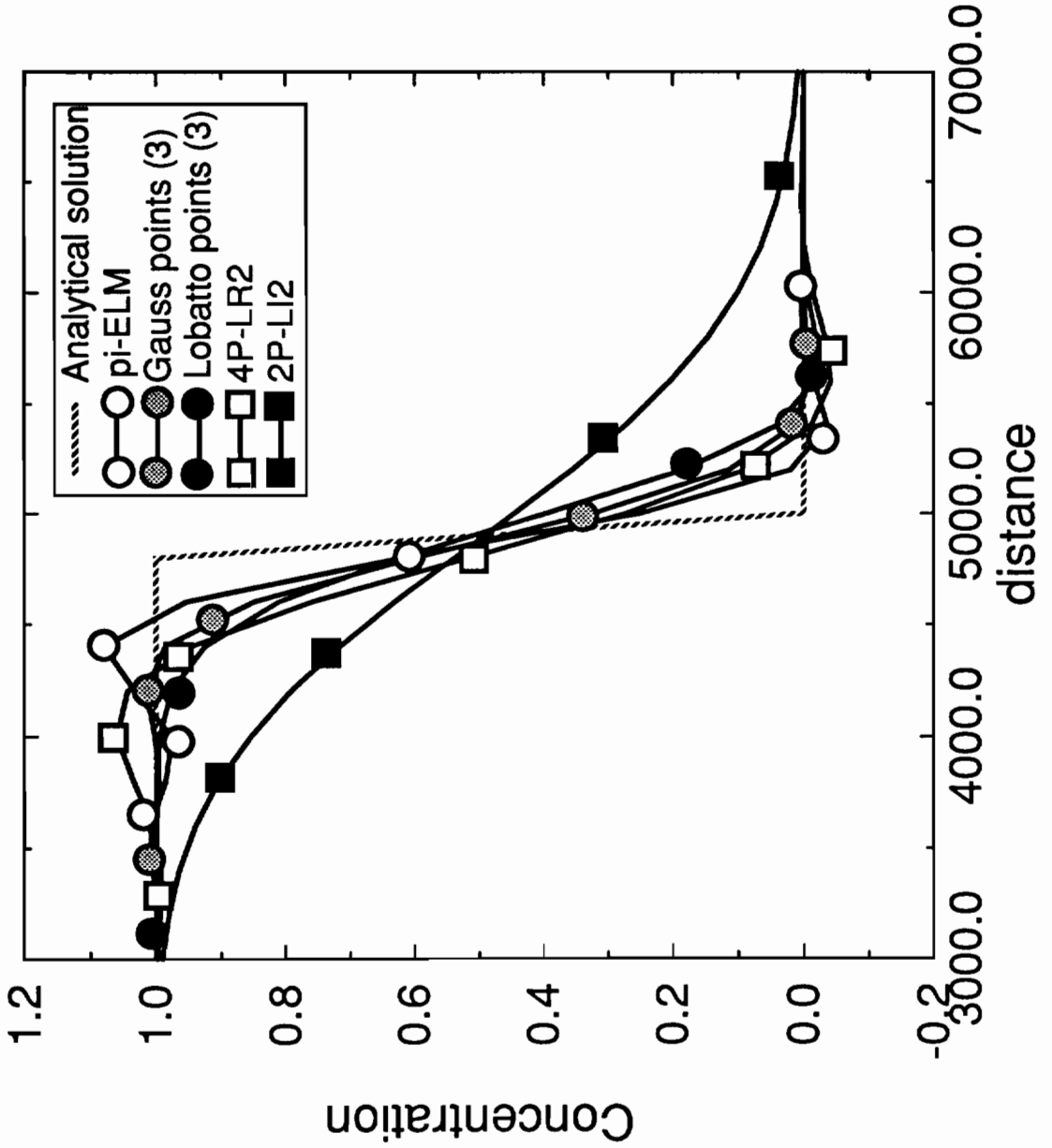

Figure 2.36 Convection-Diffusion forum - case 3A.

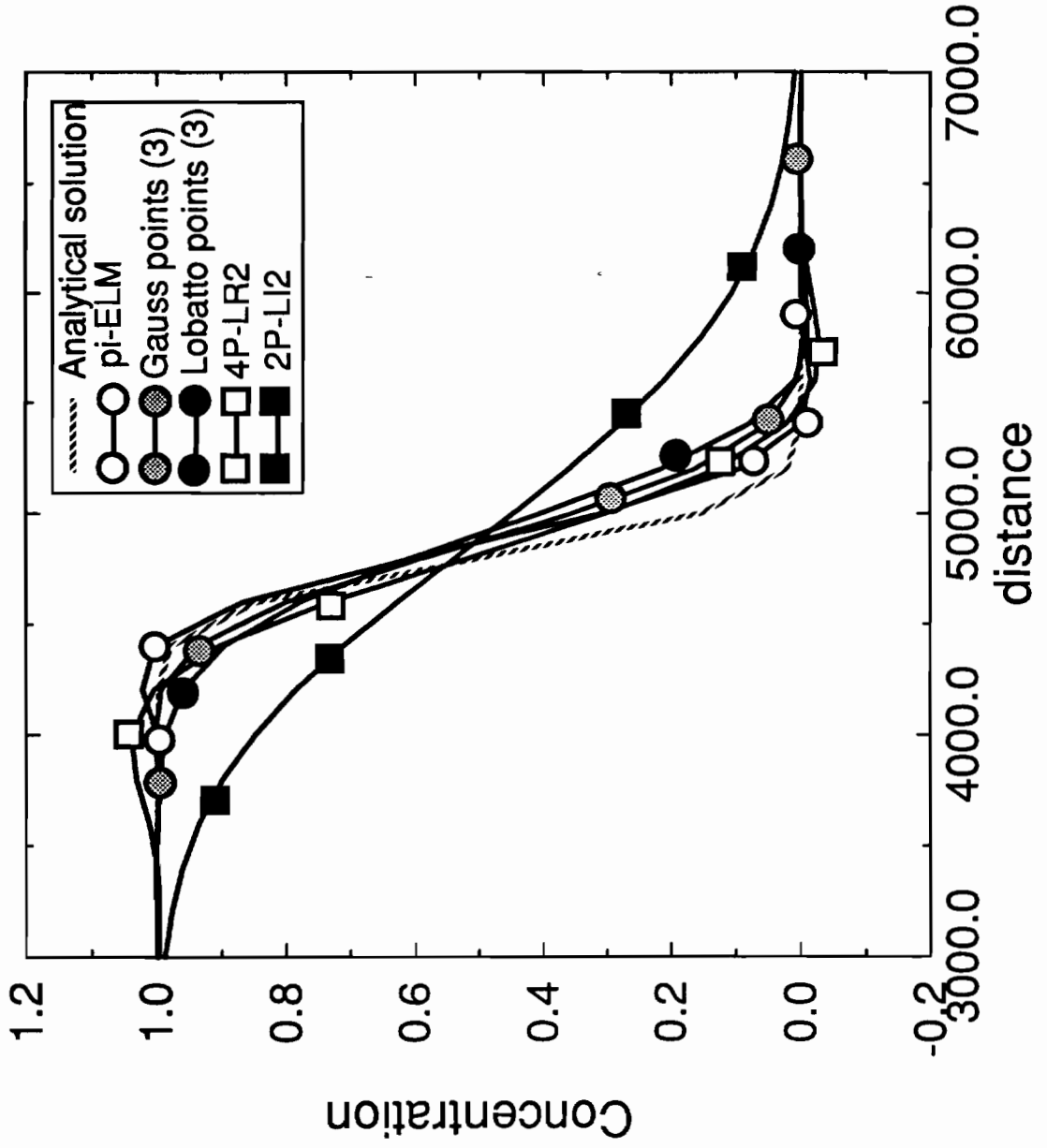

Figure 2.37 Convection-Diffusion forum - case 3B.

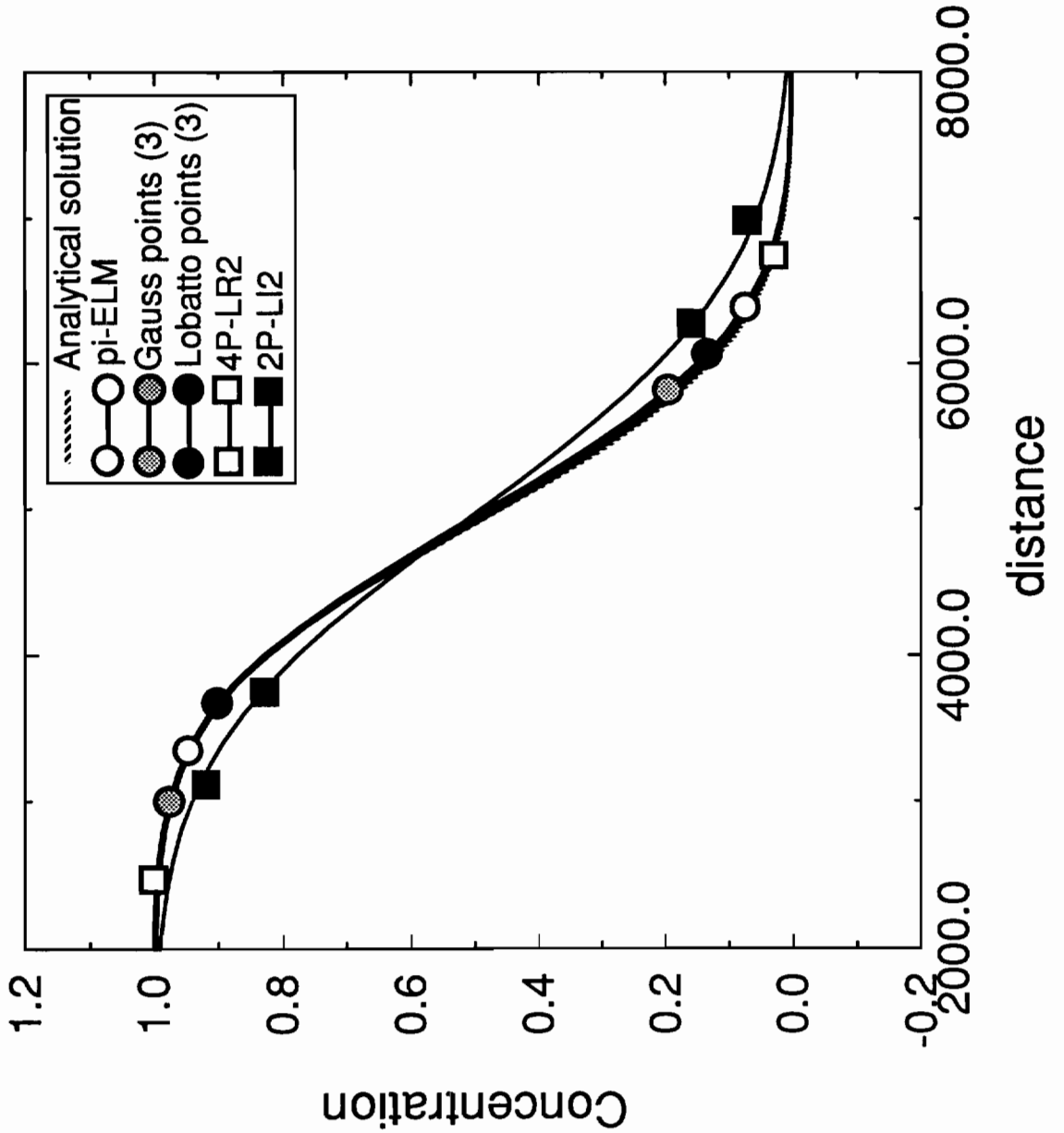

Figure 2.38 Convection-Diffusion forum - case 3C.

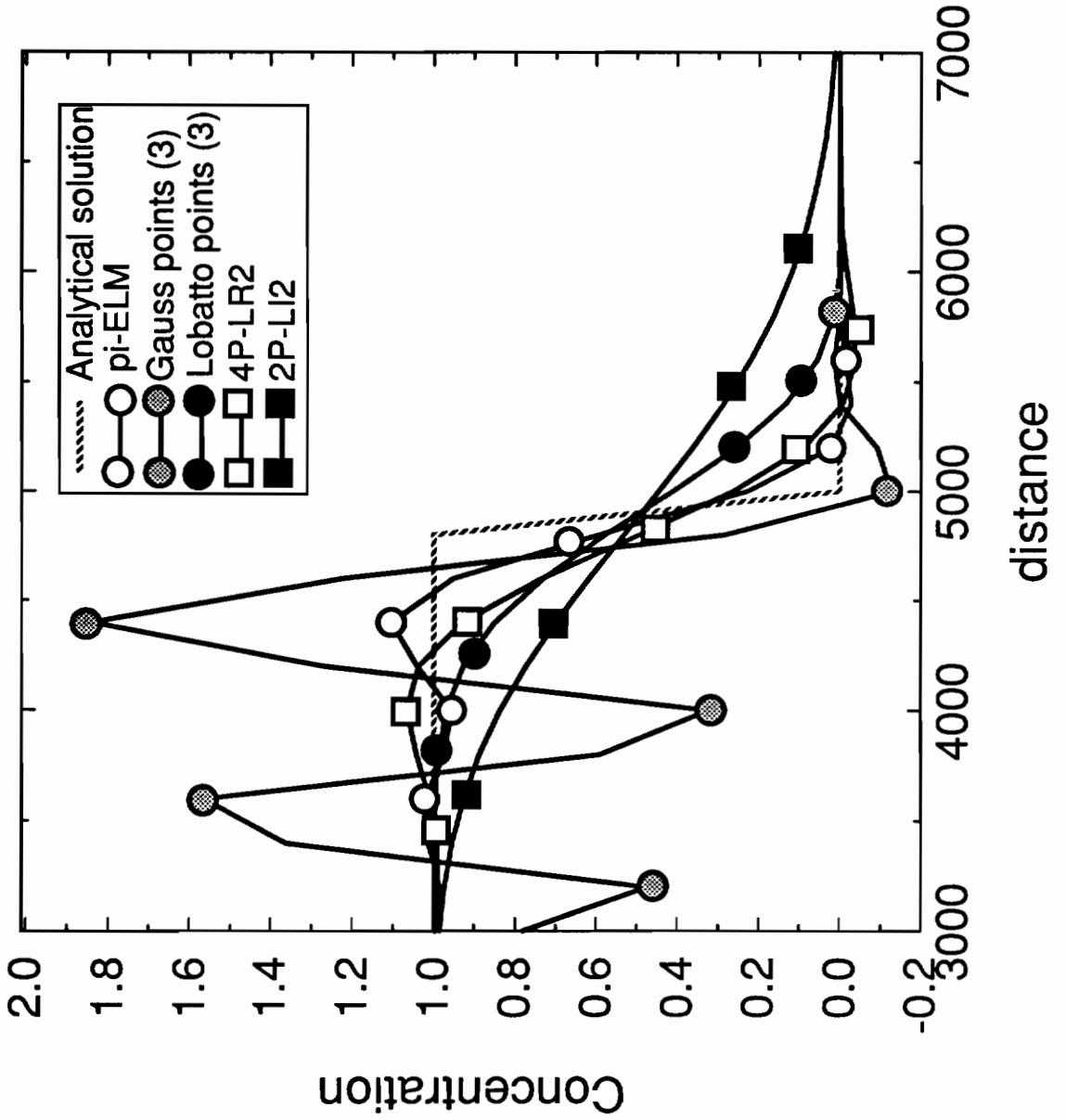

Figure 2.39 Convection-Diffusion forum - case 3F.

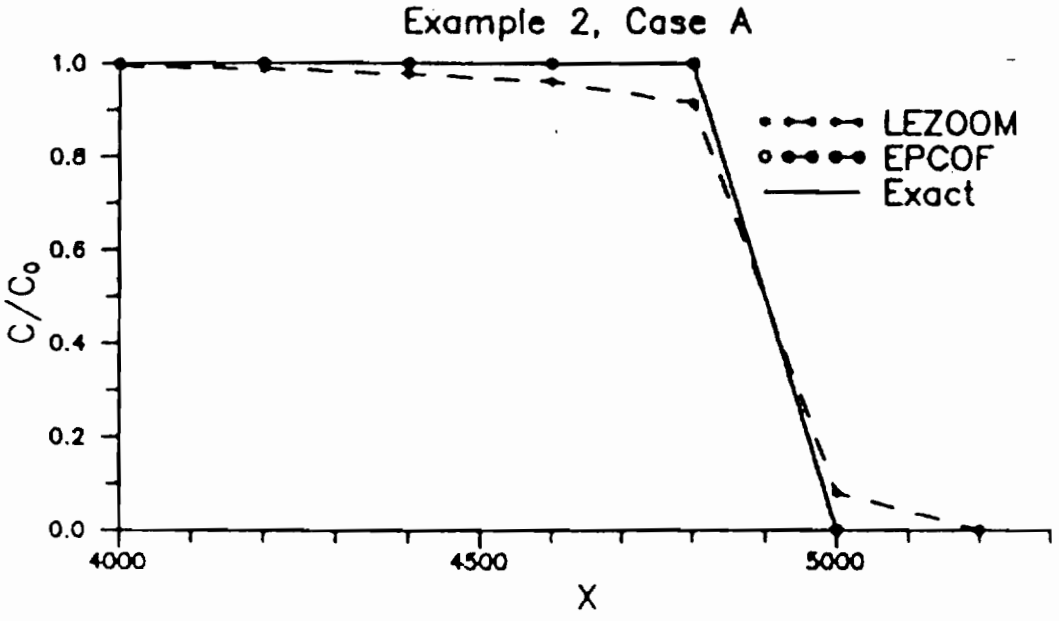

Figure 2.40 Yeh's method (EPCOF): Case 3A from the CD forum (*extracted from Yeh, et al.*, 1992)

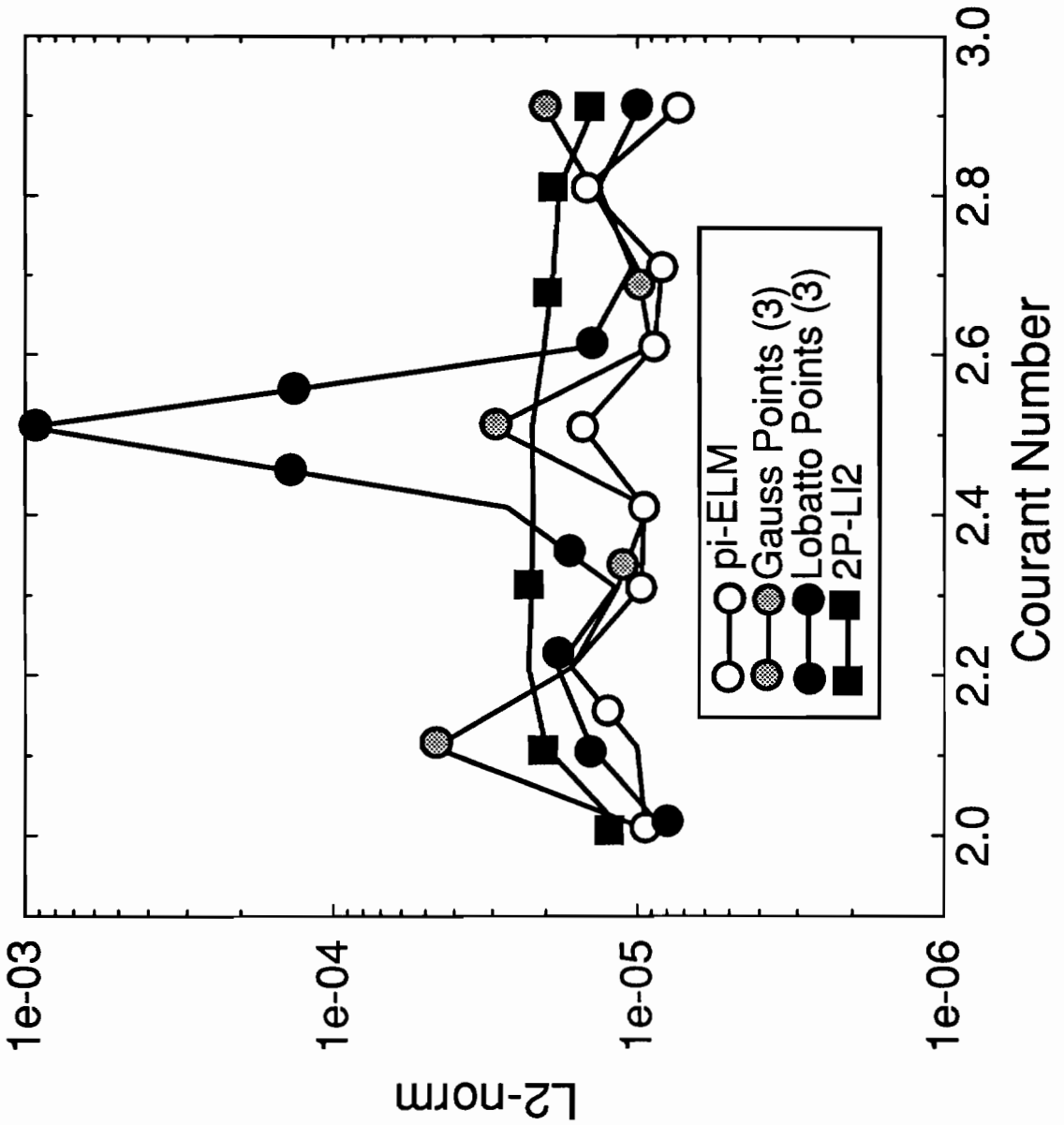

Figure 2.41(a) Influence of the fractional part of β, for an advancing front, with $D = 0$: L2-norm: pi-ELM, qu-ELM (3 Gauss points), qu-ELM (3 Lobatto points) and 2P-LI2.

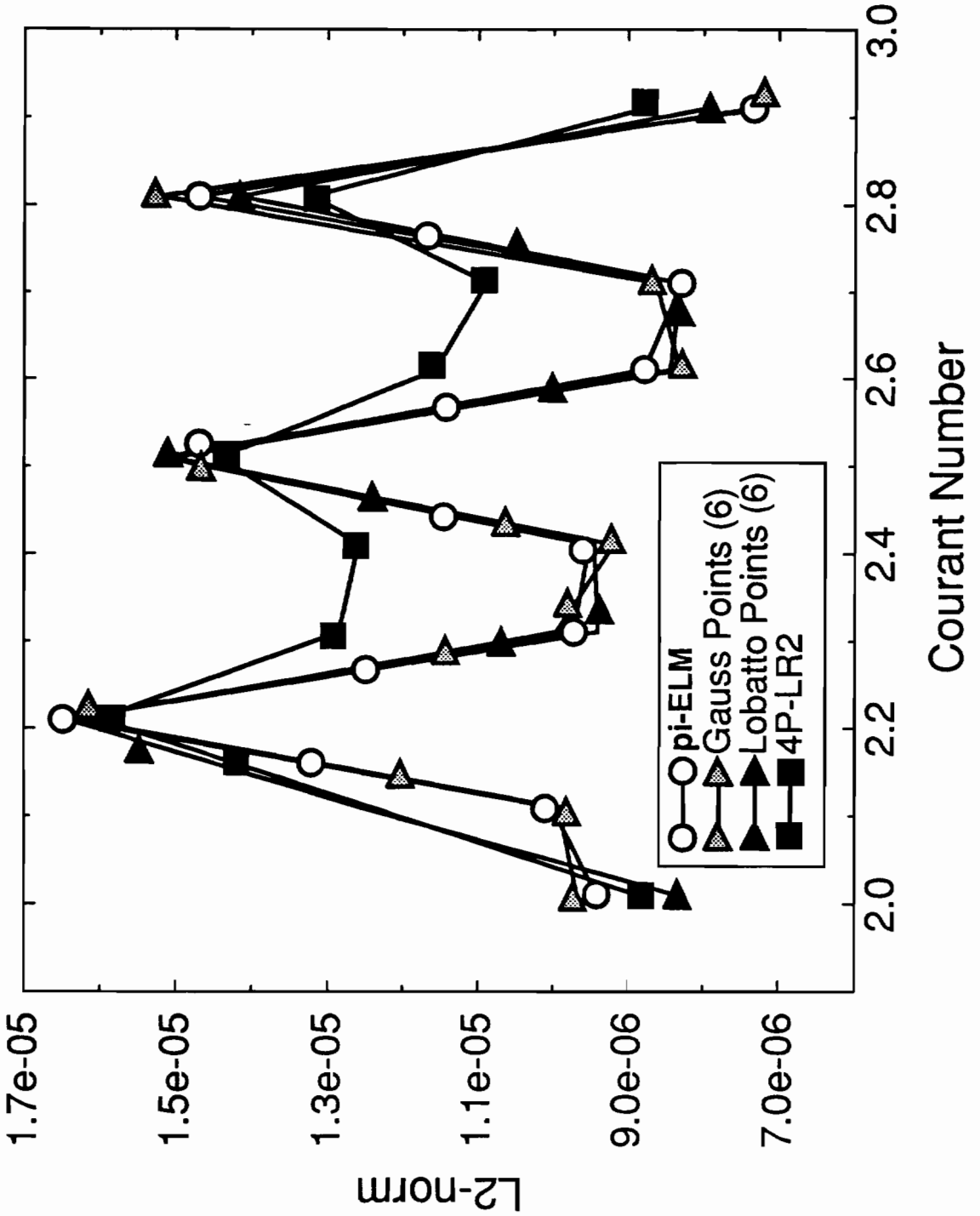

Figure 2.41(b) Influence of the fractional part of β, for an advancing front, with $D = 0$: L2-norm: pi-ELM, qu-ELM (6 Gauss points), qu-ELM (6 Lobatto points) and 4P-LI2.

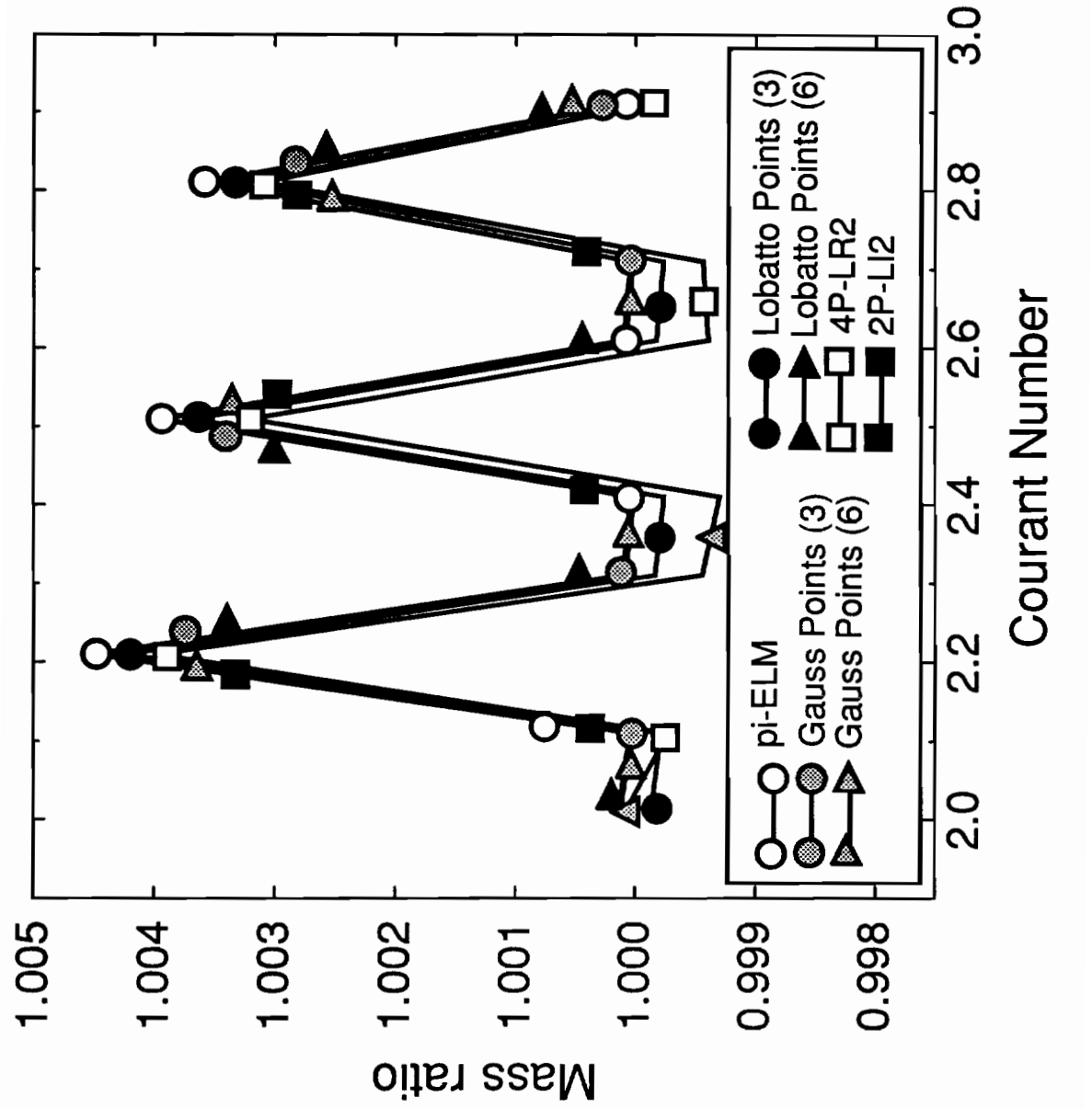

Figure 2.41(c) Influence of the fractional part of β, for an advancing front, with $D = 0$: Mass ratio.

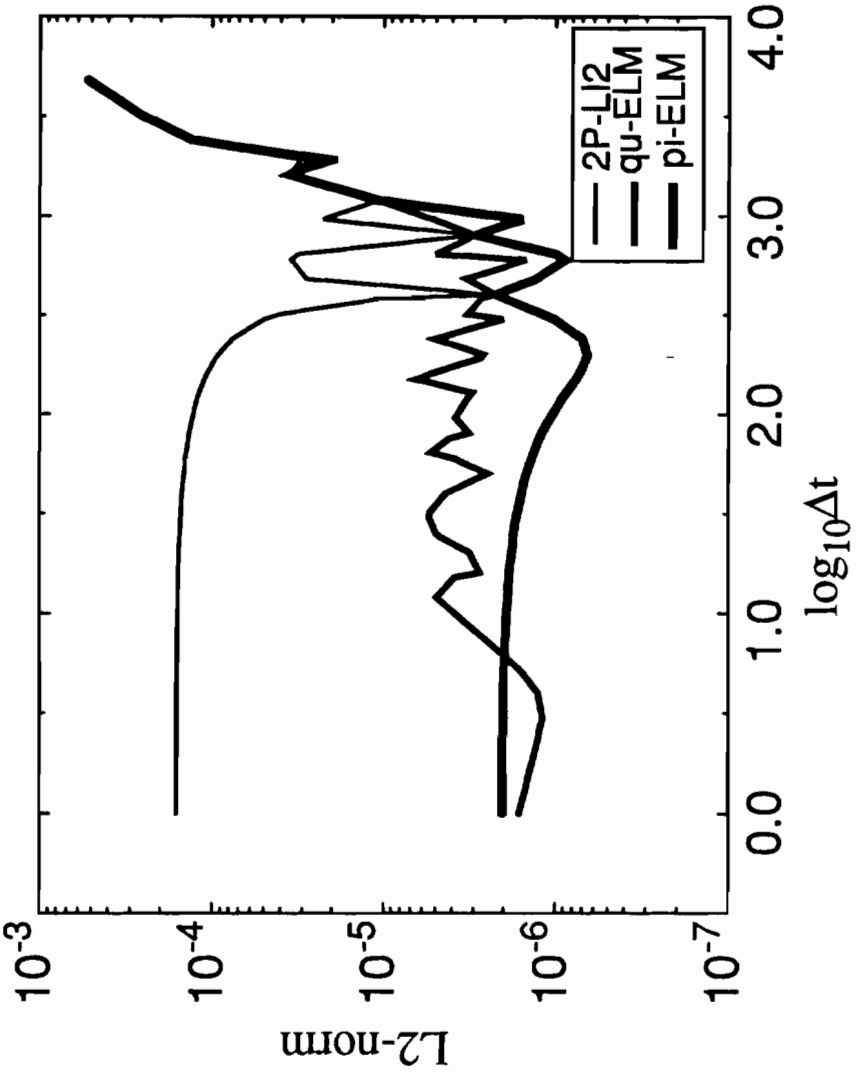

Figure 2.42 Dependence of L2-norm on the time step, for a Peclet number of 1

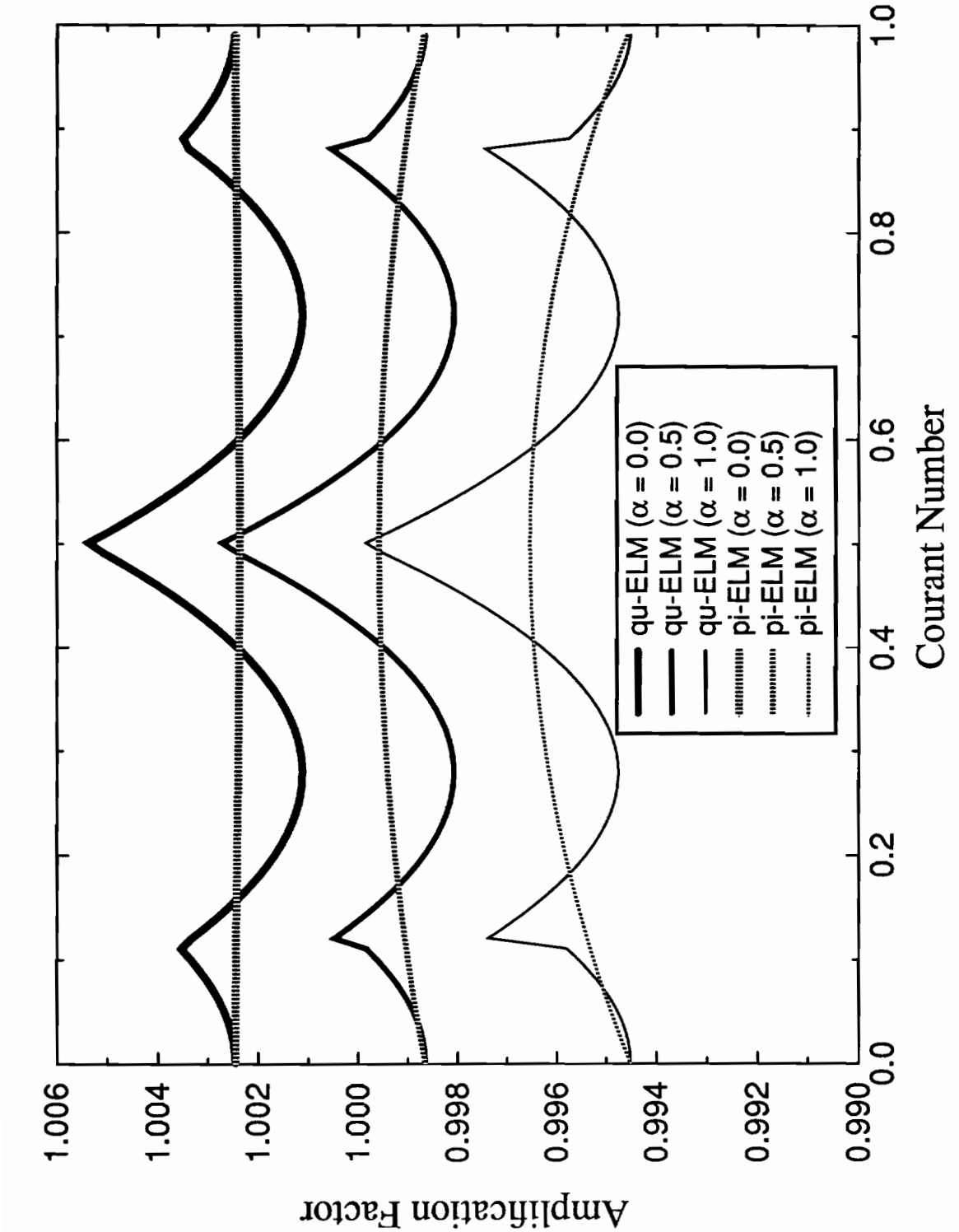

Figure 2.43 α sensitivity analysis: amplification factors for the pi-ELM and the qu-ELM with 3 Gauss points, for $L_m/\Delta x = 15$ and $D = 0.5$.

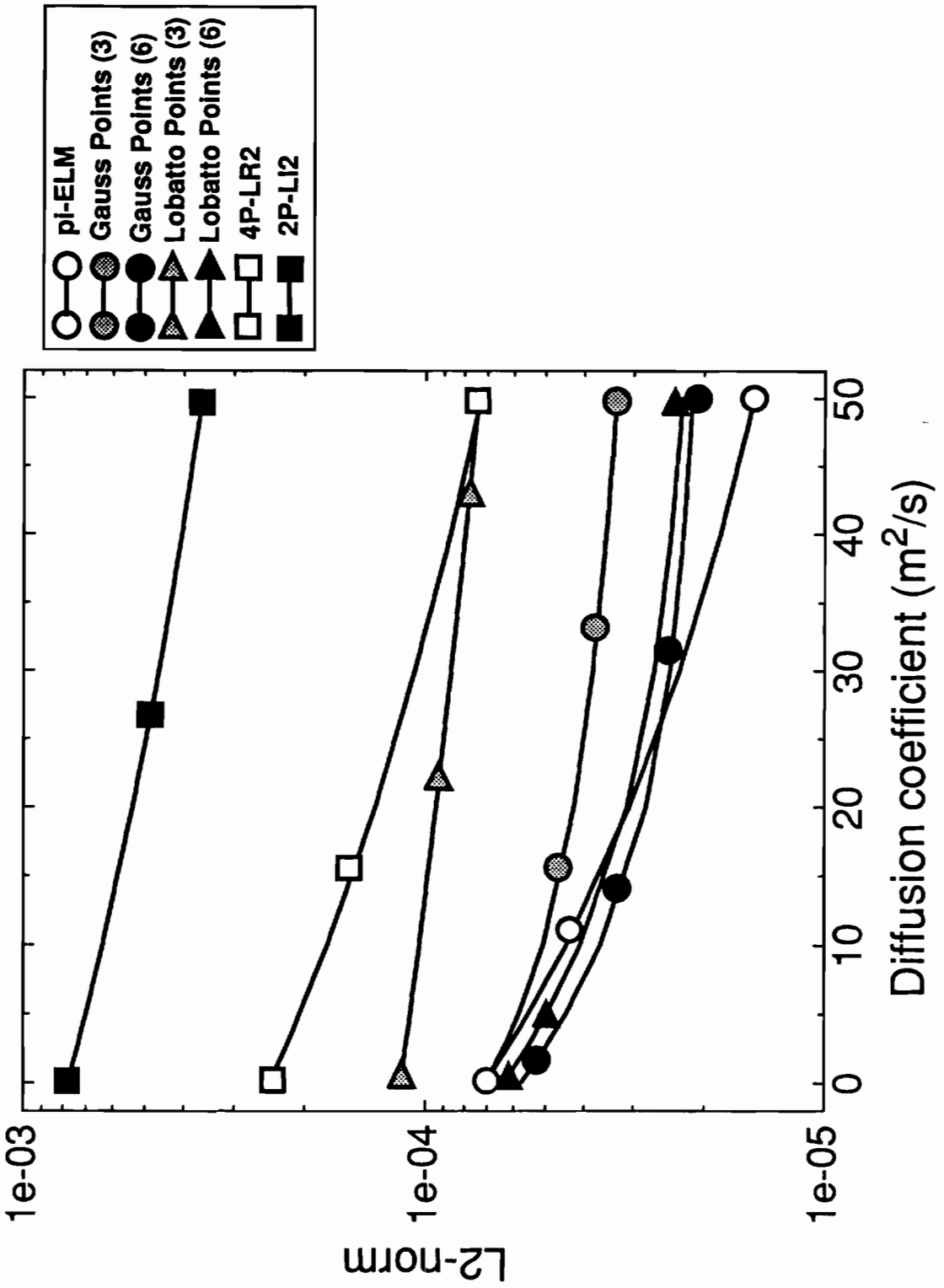

Figure 2.44(a) Influence of diffusion for a Gauss hill problem, with $\beta = 0.24$: L2-norm.

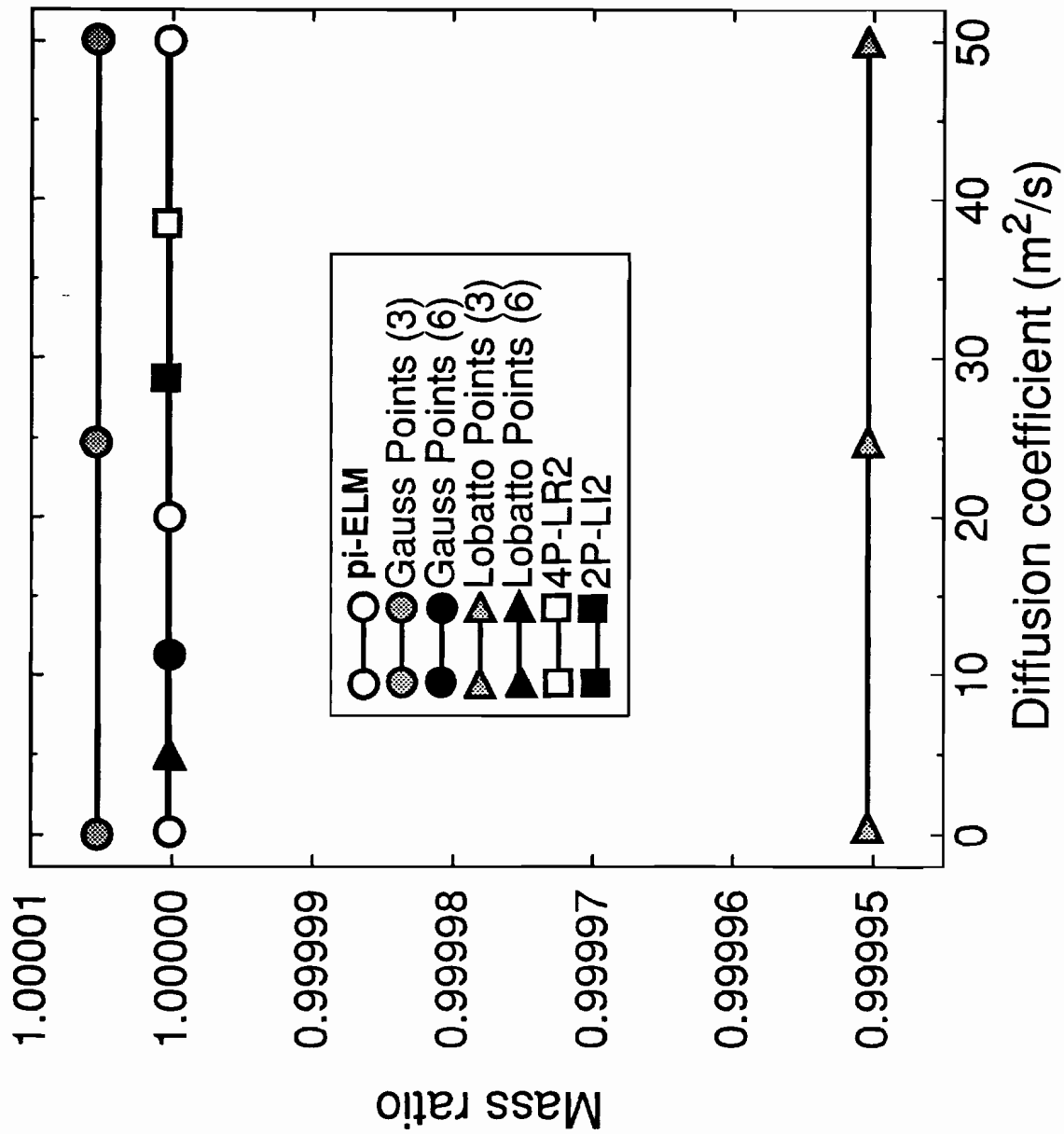

Figure 2.44(b) Influence of diffusion for a Gauss hill problem, with $\beta = 0.24$: Mass ratio.

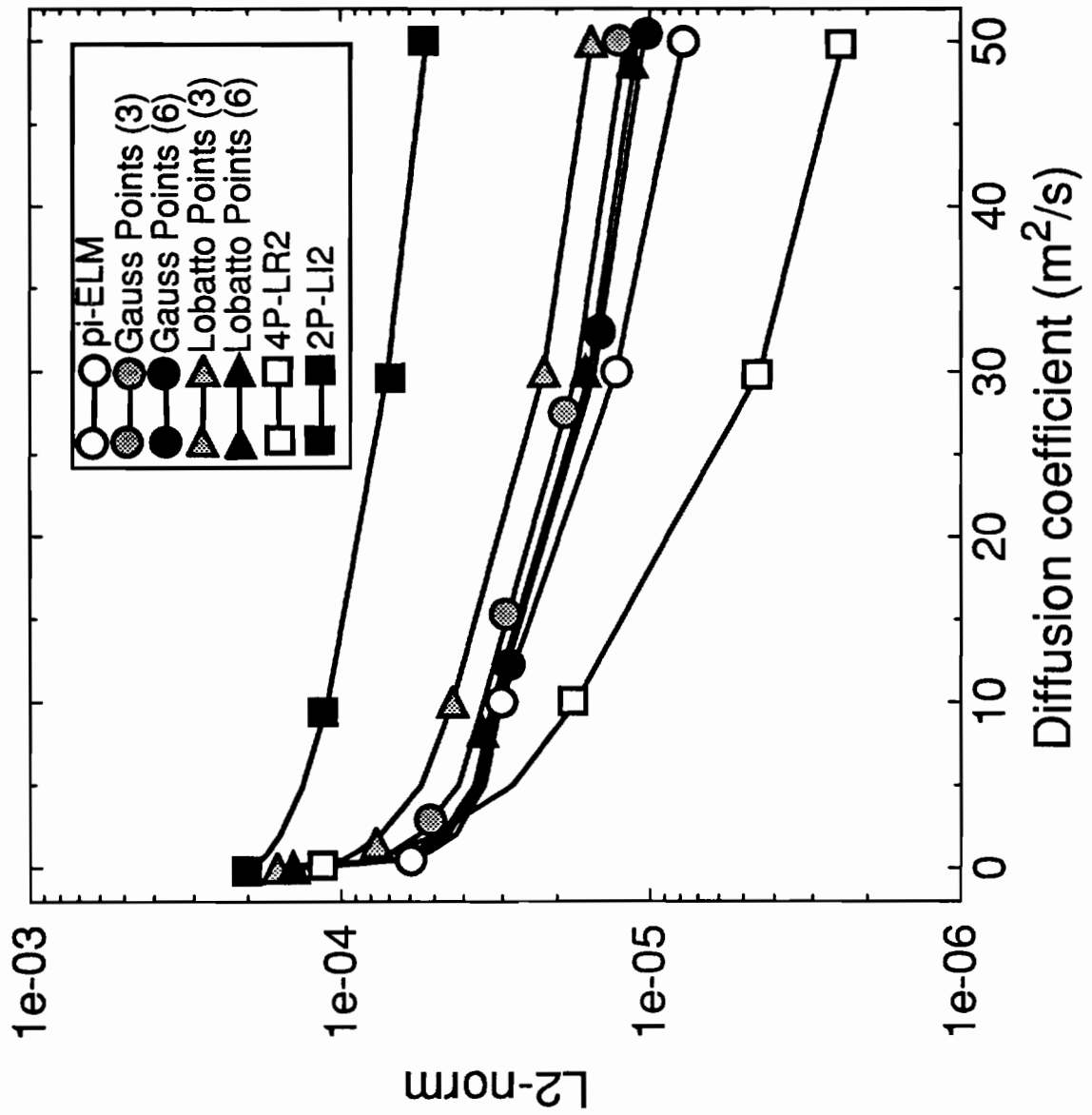

Figure 2.45(a) Influence of diffusion for an advancing front, with $\beta = 0.24$: L2-norm.

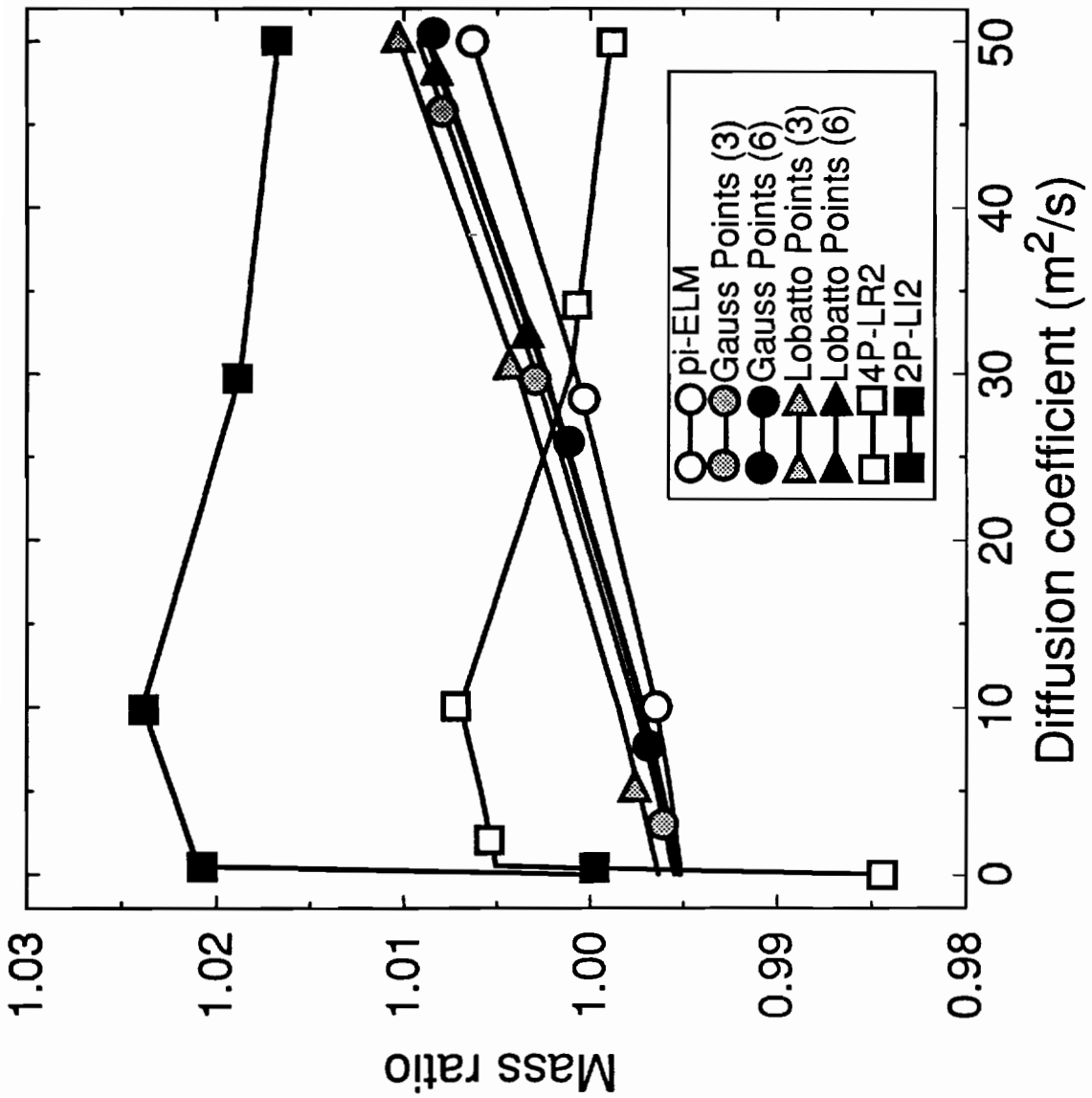

Figure 2.45(b) Influence of diffusion for an advancing front, with $\beta = 0.24$: Mass ratio.

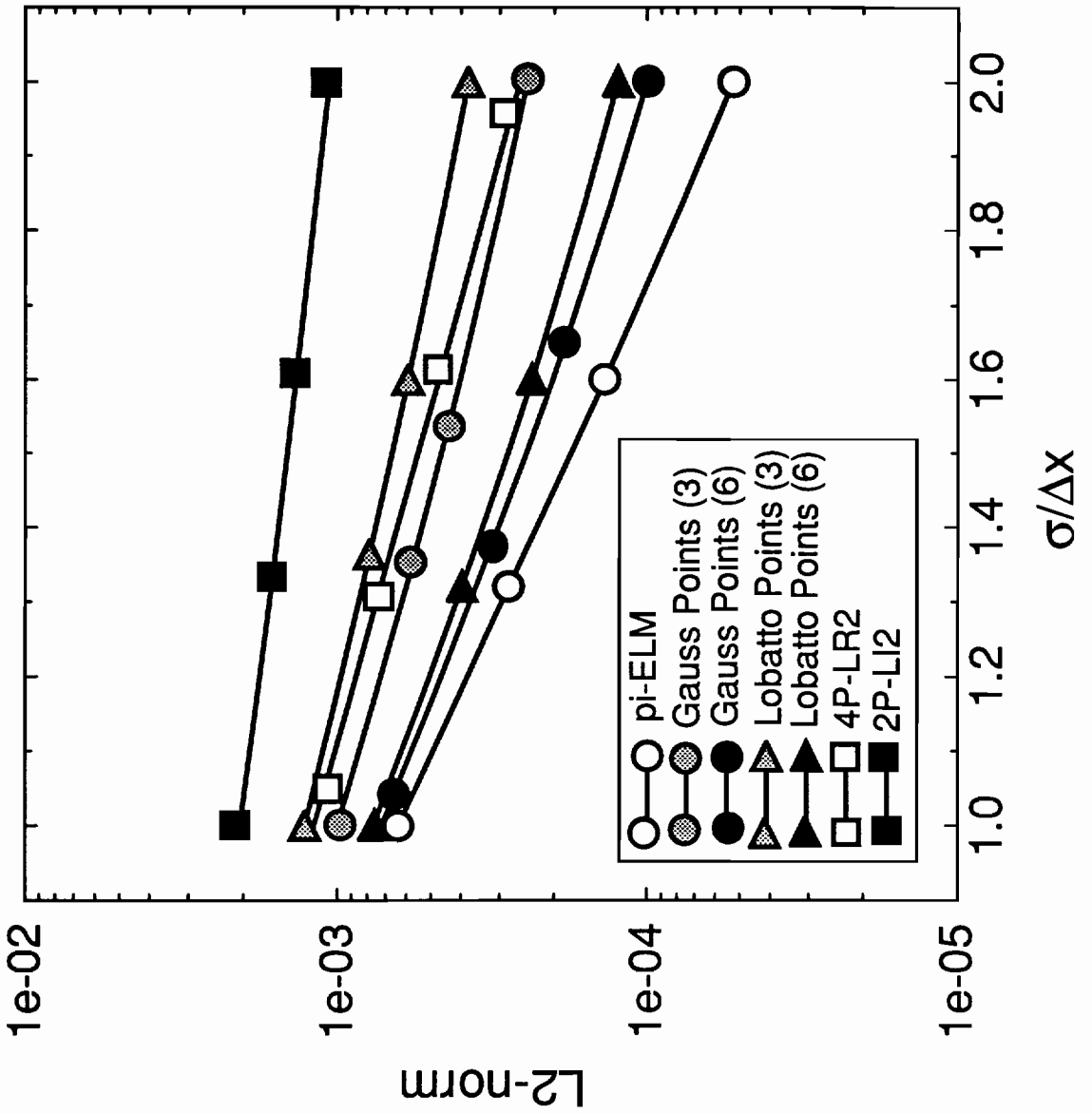

Figure 2.46(a) Influence of source discretization, for a Gauss hill, with $\beta = 0.24$ and $D = 0$: L2-norm.

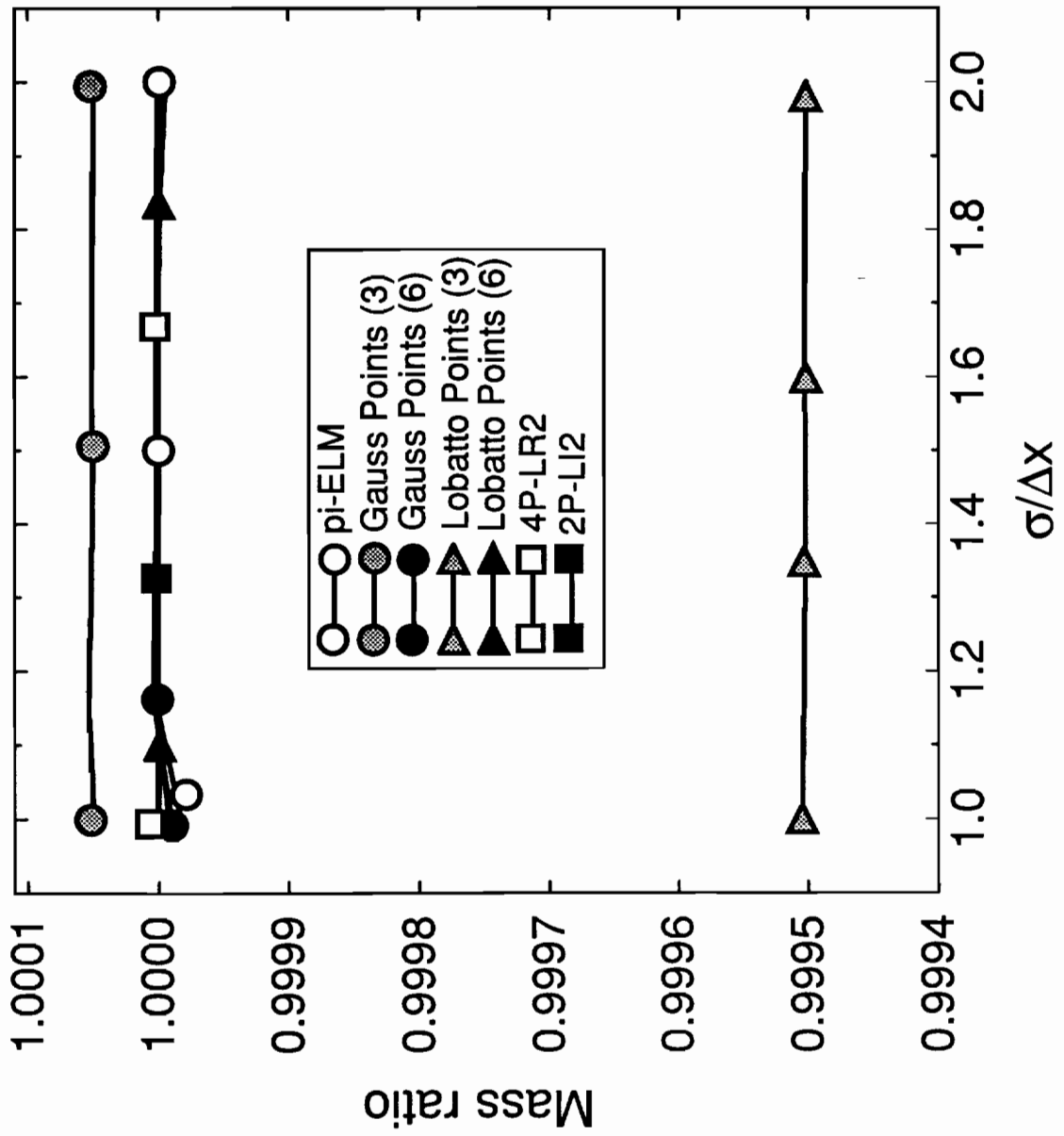

Figure 2.46(b) Influence of source discretization, for a Gauss hill, with $\beta = 0.24$ and $D = 0$: Mass ratio.

CHAPTER 3
Final considerations

Synthesis and conclusions

We have systematically compared representative interpolation and integration FE-ELMs for the solution of the 1D transport equation with constant coefficients, using both formal analysis (propagation and truncation errors analysis), and numerical experimentation.

While no method emerges as optimal, the comparison reveals marked differences between integration and interpolation methods that are worth accounting for when developing FE-ELM transport models. Integration methods tend to be more accurate than interpolation methods, for the same number of nodes and elemental shape functions. However, comparisons on a "per-node basis" may be somewhat unfair, as they do not account for the computational costs.

The piecewise integration method proposed here (pi-ELM), is unconditionally stable and among the most accurate of the methods examined in this study. However, this method cannot avoid some spatial oscillations, when very sharp gradients of concentration are present (e.g., as in pure advection or highly advection-dominated advancing front problems).

The performance of the quadrature integration methods (qu-ELMs) is highly dependent on the type and number of quadrature points used. We examined both Gauss and Lobatto quadratures, with 3 to 6 quadrature points. While the results for 3 points are only about as accurate as for the interpolation ELMs, for both types of quadrature, the for-

mulations with the larger number of points are often able to achieve the much better performance of the piecewise integration scheme. However, quadrature integration methods are only conditionally stable for pure-advective transport. While a small diffusion coefficient (smaller than the dispersion coefficients currently used in numerical simulations) is enough to stabilize the simulations, this conditional stability must be recognized when using quadrature FE-ELMs.

In the very limited context of a constant-coefficient analysis, mass is well preserved by both interpolation and integration methods. However, as discussed later in this chapter, the broad issue of mass conservation of ELMs in multi-dimensional applications with complex flows remains unresolved.

Contributions

The main contributions of this thesis are:

(1) to consolidate the current understanding of FE-ELMs; in particular:

- we explained the definition of the initial conditions for the diffusion equation as an "integration" rather than an "interpolation" problem, and placed it in the context of the evolution of ELMs. The notion of integration at the feet of the characteristic lines is conceptually appropriated for FE-ELMs and provides new opportunities in the search for more accurate algorithms;

- we explored the concept of integration ELMs by systematically analyzing the formal properties (accuracy and stability) of methods performing either a piecewise integration or a quadrature integration; these properties were studied as functions of the controlling dimensionless numbers (Courant number, diffusion number and dimensionless wavelength), providing a broad characterization of the methods that can be used for unbiased comparison;

- we related the stability and accuracy of the quadrature FE-ELMs with the number and type of quadrature points, extending work by *Morton, et al.* [1988]; we also evaluated the amount of diffusion that is necessary to guarantee stability for different choices of number and type of quadrature points.

- we showed that the characteristic loss of accuracy in the advective step for interpolation methods can be greatly reduced by integration methods; we compared the formal properties of the two integration-ELMs and two well-established interpolation ELMs, on an equal number of nodes basis.

(2) to propose a simplified piecewise integration method, which provides a controlled computational cost (time-step independent) as opposed to the original formulation [*Yeh, et al.*, 1992]. This simplified method is unconditionally stable and much more accurate than the reference methods, on a equal number of nodes comparison.

Implications

Integration ELMs emerge from our analysis as very attractive techniques. However, the analysis was done in 1D, for constant coefficients, so it is also necessary to consider the practical aspects that are relevant for real world simulations.

Practical implementation problems can compromise the development of a method in multiple dimensions. Indeed, due to these practical considerations, most application-oriented models with ELMs still use the compact quadratic interpolator or a similar approach [*Baptista, et al.*, 1984, *Cheng, et al.*, 1984, *Dimou*, 1992, *Wood and Baptista*, 1993]; more accurate methods (e.g., non-compact 8 node method) have been proposed, but not widely applied in practice.

The methods studied in this thesis constitute a class of methods that combines accuracy with simplicity of implementation. Unlike other conceptually attractive classes

of methods (e.g., non-compact methods), integration ELMs can be efficiently used with both structured and unstructured grids, and do not pose special difficulties near boundaries. Some difficulties may arise, for instance, from the evaluation of the integrals for the piecewise integration, but they are relatively minor, and can be avoided with straightforward simplifications. Therefore, integration FE-ELMs constitute a very attractive potential alternative to the interpolation ELMs in application-oriented models. In particular, we recommend that integration FE-ELMs be incorporated into the growing family of ELA water quality models [*Baptista, et al.*, 1984, *Barros and Baptista,* 1990, *Wood and Baptista*, 1993].

Our theoretical analysis can also be used to some practical purposes, if the integration ELMs are implemented in an application-oriented model. In particular, the formal analysis can provide a good criterion to the generation of finite element grids for transport simulations.

Nowadays, the same grid is typically used for both flow and transport models, for simplicity. Unfortunately, flow grids are generated through criteria that do not take into account the velocity and concentration fields, but only wave characteristics like the celerity and the period of the wave. The most used criteria for flow grids are based on the Courant number:

$$\beta_{flow} = \frac{c\,(h)\,\Delta t}{\Delta x} < \beta_{max} \tag{3.1}$$

and on the dimensionless wavelength:

$$\frac{L_m}{\Delta x}_{flow} = \frac{c\,(h)\,T}{\Delta x} > \frac{L_m}{\Delta x}_{min} \tag{3.2}$$

where h is the water depth, c and T are, respectively, the celerity and the period of the wave. The second criterion is more used for the generation of flow grids than the first one, since it does not require a previously defined time step. Usually, the dimensionless wave-

length criterion is used to generate the grid and then, the maximum time step is selected from the Courant number criterion.

These criteria will generate grids that are more discretized in shallow areas and coarser in the deep areas, since the celerity is related to the water depth. However, for transport simulations, the larger refinement is necessary where the gradients of concentration are larger, which is not considered in the above criteria. They are therefore far from optimal for transport simulations.

A transport-oriented Courant number criterion can be used to generate transport grids, when the numerical technique chosen requires a limit on β, either for accuracy or stability purposes:

$$\beta_{transp} = \frac{u\Delta t}{\Delta x} < \beta_{max} \tag{3.3}$$

However, this criterion only takes into account the flow field, being independent of the concentration field. Moreover, it cannot be applied to the generation of grids for ELMs, since this class of methods does not have limiting constraints on the Courant number.

The discretization of the pollutant's plume, or dimensionless wavelength for transport ($L_m/\Delta x$) provides a more appropriated criterion for transport grids, since it places more refinement where the concentration gradients are higher. However, the practical implementation of this criterion can be difficult since $L_m/\Delta x$ is time dependent.

One simple alternative is to generate a grid that is sufficiently refined for the entire period of the simulation, and use the same grid for the whole run. First, it is necessary to estimate the pathways of the tracer during the simulation. For instance, the flow grid can be used for a preliminary simulation. Then, the maximum gradients of concentration for each point in space can be used to generate the grid. Even though this static grid may not be optimal, it is certainly better than one optimized for flow simulations.

A conceptually more attractive approach would be to incorporate an adaptive grid generation in the transport model, since it would take into account the time-dependent nature of the problem. An example of an iterative approach is to start with the above static grid, run the model for a period of time and then refine the grid for specific time steps and run the model again. However, adaptive approaches have some implementation problems. On the one hand, it is necessary to define an error measure to evaluate the accuracy of the simulation at each time step, that does not require the knowledge of the exact solution. This measure, essential to control the refinement of the grid, is yet to be identified; elemental finite element residuals may represent the only available choice, but have not been demonstrated to be a robust error measure. On the other hand, the iterative nature of this procedure may lead to very large computational costs, due, for instance, to the duplication of runs.

Since Fourier analysis relates the amplification error associated with the numerical algorithm to the discretization of the concentration field, the analysis may provide an appropriate support for both adaptive and static generation of grids for transport simulation. If a maximum amplification error is selected by the modeler, the corresponding Dimensionless wavelength can be easily evaluated, as well as the minimum grid spacing that would guarantee the specified maximum amplification error in a constant coefficients context.

For the application of a quadrature integration model, both Fourier and truncation error analysis can be of further help to modelers, when it is necessary to select a set of parameters. If a maximum amplification error is specified, the minimum number of quadrature points required can be estimated, for a specific quadrature. Once the number and type of quadrature points is defined, the truncation error can suggest the minimum amount of diffusion required to guarantee stability.

Considerations for further research

In order to select a "best" method for application-oriented models in multiple dimensions, further research is still necessary. The simplified context in which this analysis was done excluded several aspects that can be essential to the selection procedure. Among these, we will discuss, in a qualitative form, two potential problems associated with a non-constant flow field: mass conservation and computational costs.

Mass conservation

The inherently non-conservative formulation of ELMs is one of their major drawbacks. Mass conservation problems have been detected in many applications, especially when complex flows are present, which may jeopardize the use of ELMs in applications involving tracers with complex chemical and biological transformations, and/or long-term simulations.

As mentioned in Chapter 1, the failure to preserve mass in the flow field and the errors in the evaluation of the characteristic lines can lead to considerable mass errors in the transport simulation. Both problems generate deviations in the location of the feet of the characteristic lines, leading to a distortion of the concentration field and to mass imbalances. In order to illustrate this effect, several tests were done, introducing a perturbation in the flow field. The velocity perturbation was specified as a random variable in space. A normal distribution was chosen, with zero average and a varying standard deviation (σ). Figure 3.1 shows that, as the standard deviation increases, the gauss shape is distorted, and severe phase and amplitude errors occur. The mass errors for the above standard deviations are presented in Figure 3.2, against the ratio of the standard deviation over the original velocity (σ/u). Significative mass errors occur (e.g., 17% of the mass was lost in 100 time steps, for σ/u of 30%), as a consequence of the non-conservative flow field.

While the mass errors due to the tracking are specific to ELMs, the mass problems related to non-conservative flow fields should be common to any model solving the non-

conservative form of the transport equation. The effect of the flow field's local mass imbalances in the transport simulation can be reduced either by keeping the mass errors in the flow model small, or through the compensation of these errors in the transport equation. The first alternative seems to be more effective, although it would require an innovative approach to the coupling of flow and transport models.

The mass conservation in the flow field can be improved if a more discretized grid is used. However, this refinement may be constrained by two problems. On the one hand, the refinement of the grid increases the costs of the flow simulation. On the other hand, since the same grid is traditionally used for both flow and transport simulations, a more refined grid would also increase the computational costs for the transport simulation. In order to control the transport simulation costs, different grids can be used in each simulation, but the generation of a specific grid for transport also poses some difficulties (see previous section).

A simpler but probably not very effective alternative would be to consider the conservative form of the transport equation that does not assume mass conservation in the flow field:

$$\frac{\partial}{\partial t}(cH) + \frac{\partial}{\partial x_i}(u_i cH) = \frac{\partial}{\partial x_i}(HD_{ij}\frac{\partial c}{\partial x_j}) \tag{3.4}$$

where H is the total depth. It can be written as:

$$\frac{\partial c}{\partial t} + u_i\frac{\partial c}{\partial x_i} - \frac{1}{H}\frac{\partial}{\partial x_i}(D_{ij}\frac{\partial c}{\partial x_j}) = -\frac{1}{H}(\frac{\partial H}{\partial t} + \frac{\partial}{\partial x_i}(u_i H))\, c \tag{3.5}$$

where the left hand side is the non-conservative form of the transport equation which is traditionally solved by ELMs. The right hand side of Equation (3.5) represents the correction for the failure of mass in flow and it can be either a source or a sink term. This approach will cause an arbitrary distribution of mass over the domain, that may correct the global mass, but it will not address local mass imbalances. In addition, the flow field for the tracking would still be incorrect.

Computational cost

Our analysis concentrated on stability and accuracy. However, it is also necessary to study the practical aspects that are relevant for real world simulations. In particular, some key factors like cost-effectiveness and practical implementation problems were not considered in this analysis due to its simplified context, but may compromise the use of a method for application purposes.

The computational cost in ELMs is mainly determined by the cost associated with the tracking, the evaluation of the integrals at the feet of the characteristic lines and the solution of the system of equations (for time-dependent matrices, the inversion may also be a time consuming task). The relative importance of each of these costs will depend on the specific ELM selected, and on the characteristics of the computer architecture.

Computational costs, although difficult to quantify, are important to analyze because they can compromise the expansion of the integration methods to multiple dimensions. Since the computational cost of the advective step has been recognized as one of the most time consuming tasks in traditional implementations of ELMs [*Baptista, et al.*, 1984, *Zhang*, 1990 as quoted by *Dimou*, 1992], we will qualitatively analyze it for each method. The computational cost of the advective step for the studied methods is mainly determined by two factors: the tracking of the characteristic lines and the evaluation of the integrals at the feet of the characteristic lines. Therefore, the cost of a method is directly related to the number of characteristic lines to be evaluated and to the efficiency of the integration algorithm.

The compact quadratic method (3P-LI3) is taken as reference, even though it was not studied here. It has been implemented in most application-oriented models, due to its reasonable balance between costs and accuracy [*Baptista, et al.*, 1984, *Baptista*, 1987]. Since we are looking for new methods for application purposes, it is important to compare the potential alternatives costs with the 3P-LI3's. For this method, the number of characteristic lines to be evaluated is equal to the number of nodes. The evaluation of the inte-

grals is straightforward, since the concentration is assumed to be a quadratic function defined by the interpolated concentration at the feet of the characteristic lines.

The number of characteristic lines to be tracked for the simplified pi-ELM is twice the number of nodes, since all nodes are backward and forward tracked in one time step. The evaluation of the integrals for this method can pose some problems and become extremely expensive in a 2D or 3D model, since the concentration at the feet of the characteristic lines for a specific element is a piecewise function (Figure 3.3). To overcome this problem, some simplifications can be made, with varying degrees of accuracy.

The evaluation of the integrals for the quadrature methods is straightforward, since quadrature points are used to define the concentration function. However, the tracking cost is necessarily higher than for the interpolation methods. For instance, using qu-ELMs, a minimum of 3 quadrature points is necessary to obtain a better performance than the 3P-LI3. Therefore, three characteristic lines rather than one have to be determined per element.

The qu-ELM with 2 Gauss points and quadratic elements can be another potential alternative that still keeps the tracking costs of the 3P-LI3. Although the qu-ELMs with a small number of quadrature points and linear elements are not more accurate than the interpolation approaches, the quadratic formulation will probably improve the performance of this class of methods. It would also keep the simplicity of the ELM approach, as opposed to the formality of the ELLAMs, and the straightforward evaluation of the integrals. The formal properties of the qu-ELM with quadratic elements must be studied before it can be considered a realistic alternative.

Although the above qualitative analysis covers only part of the cost controlling parameters, it has raised the question of cost-effectiveness of the integration approach. We cannot compare the total cost of the methods, but their accuracy can be compared in an 'equal tracking costs' basis. We compared the performances of the pi-ELM for the Convection Diffusion Forum problem 1A, and the 3P-LI3 for the same test but with twice the

number of nodes (Figure 3.4). Figure 3.4 shows that the differences between the accuracy of the two methods are rather small. Other tests performed for different Courant numbers confirmed these results. Since the cost of the integral evaluation is probably higher for the pi-ELM than for the 3P-LI3, the effectiveness of the new methods could be questioned. However, the integration-approach to the advective step can be more attractive and probably cost-effective, if it is implemented in an ELLAM framework.

The ELLAM approach can provide a very accurate solution that still keeps the low tracking costs of the reference solution. The number of the characteristic lines to be tracked is only the number necessary to define the elements, i.e., it is equal to the number of nodes. Since the weight function is defined at the feet of the characteristic lines, the forward tracking of the interpolated concentration is not required for a piecewise integration scheme. Therefore, the ELLAM with a piecewise integration should be about as accurate as the pi-ELM, but with a smaller computational cost. If a numerical integration is selected, then the evaluation of the integrals is as efficient as in the qu-ELMs, but the tracking cost is much smaller, since the characteristic lines of the quadrature points are not evaluated.

This qualitative analysis suggests that the ELLAMs with a numerical integration may provide a low cost solution, that is still very accurate. However, this analysis is partial, since it only considered some of the tasks to be done in an ELM. A global evaluation of the total computational cost, that also takes into account the advantages of specific computer characteristics, is necessary to select the most effective method to implement in a multiple dimension, application oriented model.

References

Baptista, A. M., E. E. Adams, and K. D. Stolzenbach, Eulerian- Lagrangian analysis of pollutant transport in shallow water, *Technical Report no. 296*, MIT R.M. Parsons Laboratory, Cambridge, Mass, 1984.

Baptista, A. M., Solution of Advection-Dominated Transport by Eulerian-Lagrangian Methods using the Backwards Method of Characteristics, Ph.D. Dissertation, Massachusetts Institute of Technology, Cambridge, Mass, 1987.

Barros, A. P. and A. M. Baptista, An Eulerian-Lagrangian model for sediment transport in estuaries, *Proceedings of the Estuarine and Coastal Modeling ASCE conference*, M. L. Spaulding, pp. 102-112, 1990,

Cheng, R. T., V. Casulli, and S. N. Milford, Eulerian-Lagrangian Solution of the Convection-Dispersion Equation in natural Coordinates, *Water Resources Research, 20*(7), pp. 944-952, 1984.

Dimou, K., 3-D Hybrid Eulerian-Lagrangian / Particle Tracking Model for Simulating Mass Transport in Coastal Water Bodies, Ph.D. Dissertation, Massachusetts Institute of Technology, Cambridge, Mass, 1992.

Morton, K. W., A. Priestley, and E. Suli, Stability of the Lagrange-Galerkin Method with Non-exact Integration, *Mathematical Modelling and Numerical Analysis, 22*(4), pp. 625-653, 1988.

Wood, T. M. and A. M. Baptista, A model for Diagnostic Analysis of Estuarine Geochemistry, *Water Resources Research, 29*(1), pp. 51-71, 1993.

Yeh, G. T., J. R. Chang, and T. E. Short, An Exact Peak Capturing and Oscillation-Free Scheme to Solve Advection-Dispersion Transport Equations, *Water Resources Research, 28*(11), pp. 2937-2951, 1992.

Zhang, X., Control of tracking error in numerical solution of advection diffusion equation by Eulerian Lagrangian method, M.S. thesis, Department of Civil Engineering, Massachusetts Institute of Technology, Cambridge, Mass, 1990.

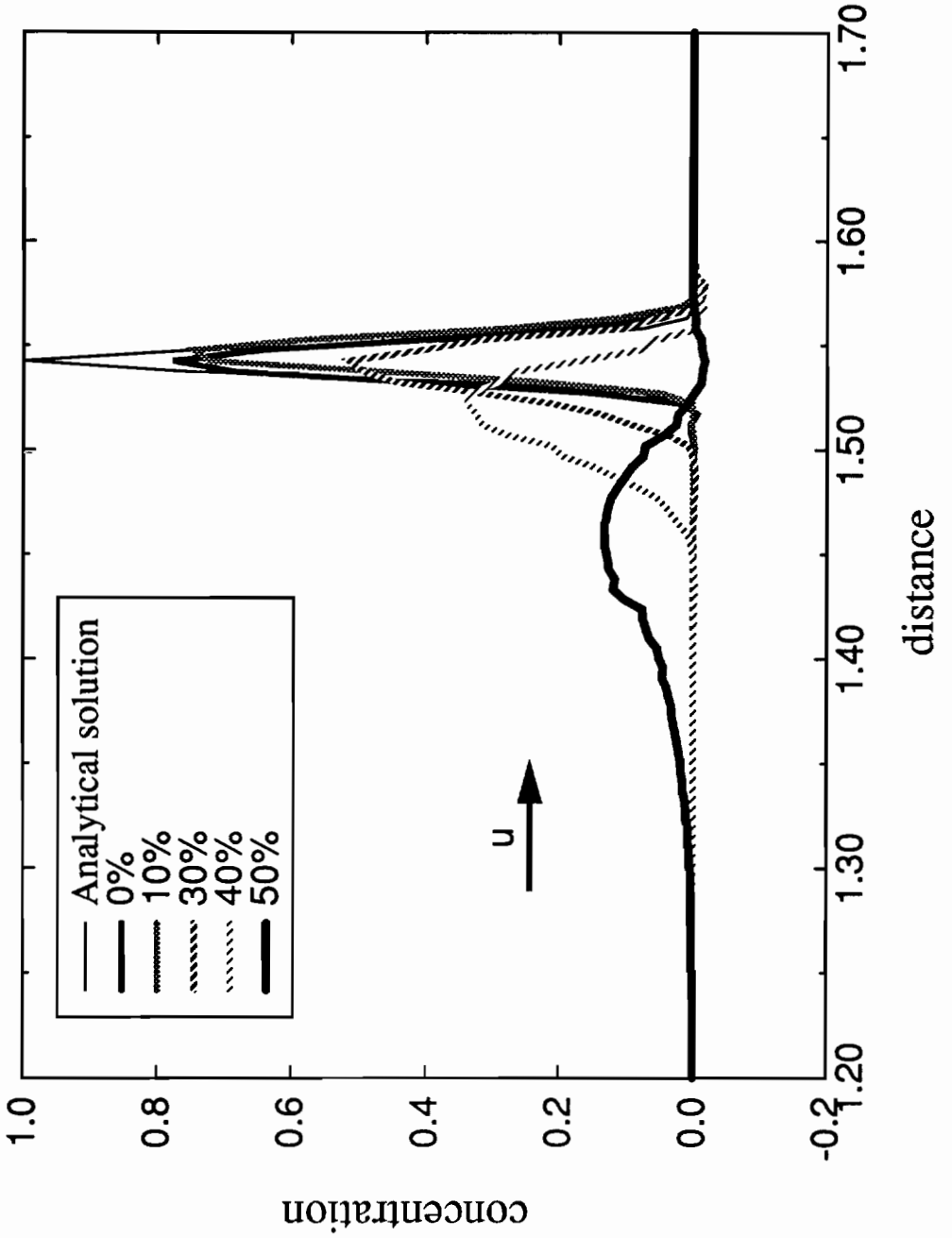

Figure 3.1 Impact of the error in velocity in a transport simulation: the percentages represent the ratios of the standard deviations of the error in the velocity over the original velocity.

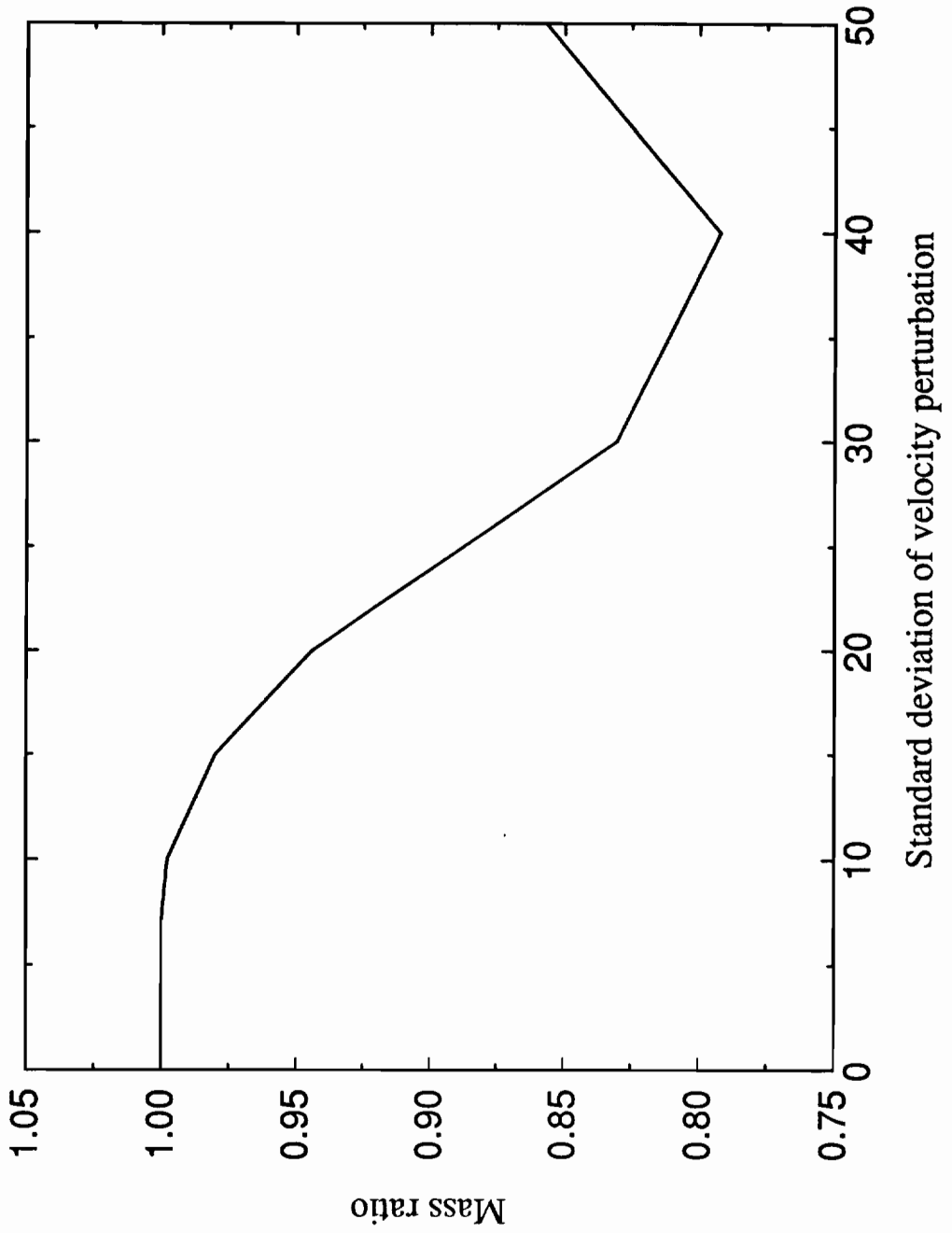

Figure 3.2 Impact of the error in velocity in the mass preservation of a transport simulation.

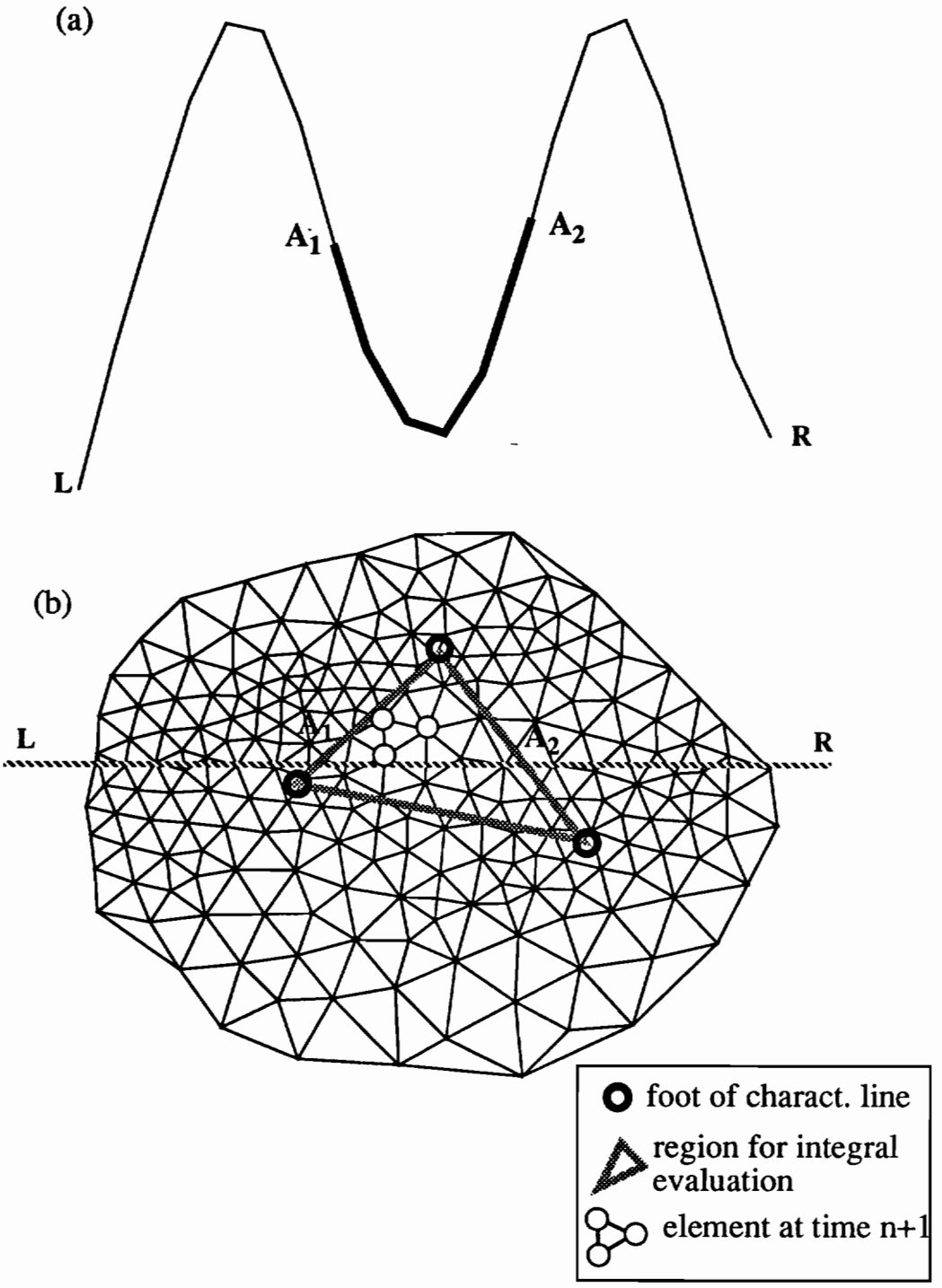

Figure 3.3 Evaluation of integrals in multiple dimensions for the pi-ELM: (a) slice of concentration field at time *n*; (b) definition of region for integral evaluation, over FE grid.

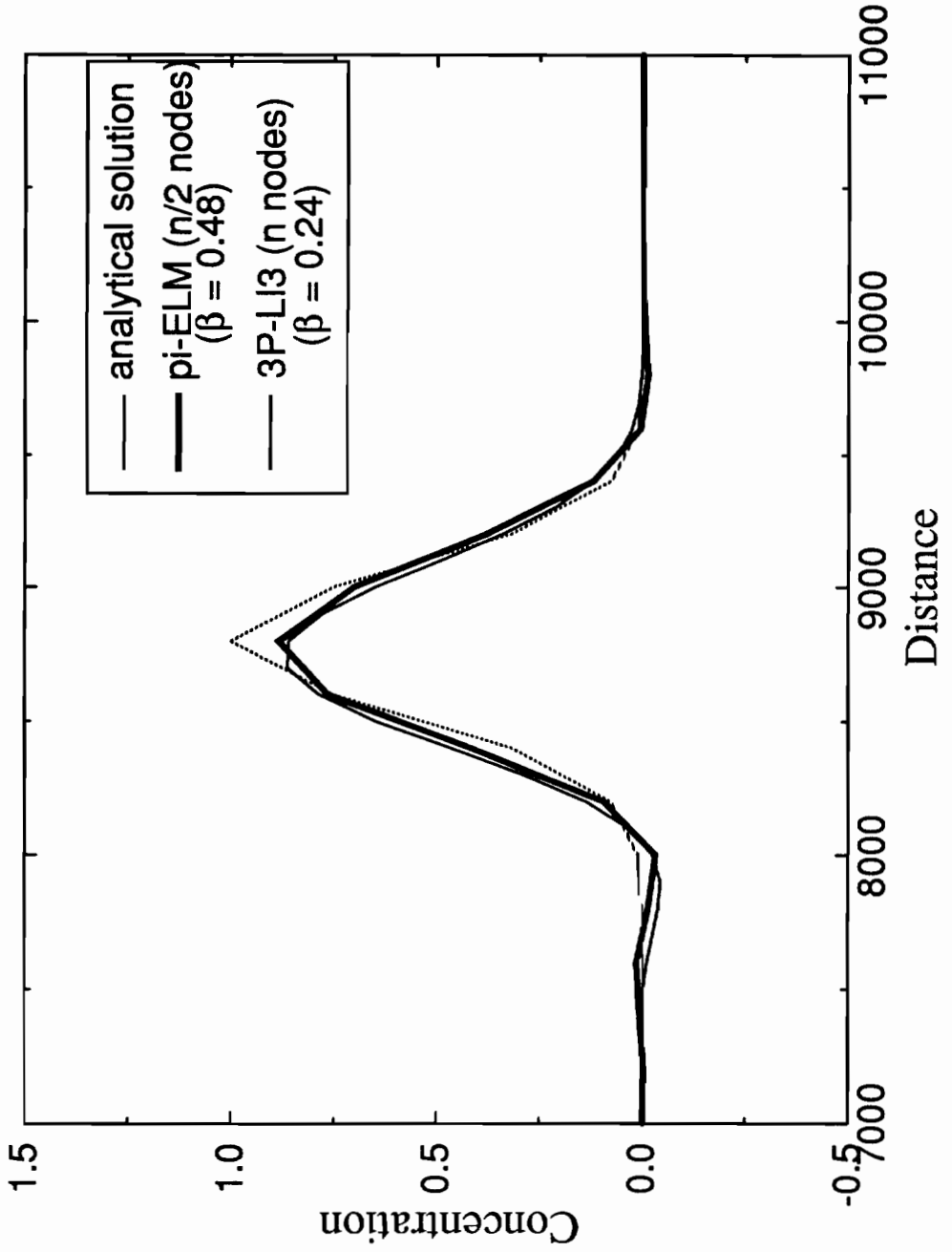

Figure 3.4 Comparison of the pi-ELM (n/2 nodes) and the 3P-LI3 (n nodes).

BIOGRAPHICAL SKETCH

The author was born on March 10, 1967, in Lisbon, Portugal. She entered Instituto Superior Técnico, Lisbon, Portugal, in October, 1985 and received her Bachelor of Science degree in Civil Engineering in September, 1990.

In September 1991, the author entered Oregon Graduate Institute of Science & Technology as a master student, under the supervision of Dr. António M. Baptista. She was awarded her Master of Science in Environmental Science and Engineering in January, 1994.